

SEISMIC BEHAVIOUR AND RETROFITTING OF URM BUILDINGS

Ph.D. THESIS

by

SHERMI C.



**DEPARTMENT OF EARTHQUAKE ENGINEERING
INDIAN INSTITUTE OF TECHNOLOGY ROORKEE
ROORKEE – 247 667 (INDIA)
DECEMBER, 2017**

SEISMIC BEHAVIOUR AND RETROFITTING OF URM BUILDINGS

A THESIS

*Submitted in partial fulfilment of the
requirements for the award of the degree*

of

DOCTOR OF PHILOSOPHY

in

EARTHQUAKE ENGINEERING

by

SHERMI C.



**DEPARTMENT OF EARTHQUAKE ENGINEERING
INDIAN INSTITUTE OF TECHNOLOGY ROORKEE
ROORKEE – 247 667 (INDIA)
DECEMBER, 2017**



**©INDIAN INSTITUTE OF TECHNOLOGY ROORKEE, ROORKEE- 2017
ALL RIGHTS RESERVED**



INDIAN INSTITUTE OF TECHNOLOGY ROORKEE ROORKEE

CANDIDATE'S DECLARATION

I hereby certify that the work which is being presented in the thesis entitled **“SEISMIC BEHAVIOUR AND RETROFITTING OF URM BUILDINGS”** in partial fulfilment of the requirements for the award of the degree of Doctor of Philosophy and submitted in the Department of **Earthquake Engineering**, Indian Institute of Technology Roorkee, Roorkee is an authentic record of my own work carried out during a period from **December, 2011 to December, 2017** under the supervision of Dr. R.N. Dubey, Assistant Professor, Department of Earthquake Engineering, Indian Institute of Technology Roorkee, Roorkee.

The matter presented in this thesis has not been submitted by me for the award of any other degree of this or any other Institute.

(SHERMI C.)

This is to certify that the above statement made by the candidate is correct to the best of my knowledge.

(R.N. Dubey)
Supervisor

Date:

The Ph.D. Viva-Voce Examination of Shermi C., Research Scholar, has been held on.....

Chairman, SRC

Signature of External Examiner

This is to certify that the student has made all the corrections in the thesis.

Signature of Supervisor

Head of the Department

ABSTRACT

Earthquakes are natural hazards under which disasters are mainly caused by damage to or collapse of buildings and other man-made structures. The unreinforced masonry (URM) buildings have proved to be the most vulnerable to earthquake forces and have suffered maximum damage during the past earthquakes worldwide. Unreinforced masonry is an old age traditional method used for most of the low to medium rise buildings in many countries, including India. In most cases, neither seismic loads are considered while designing nor earthquake resistant features are incorporated in masonry buildings leading to their excessive damage during earthquakes. Understanding the failure mechanism of these buildings subjected to seismic loads will help in improving their performance. Thus, the various failure mechanism of different masonry buildings subjected to seismic loads has been presented herein.

To improve the seismic performance of masonry buildings, a number of techniques have been adopted to strengthen the existing masonry buildings. A review of the existing strengthening technology used for strengthening masonry has been comprehensively discussed in this thesis. In addition, a detailed review of existing codal recommendations and guidelines have also been presented. Numerical modeling which serves as a powerful tool has also been reviewed with respect to masonry modeling.

The procedure adopted for the strengthening of URM recommended in Indian standard code of practice IS 13935: 2009, using welded wire mesh (WWM) and coarse cement sand mortar has been adopted and presented in detail for all considered test specimens. The conventional masonry panels were constructed and tested to obtain the material properties and to develop a non-linear material model for finite element (FE) modeling. Concrete Damaged Plasticity (CDP) constitutive model has been used in this study to simulate the non-linear behavior of masonry. Experiments have been conducted to evaluate the in-plane and out-of-plane behavior of both reinforced and unreinforced masonry panels. Two half-scale masonry models have also been tested on shake table whose sequential construction details are also presented herein. The experimental results of URM and reinforced masonry (RM) panels, as well as the two half-scale masonry models, have been compared with numerical simulations.

In the first phase, masonry panels of size 500 mm x 500 mm x 230 mm have been tested for diagonal compression as per ASTM E519 to study the in-plane behavior of URM panels. The URM specimens were strengthened using WWM (1 inch, 1.5 inch, and 2 inch spacing) and 1:3 coarse sand mortar as per IS 13935: 2009. The behavior of both strengthened and URM panels

have been compared in terms of strength, stiffness and ductility. The incorporation of WWM reinforcement on URM masonry panels resulted in an average increase of strength ranging from 1.88, 2.35 and 2.42 times more compared to control specimen of 1:4 mortar masonry samples. In case of 1:6 mortar masonry samples increase in strength varied from 11.51, 12.24, 13.00 times the controlled specimen in 1 inch, 1.5 inch and 2 inch spacing WWM respectively. The numerical results simulated with CDP model were compared with the experimental findings in terms of damage pattern and shear stress-strain plots.

In the second phase, the URM panels were investigated for out-of-plane behavior as per ASTM E518. Masonry panels of size 1000 mm x 500 mm x 230 mm were tested under four-point loading condition to study the out-of-plane behavior of both URM and RM panels. The enhancement in flexural strength of RM specimen compared to URM specimen was investigated in terms of load carrying capacity, displacement, and ductility. The flexural load carrying capacity of masonry has significantly increased at an order of four in case of strengthened specimen compared to that of conventional URM panels. The experimental test results were numerically validated in terms of load-deflection plots and damage pattern.

In the third phase, two half-scale masonry models, one URM and the other strengthened with 1.5 inch spacing WWM and 1:3 coarse sand mortar has been evaluated using shake table test facility in the Department of Earthquake Engineering, IIT Roorkee. Initially, free vibration test was carried out on both the models to compute the time period and natural frequency of the URM and RM models. The models have been tested on a shake table for a series of artificially generated acceleration time history compatible with Indian standard response spectra for seismic zone V on hard soil. These ground motions were applied at the base of the model and response has been recorded at the base and at the top of these models. The URM model experienced extensive damage confirming that URM buildings are highly unsafe during the earthquake and require retrofitting/strengthening. Acceleration at the top of the models was observed and recorded during testing. The RM model was able to withstand three times more intense load (ground motion) compared to the URM model without any sign of distress. The modes of failure were observed and roof acceleration was recorded. The experimental results were validated numerically using finite element analyses. The results obtained from the numerical simulation were found to be in good agreement with the damage pattern and peak ground acceleration obtained from the experimental results. The RM model performed well during the dynamic testing confirming that the adopted technique can be effectively used for strengthening/ retrofitting of existing masonry structures.

ACKNOWLEDGEMENT

I express sincere gratitude to my supervisor, **Dr. R.N. Dubey** for his guidance, constant encouragement, inspiration and continuous support throughout my research work. He always showed confidence in me and provided freedom in thoughts and work. I really feel privileged to have worked under his supervision. I would also like to express my gratitude and appreciation to **Prof. Yogendra Singh**, Head of Earthquake Engineering Department, for his critical suggestions, constant encouragement and inspiration.

I would like to thank Dr. Umesh Kumar Sharma, Civil Engineering Department, Prof. Pankaj Agarwal and Prof. J.P. Narayan of Earthquake Engineering Department for their constructive comments and suggestion during my research committee meetings. I am highly indebted to Prof. M.L. Sharma, former Head of the Department for providing facilities and support to enable my research work. My sincere thanks to Prof. Ashok Kumar Mathur, Prof. Manish Shrikhande for their help and support. I am very thankful to Mr. Joshua Daniel, Dr. Sachin Kadam, Ms. Mounika Bhemineni, Ms. Bharathi, Mr. Dhiraj Raj, Mr. Amit Goyal, Mr. Banu Prathap Chamoli from Earthquake Engineering Department, Dr. Manju, Dr. Purushothaman Parthasarathy, Dr. Nirupama Prasad, Dr. Shugandha Panwar, former research scholars at IIT Roorkee for their timely help and support.

I would like to express my special thanks of gratitude to Dr. Siva Chidambaram and Dr. Franklin Frederick former research scholars at IIT Roorkee for their continuous help and support throughout experimental work.

I would also like to acknowledge the staff of shake table test facilities, quasi-static test facilities and workshop of the Earthquake Engineering Department, IIT Roorkee for their help during the instrumentation and fabrication of test setup and testing of specimens. I am indebted to Mr. Rishi Chand and all the supporting staff for their help during the casting and testing of specimens and models. I also extend my sincere thanks to Dr. Umesh Kumar Sharma, for permitting me to use Heavy Testing Laboratory at Department of Civil Engineering, IIT Roorkee for conducting necessary experiments. I am also thankful to Mr. Chetan and his team, Technical Staffs, Heavy Testing Laboratory of Civil Engineering Department for their help during the testing of the specimens.

I have no words to express the deepest appreciation and blessings from my parents Mr. Chellappa and Smt. Grace. I am extremely grateful to my parent-in-laws Mr. Anasco Roy and Smt. Roselet, who gave me wholehearted moral support and never-ending endurance.

Acknowledgement will not be complete without thanking my husband Dr. A.B. Danie Roy and my daughter, Jane for their unwavering patience, as the present work could not be possible without their personal sacrifices and support, for which I shall ever remain indebted.

Finally, I want to express my deepest gratitude to all those who have contributed directly or indirectly to my research work. Last but not the least; I am grateful to the Almighty for making this happen.



TABLE OF CONTENTS

ABSTRACT.....	i
ACKNOWLEDGEMENT	iii
TABLE OF CONTENTS.....	v
LIST OF FIGURES	ix
LIST OF TABLES.....	xv
LIST OF ABBREVIATIONS.....	xvii
LIST OF NOTATIONS	xix
CHAPTER – 1	1
INTRODUCTION	1
1.1 GENERAL	1
1.2 MERITS AND LIMITATIONS OF BRICK MASONRY	3
1.3 COMMON FAILURE MECHANISM OF UNREINFORCED MASONRY BUILDING..	4
1.3.1 Out-of-plane Failure	4
1.3.2 In-plane Failure	4
1.3.3 Combined In-plane and Out-of-plane Failure	5
1.3.4 Diaphragm Failure.....	6
1.3.5 Pounding.....	6
1.3.6 Failure of Connection & Non-structural Components	7
1.4 CODAL RECOMMENDATIONS/ GUIDELINES	7
1.5 OBJECTIVES	8
1.6 SCOPE AND METHODOLOGY.....	8
1.7 ORGANIZATION OF THESIS.....	9
CHAPTER – 2	11
IN-PLANE BEHAVIOR OF UNREINFORCED AND REINFORCED MASONRY PANELS	11
2.1 INTRODUCTION.....	11
2.2 RESEARCH SIGNIFICANCE	13
2.3 EXPERIMENTAL PROGRAM	13
2.3.1 Material Properties	13
2.3.2 Mixing, Casting and Curing of Masonry Specimens	14
2.4 STRENGTHENING PROCEDURE.....	16
2.5 INSTRUMENTATION AND TEST SETUP	17
2.6 ANALYSIS AND DISCUSSION OF EXPERIMENTAL RESULTS.....	18

2.6.1 Test Observations and Failure Modes	18
2.6.2 Influence on Strengthening	21
2.6.3 Test Discussion	25
2.7 THE DIFFERENT MODELING APPROACHES FOR MASONRY	25
2.7.1 Modeling with FEM	25
2.7.2 Modeling with Interface Elements	26
2.7.3 Modeling with DEM	27
2.8 NON-LINEAR MATERIAL MODEL	28
2.9 CONCRETE DAMAGE PLASTICITY (CDP)	28
2.10 DAMAGE AND STIFFNESS DEGRADATION	29
2.11 MATERIAL PROPERTIES OF MASONRY	32
2.11.1 Material Properties of Coarse Sand Mortar	37
2.11.2 Welded Wire Mesh (WWM)	39
2.12 FINITE ELEMENT MODELING OF STRENGTHENED MASONRY	40
2.13 SIMULATION OF DIAGONAL COMPRESSION TEST ON RETROFITTED MASONRY PANEL	41
2.14 SUMMARY	44
CHAPTER – 3	47
OUT-OF-PLANE BEHAVIOR OF UNREINFORCED AND REINFORCED MASONRY PANELS	47
3.1 INTRODUCTION	47
3.2 RESEARCH SIGNIFICANCE	48
3.3 EXPERIMENTAL PROGRAM	49
3.4 STRENGTHENING PROCEDURE	49
3.5 INSTRUMENTATION AND TEST SETUP	51
3.6 TEST OBSERVATION AND FAILURE MODES	52
3.6.1 Strength, Stiffness and Deformation Characteristics	52
3.7 SIMULATION OF FLEXURE TEST ON RETROFITTED PANELS	65
3.8 SUMMARY	72
CHAPTER – 4	75
DYNAMIC TESTING AND SIMULATION OF HALF-SCALE URM AND RM MODELS	75
4.1 INTRODUCTION	75
4.2 EXPERIMENTAL PROGRAM	76
4.3 CONSTRUCTION OF MASONRY MODEL	76

4.3.1 Unreinforced Masonry Model	76
4.3.2 Reinforced Masonry Model.....	79
4.4 TESTING PROCEDURE	83
4.4.1 Free Vibration Test.....	83
4.5 ANALYSIS OF FREE VIBRATION DATA	84
4.6 SHAKE TABLE TESTING	85
4.6.1 Shake Table Specification	85
4.6.2 Sensors and Data Acquisition.....	86
4.6.3 Input Acceleration	86
4.7 BEHAVIOR OF URM MODEL.....	88
4.7.1 First Shake	88
4.7.2 Second Shake.....	89
4.8 BEHAVIOR OF RM MODEL.....	90
4.8.1 First Shake	90
4.8.2 Second Shake.....	91
4.8.3 Third Shake	91
4.8.4 Fourth Shake.....	92
4.9 CLASSIFICATION OF DAMAGE.....	92
4.9.1 Structural Failure Mechanism	93
4.10 SIMULATION OF DYNAMIC TESTING OF URM AND STRENGTHENED MASONRY BUILDING MODELS	93
4.10.1 Material Properties of Concrete.....	93
4.10.2 Material Properties of Steel Reinforcement	96
4.11 MODELING OF URM MODEL	97
4.11.1 Modeling of Strengthened Masonry Model	98
4.12 SUMMARY	102
CHAPTER – 5	105
CONCLUSION AND SCOPE FOR FUTURE WORK.....	105
5.1 GENERAL	105
5.2 URM PANELS.....	105
5.3 RM PANELS	106
5.4 DYNAMIC TESTING AND SIMULATION OF BUILDING MODELS.....	107
BIBLIOGRAPHY	111
LIST OF PUBLICATIONS	133



LIST OF FIGURES

Figure 1. 1 : (a) Out-of-plane failure of Zila Panchayat building at Bhuj (Dubey, 2011) (b) Out-of-plane failure of a long unsupported masonry wall at Engineering College, Morbi (Dubey, 2011)	4
Figure 1. 2 : (a) In-plane failure of the wall of District court building at Bhuj (Dubey, 2011) (b) Diagonal cracks in short pier in Zila Panchayat building at Bhuj (Dubey, 2011).....	5
Figure 1. 3 : (a) Combined in-plane and out-of-plane failure of a two-storeyed house in Anjar (Dubey, 2011). (b) Improper placement of lintel band causing severe damage to the primary school building in Kukma (Dubey, 2011)	6
Figure 1. 4 : (a) Total collapse of Bhachau railway station building (Dubey, 2011) (b) Two storeyed houses in Bhachau collapsed because of roof failure (Dubey, 2011)	6
Figure 1. 5 : Pounding	7
Figure 2. 1 : Unreinforced specimen size details.....	14
Figure 2. 2 : Specimen reinforcement and size details	15
Figure 2. 3 : Stages of strengthening unreinforced specimen with WWM	17
Figure 2. 4 : Test set up and arrangement of instruments on control specimen and on strengthened specimen.....	17
Figure 2. 5 : URM specimen after testing.....	19
Figure 2. 6 : High strength mortar (1:4) retrofitted panel with 1 inch, 1.5 inch and 2 inch spacing WWM	20
Figure 2. 7 : Low strength mortar (1:6) retrofitted panel with 1 inch, 1.5 inch and 2 inch spacing WWM	20
Figure 2. 8 : Specimen reinforced with 1 inch spacing WWM and coarse sand mortar 1:3	21
Figure 2. 9 : Specimen reinforced with 1.5 inch spacing WWM and coarse sand mortar 1:3	22
Figure 2. 10 : Specimen reinforced with 2 inch spacing WWM and coarse sand mortar 1:3	22
Figure 2. 11 : Specimen reinforced with 1 inch spacing WWM and coarse sand mortar 1:3	22
Figure 2. 12 : Specimen reinforced with 1.5 inch spacing WWM and coarse sand mortar 1:3 ..	23
Figure 2. 13 : Specimen reinforced with 2 inch spacing WWM and coarse sand mortar 1:3	23
Figure 2. 14 : Bilinear curve	24
Figure 2. 15 : Modeling strategies for masonry: (a) Masonry sample; (b) Detailed micro modeling (discrete crack); (c) Simplified micro-modeling (discrete crack);and (d) Micro modeling (smeared crack) (Lourenco et al. 1997).....	27
Figure 2. 16 : Degeneration of continuum element into 'joint' element (Giordano 2002)	27
Figure 2. 17 : Response of concrete to uni-axial loading in tension (Abaqus 2013).....	31

Figure 2. 18 : Response of concrete to uni-axial loading in compression (Abaqus 2013).....	31
Figure 2. 19 : Compression behavior of 1:4 masonry in non-linear range.....	33
Figure 2. 20 : Compression damage of 1:4 masonry.....	34
Figure 2. 21 : Tension behavior of 1:4 masonry in non-linear range.....	34
Figure 2. 22 : Tension damage of 1:4 masonry.....	35
Figure 2. 23 : Compression behavior of 1:6 masonry non-linear range.....	35
Figure 2. 24 : Compression damage of 1:6 masonry.....	36
Figure 2. 25 : Tension behavior of 1:6 masonry in non-linear range.....	36
Figure 2. 26 : Tension damage of 1:6 masonry.....	37
Figure 2. 27 : Compression behavior of coarse sand mortar in non-linear range expressed as a function of crushing.....	37
Figure 2. 28 : Compression damage of coarse sand mortar.....	38
Figure 2. 29 : Tension behavior of coarse sand mortar in non-linear range expressed as a function of crushing.....	38
Figure 2. 30 : Tension damage of coarse sand mortar.....	38
Figure 2. 31 : Stress-strain curve for 1 inch spacing WWM.....	39
Figure 2. 32 : Stress-strain curve for 1.5 inch spacing WWM.....	39
Figure 2. 33 : Stress-strain curve for 2 inch spacing WWM.....	40
Figure 2. 34 : Diagonal compression test specimens with tie constraint used for simulating interaction between different materials.....	40
Figure 2. 35 : Linear 2-noded truss element (T3D2) used for modeling of WWM in simulation of diagonal shear test of strengthened masonry panel.....	41
Figure 2. 36 : Meshing of composite masonry-WWM- coarse sand panel.....	41
Figure 2. 37 : Modeling of loading and support condition in case of strengthened masonry panels.....	42
Figure 2. 38 : Minimum principal stress and deformation of 1:4 and 1:6 strengthened masonry panel.....	42
Figure 2. 39 : Tension damage of 1:4 strengthened masonry panel.....	42
Figure 2. 40 : Numerical and experimental shear stress vs shear strain curves for 1:4 strengthened masonry panel.....	43
Figure 2. 41 : Numerical and experimental shear stress vs shear strain curves for 1:6 strengthened masonry panel.....	43
Figure 2. 42 : Numerical and experimental shear stress vs shear strain curves for unreinforced masonry panel.....	44

Figure 3. 1 : Stages strengthening unreinforced specimen with WWM.....	50
Figure 3. 2 : Test set up	51
Figure 3. 3 : Load-deflection behavior of low strength URM sample.....	62
Figure 3. 4 : Load-deflection behavior of high strength masonry reinforced with 1 inch spacing WWM and 1:3 mortar.....	62
Figure 3. 5 : Load-deflection behavior of high strength masonry reinforced with 1.5 inch spacing WWM and 1:3 mortar.....	63
Figure 3.6: Load-deflection behavior of high strength masonry reinforced with 2 inch spacing WWM and 1:3 mortar.....	63
Figure 3. 7 : Load-deflection behavior of low strength masonry reinforced with 1 inch spacing WWM and 1:3 mortar.....	64
Figure 3. 8 : Load-deflection behavior of low strength masonry reinforced with 1.5 inch spacing WWM and 1:3 mortar.....	64
Figure 3. 9 : Load-deflection behavior of low strength masonry reinforced with 2 inch spacing WWM and 1:3 mortar.....	65
Figure 3. 10 : Solid 8-noded brick elements used for modeling of coarse sand mortar in flexure test simulation of strengthened panels	65
Figure 3. 11 : Linear 2-noded truss elements used for modeling of WWM.....	66
Figure 3. 12 : Meshing of composite masonry WWM-coarse sand panel in flexure test simulation of strengthened panels.....	66
Figure 3. 13 : Modeling of loading and support conditions in flexure test simulation of strengthened panels.....	66
Figure 3. 14 : Minimum principal stress and deformation of strengthened masonry panel (1:4 masonry)	67
Figure 3. 15 : Minimum principal stress and deformation of strengthened masonry panel (1:6 masonry)	67
Figure 3. 16 : Tension damage of strengthened panel (1:4 masonry)	67
Figure 3. 17 : Tension damage of strengthened panel (1:6 masonry)	68
Figure 3. 18 : Numerical and experimental load-deflection curves for 1:4 masonry panel	68
Figure 3. 19 : Numerical and experimental load-deflection curves for 1:6 masonry panel	69
Figure 3. 20 : Numerical and experimental load-deflection curves for 1 inch spacing 1:4 strengthened masonry panel.....	69
Figure 3. 21 : Numerical and experimental load-deflection curves for 1.5 inch spacing 1:4 strengthened masonry panel.....	70

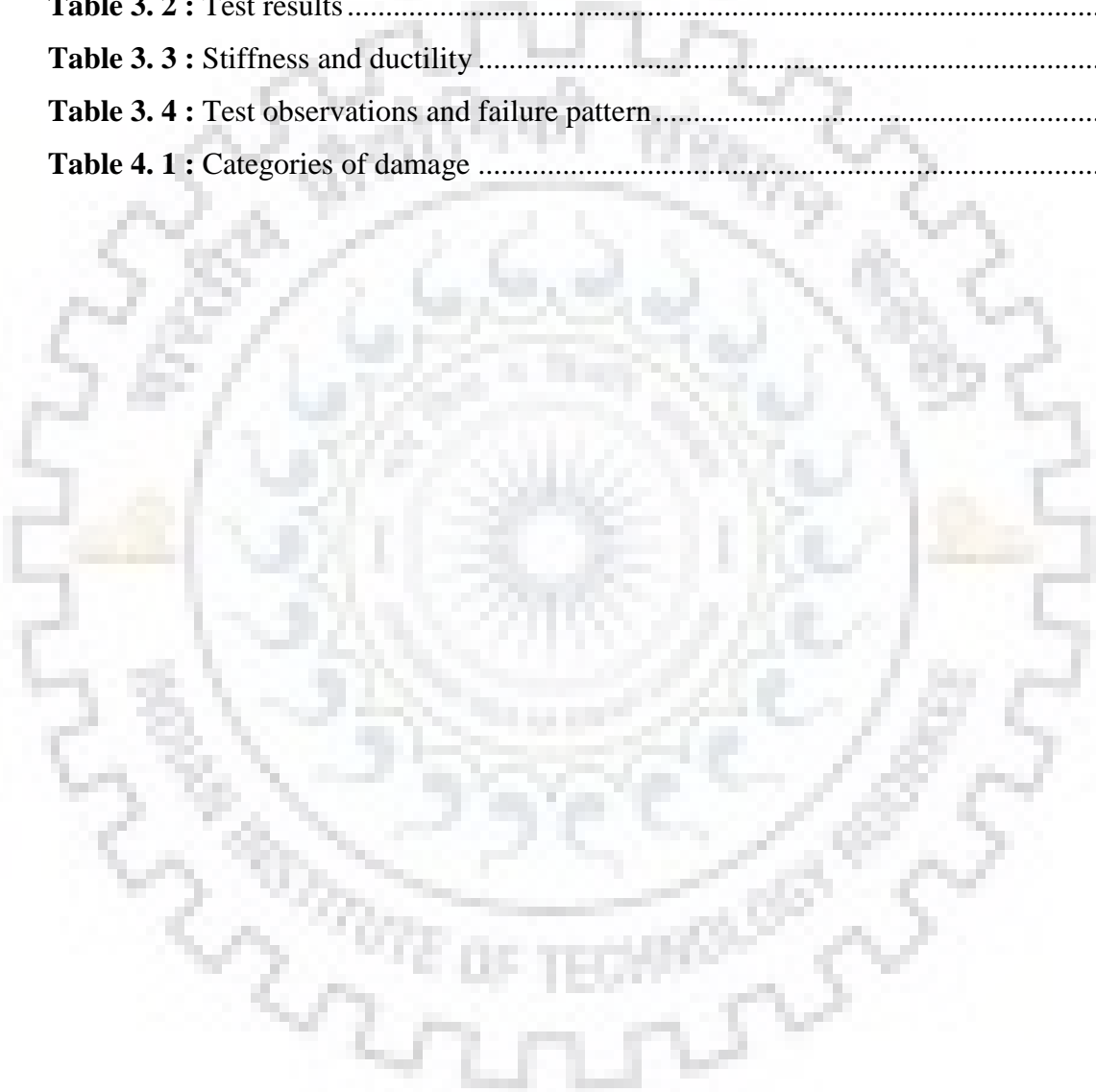
Figure 3. 22 : Numerical and experimental load-deflection curves for 2 inch spacing 1:4 strengthened masonry panel	70
Figure 3. 23 : Numerical and experimental load-deflection curves for 1 inch spacing 1:6 strengthened masonry panel	71
Figure 3. 24 : Numerical and experimental load-deflection curves for 1.5 inch spacing 1:6 strengthened masonry panel	71
Figure 3. 25 : Numerical and experimental load-deflection curves for 2 inch spacing 1:6 strengthened masonry panel	72
Figure 4. 1 : Plan	77
Figure 4. 2 : Window side section and front door section.....	77
Figure 4. 3 : Angle section welded on plate	78
Figure 4. 4 : Casting of foundation.....	78
Figure 4. 5 : Laying of bricks above foundation	78
Figure 4. 6 : URM model up to roof.....	78
Figure 4. 7 : Casting of roof slab.....	79
Figure 4. 8 : Front facing URM building model	79
Figure 4. 9 : Fully completed model N-E.....	79
Figure 4. 10 : Retrofitted window side section and door side section of RM model.....	80
Figure 4. 11 : RM model construction process	81
Figure 4. 12 : Model strengthening process	82
Figure 4. 13 : RM model after completion.....	83
Figure 4. 14 : Free vibration setup for URM model and RM model.....	83
Figure 4. 15 : Free vibration data of URM model.....	84
Figure 4. 16 : Free vibration data of RM model.....	84
Figure 4. 17 : Response spectra of input acceleration time history -DBE	87
Figure 4. 18 : Response spectra of input acceleration time history -MCE.....	87
Figure 4. 19 : (a)-(b) Input acceleration time history	87
Figure 4. 20 : Failure pattern after first shake	88
Figure 4. 21 : Acceleration at roof level in X direction of URM model - DBE.....	88
Figure 4. 22 : Failure pattern after second shake	89
Figure 4. 23: Acceleration at roof level in the X direction in URM model - MCE	90
Figure 4. 24: Acceleration at roof level in the X direction in RM model - DBE.....	90
Figure 4. 25 : Acceleration at roof level in the X direction in RM model - 2 DBE.....	91
Figure 4. 26 : Acceleration at roof level in the X direction in RM model – 3 DBE	91

Figure 4. 27 : Acceleration at roof level in the X direction in RM model – 4 DBE.....	92
Figure 4. 28 : Compression behavior of concrete in non-linear range expressed as a function of crushing.....	95
Figure 4. 29 : Compression damage of concrete	95
Figure 4. 30 : Tension behavior of concrete in non-linear range expressed as a function of crushing.....	96
Figure 4. 31 : Tension damage of concrete.....	96
Figure 4. 32 : Stress-plastic strain curve for steel.....	97
Figure 4. 33 : Finite element model of URM model with mesh.....	97
Figure 4. 34 : Finite element model of strengthened masonry model with mesh.....	98
Figure 4. 35 : Numerical acceleration at roof level in the X direction in URM model - DBE....	99
Figure 4. 36 : Numerical acceleration at roof level in the X direction in URM model - MCE...	99
Figure 4. 37 : (a)-(d) Damage in URM model after shake loading	100
Figure 4. 38 : Numerical acceleration at roof level in the X direction in RM model - DBE	100
Figure 4. 39 : Numerical acceleration at roof level in the X direction in RM model - 2 DBE .	101
Figure 4. 40 : Numerical acceleration at roof level in the X direction in RM model – 3 DBE.	101
Figure 4. 41 : Numerical acceleration at roof level in the X direction in RM model – 4 DBE.	101
Figure 4. 42 : No damage in strengthened model after shake loading	102



LIST OF TABLES

Table 2. 1 : Mechanical properties of masonry.....	14
Table 2. 2 : Mechanical properties of WWM reinforcement.....	14
Table 2. 3 : Specimen details	15
Table 2. 4 : Experimental results of shear-compression tests.....	24
Table 3. 1 : Specimen details	50
Table 3. 2 : Test results	54
Table 3. 3 : Stiffness and ductility	55
Table 3. 4 : Test observations and failure pattern.....	56
Table 4. 1 : Categories of damage	92





LIST OF ABBREVIATIONS

ACI	American Concrete Institute
ADC	Analog to Digital Converters
ASTM	American Society for Testing and Materials
C3D8	Solid 8-Noded Linear Hexahedral Elements
CDP	Concrete Damaged Plasticity
DAC	Digital to Analog Converter
DBE	Design Basis Earthquake
DEM	Distinct Element Method
ECC	Engineered Cementitious Composites
EFM	Equivalent Frame Method
FEM	Finite Element Method
FRP	Fibre Reinforced Polymer
GFRP	Glass Fibre Reinforced Polymer
IS	Indian Standard
LVDT	Linear Variable Displacement Transducers
MCE	Maximum Considered Earthquake
MSJC	Masonry Standard Joint Committee
NBCC	National Building Code of Canada
NSM	Near Surface Mounting
PAM	Pier Analysis Method
PGA	Peak Ground Acceleration
RCC	Reinforced Cement Concrete
RDSS	Reinforced Diagonal Shear Specimen
RM	Reinforced Masonry
RMFST	Reinforced Masonry Flexural Specimen
SRG	Steel Reinforced Grout
T3D2	2-Noded Linear Truss Element
TMS	The Masonry Society
UDSS	Unreinforced Diagonal Shear Specimen
URM	Unreinforced Masonry
URMFST	Unreinforced Masonry Flexural Specimen
UTM	Universal Testing Machine

WWM Welded Wire Mesh
ZPA Zero Period Acceleration



LIST OF NOTATIONS

Symbol	Explanation
γ	Shear strain
μ	Ductility
ρ_h	Horizontal reinforcement ratio
τ_{max}	Maximum shear stress
ρ_v	Vertical reinforcement ratio
$\dot{\epsilon}^{el}$	Elastic strain rate
$\dot{\epsilon}^{pl}$	Plastic strain rate
$\bar{\sigma}^{def}$	Effective stress
D_0^{el}	Initial undamaged elastic stiffness
D^{el}	Degraded elastic stiffness
$\dot{\epsilon}$	Strain rate total
$\dot{\epsilon}^{pl}$	Plastic strain rate
d_u	Ultimate drift corresponding to 0.8τ
d_y	Yield drift
f_b	Compressive strength of brick
f_c	Compressive strength of mortar
f_m	Compressive strength of masonry
g	Gauge length
H	Height of the panel
L	Length of the panel
P	Diagonal force measured experimentally
p_{max}	Maximum applied load
t	Thickness of the panel
ΔH	Diagonal elongation measured perpendicular to the axis of applied force
ΔV	Diagonal shortening along the axis of applied force
τ	Shear stress
d	Scalar stiffness degradation variable
ϵ	Total strain
σ	Effective stress
$\bar{\sigma}$	Effective cohesive stress

$\dot{\epsilon}_t^{pl}$	Tensile plastic strain rate
$\dot{\epsilon}_c^{pl}$	Compressive plastic strain rate
σ_t	Uniaxial tensile load
$\tilde{\epsilon}_t^{pl}$	Tensile plastic strain rate
$\dot{\tilde{\epsilon}}_t^{pl}$	Equivalent tensile plastic strain rate
θ	Temperature
f_i	Another predefined field variable
σ_c	Uniaxial compressive load
d_t	Tension damage variable
d_c	Compression damage variable
$\bar{\sigma}_t$	Effective uniaxial tensile cohesive stress
$\bar{\sigma}_c$	Effective uniaxial compressive cohesive stress
f_t	Tensile strength
E_t	Elastic modulus of tension
K_r	Rate of tension softening
ϵ_V	Strain corresponding to zero stress
P_y	Yield load
P_u	Ultimate load
μ_Δ	Deflection ductility
μ_E	Energy ductility
Δ_u	Mid span deflection at ultimate load
Δ_y	Mid span deflection at tension steel yielding
E_u	Area under the load-deflection diagram at ultimate load
E_y	Area under the load-deflection diagram up to yielding of tension steel
P_{umax}	Ultimate maximum load
R	Modulus of rupture
R/R_o	Ratio of modulus of rupture of strengthened specimen to that of unreinforced specimen
E_c	Modulus of elasticity of concrete
ϵ_c	Total compressive strain
R_E	Modular ratio
R_ϵ	Stress ratio
R_σ	Stain ratio

f'_c	Ultimate yield stress of concrete
ϵ_{cr}	Cracking strain
f_{cr}	Flexural strength of concrete
C_1	Modification factor to relate expected maximum inelastic displacements to displacements calculated for linear elastic response
C_2	Modification factor to represent the effect of pinched hysteresis shape, cyclic stiffness degradation, and strength deterioration on maximum displacement response
E_0	Initial (undamaged) elastic stiffness of material
ϵ_0	Strain corresponding to f'_c





CHAPTER – 1

INTRODUCTION

1.1 GENERAL

Masonry structures were built during ancient times when no appropriate theory and good engineering knowledge were available. People usually built their houses according to the traditions and experience in vogue at that time. So, many buildings which still exist do not satisfy the present codal guidelines for earthquake resistant construction. The recent worldwide earthquakes have also made the people more conscious about the safety of life and property.

The mechanical behaviour of masonry is complex and its form, type of units and quality of mortar varies world-wide. This variation makes the design and retrofitting of masonry buildings a more challenging task. Despite wide spread use of masonry world-wide, a thorough understanding of behavior of masonry is still lacking and it is considered as a non-engineered material. Recently, there has been renewed research interest, particularly in estimating the seismic vulnerability of masonry buildings and a number of projects have been undertaken worldwide on estimating seismic vulnerability/ response of masonry structures. As a result, masonry is gradually being recognized as a reliable construction material even for seismic areas.

The strengthening of existing masonry structures in earthquake prone areas seems to be a serious issue to be dealt with. Many strengthening techniques are being used in practice while many more are being developed. A most effective economical easy to use technique is still a target for many researchers. Strengthening using fibre reinforced polymers (FRP), ferrocement, bamboo, rubber tyres, twisted steel bars, steel reinforcement, etc. have successively been used in practice, but their behaviour in in-plane and out-of-plane action are yet to be explored in detail.

In this study, an attempt has been made to study the in-plane and out-of-plane behaviour of URM (Unreinforced Masonry) strengthened with WWM (Welded Wire Mesh) with various spacing and coarse sand (which is proposed in IS 13935: 2009), both numerically and experimentally. The behavior is studied in terms of damage pattern, strength, load carrying capacity and ductility. The results of URM and RM (Reinforced Masonry) were compared to understand the effectiveness of the retrofitting technique used. The dynamic behavior of URM and RM was also studied, both numerically and experimentally.

Two types of modeling approaches, namely micro-modeling and macro-modeling, are being used to simulate the seismic behavior of masonry buildings. Finite Element Method (FEM) and Distinct Element Method (DEM) are the most common techniques used for the former approach, whereas Pier Analysis Method (PAM) and Equivalent Frame Method (EFM) are used in macro modeling. The micro modeling approach is computationally demanding and has the potential of simulating the detailed behavior and failure pattern. Whereas, the macro modeling approach is more suitable to simulate the global behavior.

The research effort has been made to develop mathematical models for different failure modes of masonry subjected to seismic loads. Magenes et al. (1997), Abrams et al. (1997, 2001), Priestly et al. (2007) and several other researchers have studied the behavior of masonry based on the numerical and experimental evaluation. Based on these studies the typical modes of failure in masonry piers are rocking (flexure), diagonal shear, and sliding shear. Rocking has been considered as a more desirable mode of failure as it has large deformation capacity without losing much strength and energy dissipation capacity in successive cycles. The sliding mode of failure also has good deformation capacity. In this mode of failure, frictional forces continue to resist lateral forces after the formation of cracks, if the vertical load is present. On the other hand, the diagonal shear mode is not a desirable mode of failure, since very little ductility is experienced in this mode of failure.

More than half of the Indian houses are made up of unreinforced masonry and their performance in the past earthquakes (Bihar-Nepal, 1988; Uttarkashi, 1991; Killari, 1993; Jabalpur, 1997; Chamoli, 1999; Bhuj, 2001; Sumatra, 2004; Kashmir, 2005; Sikkim, 2006 and 2011; Nepal-India, 2015) have created a necessity to review the capability of existing structures for future earthquakes (Jagadish et al. (2003), Hashmi et al. (2008), Jain (2016)), and to find a suitable strengthening technique to strengthen or to retrofit masonry structures. Due to low cost and less skilled labour, masonry buildings are still very much popular in use in many countries.

Strengthening of existing masonry structures in earthquake prone areas seems to be a serious issue to be dealt with. So far various strengthening techniques are being used in practice and more new methodologies are being developed. Strengthening of masonry buildings using fiber reinforced polymers (FRP), ferrocement, bamboo, twisted steel bars, steel reinforcement etc. have successively been used in practice. There is a number of research carried out on strengthening/ retrofitting of masonry structures both in India and abroad. Strengthening of masonry using FRP, polymeric meshes, textile reinforcement and reinforcing steel wires have been reported by many researchers including D'Ambrisi et al. (2013), Mohammad, et al. (2012),

Papanicolaou et al. (2011), El Gawady et al. (2004), Kiang et al. (2004), Ayman et al. (2007), Khaled et al. (2010), Papanicolaou et al. (2008), Saleem et al. (2016) etc. Application of ferrocement on masonry structures to improve the behavior of URM has been commonly used for retrofitting existing URM buildings in India and South Asian countries as recommended by IS 13935: 2009. The behavior of masonry building after retrofitting using ferrocement is not clearly understood and it requires extensive investigation. In the present study, experimental and numerical investigations have been performed on both URM and RM specimens to quantify enhancement in strength and ductility. The efficiency of this technique has been demonstrated by conducting shake table tests on half-scale models.

1.2 MERITS AND LIMITATIONS OF BRICK MASONRY

Brick masonry can be classified as a homogenous material, brittle in nature, bonded together with cement mortar. Due to the layered configuration of brick masonry, it can accommodate minor disturbances which may result due to differential settlement of foundation etc. It has a good resistance to weathering and is highly durable. It can be easily built with available semi-skilled workers and the materials are available at a relatively low cost. Repairing of brick masonry can be easily done by replacing the damaged portions with new bricks. Masonry behaves fairly well under normal gravity loading. But in the event of an extreme loading like an earthquake, brick masonry attains partial to total collapse resulting in large scale loss of lives and property. The failure may be attributed to the following reasons:

- i. Due to its brittle nature and high self-weight, masonry undergoes sudden brittle failure without much prior warning and hence the occupants do not have enough time to run to safety.
- ii. Bricks available in the developing countries have a varying crushing strength depending upon the quality of locally available brick earth/ soil.
- iii. The failure of masonry is mainly against horizontal forces resulting in flexure due to out-of-plane bending and shear due to in-plane bending. As masonry cannot resist tensile stresses induced by these forces, there will be a sudden collapse. Cracks develop along the bed joint in flexure due to out-of-plane forces acting normal to the wall. Diagonal cracks occur due to in-plane forces acting in the plane of the wall.

The types of failures observed in masonry structures globally during the past earthquakes have been summarized in the following section.

1.3 COMMON FAILURE MECHANISM OF UNREINFORCED MASONRY BUILDING

1.3.1 Out-of-plane Failure

The structural wall perpendicular to seismic motion is subjected to out-of-plane bending which results in development of vertical cracks at the corner and in the middle of the wall (Figure 1.1). Unreinforced masonry buildings are most vulnerable to out-of-plane flexural failure. The causes of the out-of-plane failure of the wall are the inadequate anchorage of the masonry wall into the roof diaphragm and limited tensile strength of the masonry and mortar. The resulting flexural stress apparently exceeds the tensile strength of the masonry leading to its rupture followed by collapse.

Out-of-plane wall movement is characterized by the partial collapse of the exterior wall, wythe separation or peeling of the outer wythe or veneer units, and crack formation at lintel and top of slender piers near the opening (Figure 1.1). These types of failures are almost non-existent in the lower storey.

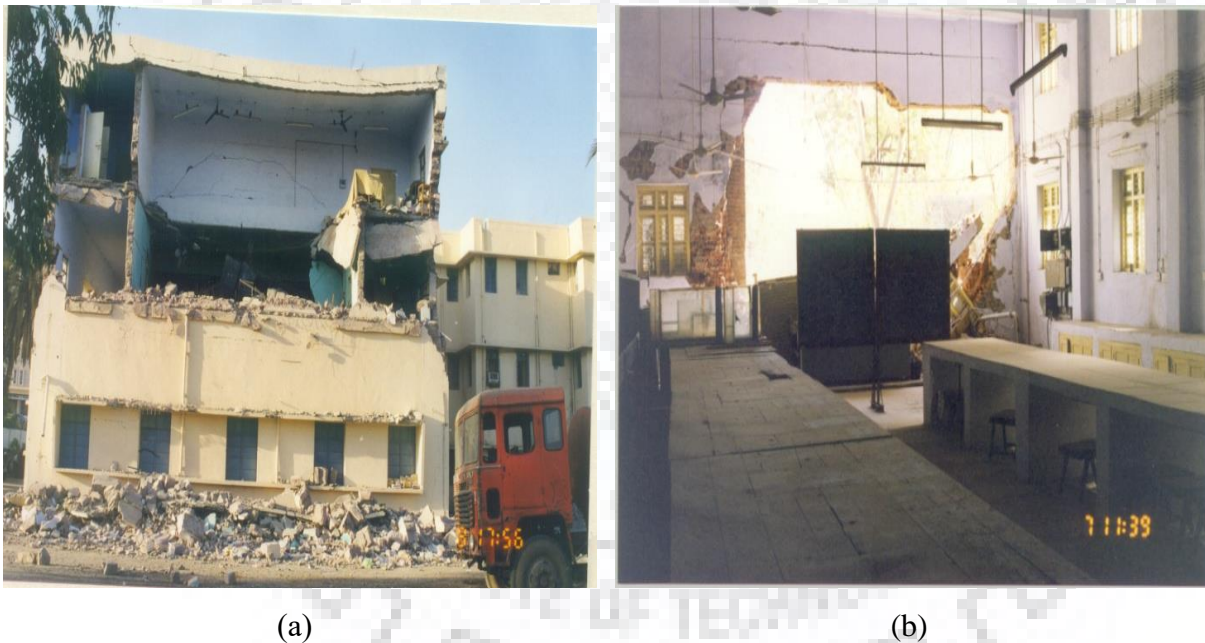


Figure 1. 1 : (a) Out-of-plane failure of Zila Panchayat building at Bhuj (Dubey, 2011) (b) Out-of-plane failure of a long unsupported masonry wall at Engineering College, Morbi (Dubey, 2011)

1.3.2 In-plane Failure

The structural wall parallel to seismic motion is subjected to in-plane bending which results in development of horizontal and diagonal cracks in the wall. Excessive bending or shear may produce in-plane failure of the walls as illustrated in Figure 1.2. For unreinforced masonry

walls, shear in-plane failure is more common, as expressed by double-diagonal (X) shear cracking, Figure 1.2. This cracking pattern is common in cyclic loading. The cracks indicate that the plane of principal tensile stress in the walls remains incapable of withstanding repeated load reversals thus leading to total collapse. As the ground motion takes place for a short duration the walls are subjected to only one or two significant loading reversals and do not collapse totally. By the time the shear cracks become unduly severe, the gravity load carrying capacity of the wall is not jeopardized.

Diagonal tension “X” cracks occurs mainly in short piers, and rocking (cracks top and bottom) in slender piers. These cracks were worst at the lower storey as depicted in Figure 1.2 during Bhuj earthquake.



(a)



(b)

Figure 1. 2 : (a) In-plane failure of the wall of District court building at Bhuj (Dubey, 2011) (b) Diagonal cracks in short pier in Zila Panchayat building at Bhuj (Dubey, 2011).

1.3.3 Combined In-plane and Out-of-plane Failure

Earthquake forces are bi-directional in nature, but each URM element behaves independently in both in-plane and out-of-plane direction. As in-plane shear cracking occurs, some triangular wedges are produced whose out-of-plane strength is significantly weaker than that of the original un-cracked wall panel. Pounding against adjacent structure can also accelerate this combined failure mode (Figure 1.3).



(a)



(b)

Figure 1.3 : (a) Combined in-plane and out-of-plane failure of a two-storeyed house in Anjar (Dubey, 2011). (b) Improper placement of lintel band causing severe damage to the primary school building in Kukma (Dubey, 2011)

1.3.4 Diaphragm Failure

The failure of the diaphragm due to seismic excitations is a rare phenomenon. Damage to the diaphragm never impairs its gravity load carrying capacity. Lack of tension anchorage produces a non-bending cantilever action of the entire wall about its base resulting from the pushing of the diaphragm, against the wall. The in-plane rotation of the diaphragm's end induces damage at the corner of the wall. The absence of a good shear transfer between diaphragms and reaction wall also accounts for damage at the corners of the walls. The diaphragm failure is illustrated in Figure 1.4.



(a)



(b)

Figure 1.4 : (a) Total collapse of Bhachau railway station building (Dubey, 2011) (b) Two storeyed houses in Bhachau collapsed because of roof failure (Dubey, 2011)

1.3.5 Pounding

When adjacent roof levels of two buildings and vertical brickwork faces flush with one another, the pounding action causes structural distress due to out-of-plane vibrations (Figure 1.5).



Figure 1. 5 : Pounding

1.3.6 Failure of Connection & Non-structural Components

Seismic inertia forces originate in all elements of a building and are delivered through structural connections to horizontal diaphragms. The diaphragms distribute these forces to vertical elements which in turn transfers these forces to the foundation. An adequate connection between the diaphragm and the vertical elements is essential for the satisfactory performance of any structure. The connection must be capable of transferring the in-plane shear stress from the diaphragm to the vertical elements and must be capable of providing support to out-of-plane forces on the vertical elements.

The non-structural components in masonry buildings may include parapet walls, partition walls, water tanks, canopies, projections, staircase etc. These non-structural elements behave, if unrestrained, as cantilevers extending beyond the roof line located at the top of the building. These components may be subjected to greater amplification of the ground motion, and hence prone to failure.

1.4 CODAL RECOMMENDATIONS/ GUIDELINES

In the United States, after the 1933 Long Beach earthquake, use of reinforced masonry was promoted and ACI published a code on concrete masonry in 1979 (ACI 531). New Zealand also developed codal provisions for earthquake resistant design of masonry (NZS 4230 1990). This code was later revised in 2004 entitled “Design of Reinforced Concrete Masonry Structures” (NZS 4230 2004). In 1997, FEMA 273 outlined the procedure for performance evaluation of buildings including masonry buildings. The guidelines have been further improved in FEMA 356 (2000) and ASCE-41 (2007). The European committee for standardization has developed Eurocode 6 (1996) for the design of masonry buildings and Eurocode 8 (2004) for the design of

structures for earthquake resistance. Recently, The Masonry Society (TMS) and American Concrete Institute (ACI) have developed a new code called Masonry Standard Joint Committee (MSJC, 2013). This code deals with design and retrofit aspects of masonry buildings. However, the emphasis in this code has been on reinforced masonry. The National Building Code of Canada (NBCC, 2010) and the masonry design standard CSA S304.1-04 have been practiced in Canada for seismic design provisions of unreinforced and reinforced masonry structures.

The Indian standard on masonry design, IS 1905 was first published in 1960 and was revised in 1969 and 1980. The recent revision was made in 1987 and is supported by a separate handbook, SP 20: 1991. IS 1905 deals with the properties and specifications of masonry and constituent materials and provides guidelines for the design of URM walls and columns under different actions. The Earthquake Resistant Design and Construction of Buildings - Code of Practice, IS 4326: 2013 deals with standard provisions for the seismic safety of load bearing and non-load bearing URM walls. Indian standard IS 13828: 1993 provides Guidelines for Improving Earthquake Resistance of Low Strength Masonry Buildings and IS 13935: 2009 has exclusive provisions for Seismic Evaluation Repair and Strengthening of Masonry Buildings. This code presents various techniques and materials for seismic strengthening of masonry.

1.5 OBJECTIVES

The present study has been conducted with the following objectives

1. To study the in-plane and out-of-plane behavior of URM and RM panels experimentally and to simulate the results numerically.
2. To investigate the effectiveness of various sizes of welded wire mesh, used to strengthen the unreinforced masonry panels, in both in-plane and out-of-plane action.
3. To study the behavior of URM and RM building models tested on the shake table subjected to artificial time history compatible with IS code response spectra for seismic zone V on hard soil.
4. To carry out a numerical study for URM and RM building models and validate the experimental results obtained from shake table test.

1.6 SCOPE AND METHODOLOGY

The main aim of the proposed research is to study the in-plane and out-of-plane behavior of URM and RM model, the effectiveness of strengthening technique and development of numerical models using Abaqus/CAE to simulate the seismic behavior of URM and RM. As a

first step, masonry panels have been constructed in a conventional manner and these were tested to obtain the properties required to develop a non-linear material model for FE modeling. Non-linear FE analyses using Concrete Damaged Plasticity (CDP) constitutive model have been performed to simulate the in-plane and out-of-plane behavior of masonry which were tested experimentally. Though the CDP model was developed for simulating the behavior of concrete, it has been demonstrated by many researchers that CDP model could be applicable to masonry and other brittle materials as well. The URM specimens were strengthened using welded wire mesh (1 inch, 1.5 inch, and 2 inch spacing) and coarse sand mortar as per IS 13935: 2009. Experimental and numerical validation of RM panels strengthened with WWM of various spacing and coarse sand mortar has also been carried out to study the difference in behavior of URM and RM panels.

The effectiveness of the proposed retrofitting technique has also been studied by performing dynamic tests on two half-scale masonry models, one URM and other RM model strengthened with proposed retrofitting method. The tests were conducted on the shake table testing facility. The models were given artificial ground motion compatible with IS 1893 (Part 1): 2002 response spectrum in seismic zone V on hard soil.

1.7 ORGANIZATION OF THESIS

The thesis is organized into the following chapters

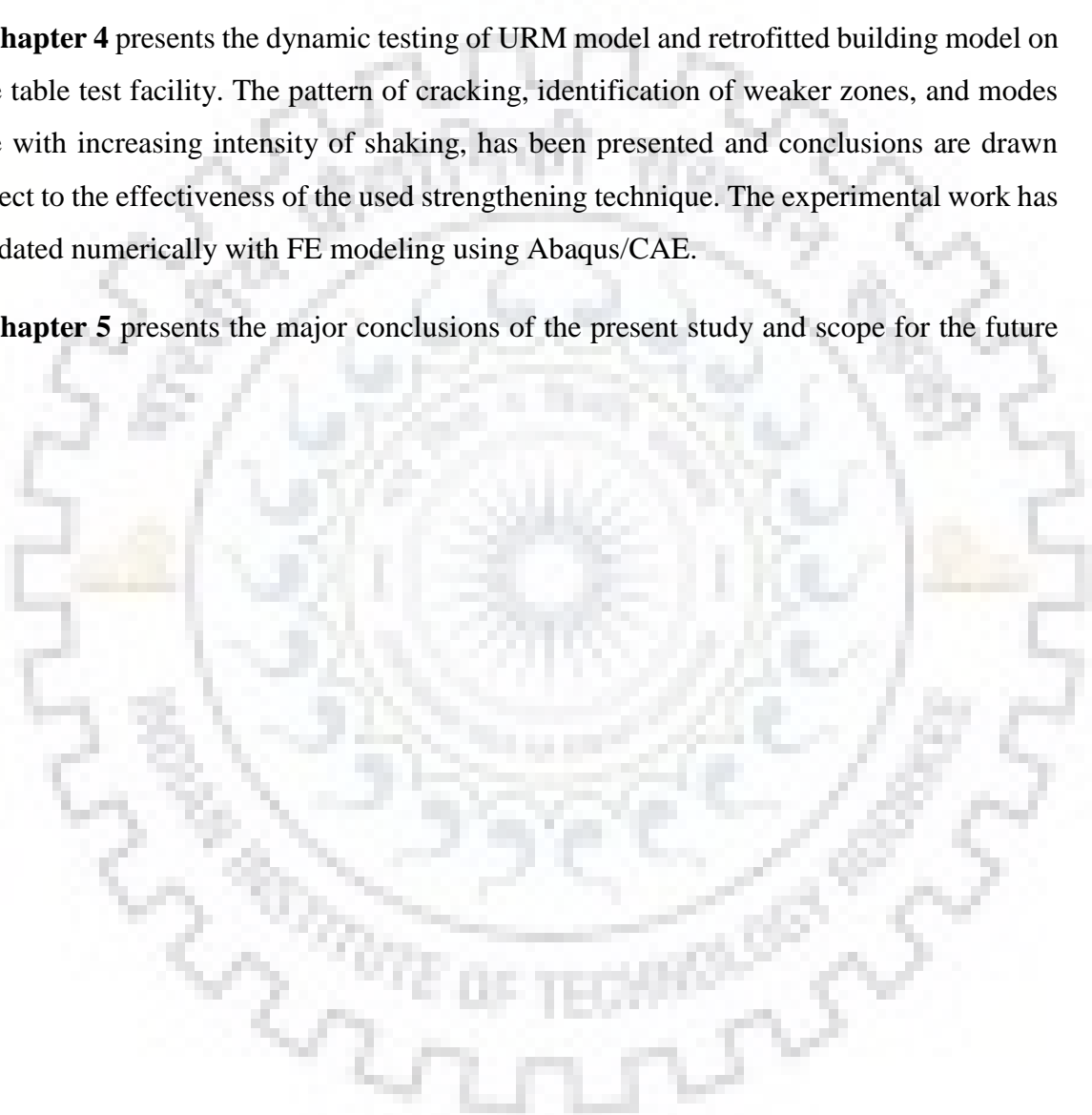
Chapter 1 briefly describes the seismic behavior of URM buildings with different failure modes observed during past earthquakes. A brief overview of different national codes on masonry buildings is also presented. The chapter introduces different techniques and associated challenges in numerical modeling of masonry structures. This chapter also describes the need, objectives, scope and methodology of the present study.

Chapter 2 reviews the various strengthening technique used to improve the in-plane behavior of URM wall and modeling of masonry buildings, advantage and disadvantages of different modeling techniques for simulating the global seismic response of URM buildings. The URM and RM specimens strengthened using WWM and 1:3 coarse sand mortar, has been tested experimentally as per ASTM E519/ E519M-10 to investigate the effect of strengthening on the in-plane behavior of masonry in terms of failure mode, strength and ductility. The tests were simulated using FE modeling and compared with the experimental test results.

Chapter 3 reviews the various strengthening technique used to enhance the out-of-plane behavior of URM wall. The experimental study on URM and RM specimens strengthened using WWM and 1:3 coarse sand mortar has been carried out to investigate the effectiveness of strengthening on the out-of-plane behavior of masonry in terms of failure mode, strength and ductility. The numerical simulation was carried out using FE modeling and the results were compared with the experimental findings.

Chapter 4 presents the dynamic testing of URM model and retrofitted building model on the shake table test facility. The pattern of cracking, identification of weaker zones, and modes of failure with increasing intensity of shaking, has been presented and conclusions are drawn with respect to the effectiveness of the used strengthening technique. The experimental work has been validated numerically with FE modeling using Abaqus/CAE.

Chapter 5 presents the major conclusions of the present study and scope for the future work.



CHAPTER – 2

IN-PLANE BEHAVIOR OF UNREINFORCED AND REINFORCED MASONRY PANELS

2.1 INTRODUCTION

Unreinforced masonry (URM) structures are the most common and oldest form of building construction technique existing in the world. In most of the developed and developing countries masonry is still being widely used in practice due to its low cost and easy construction technique. URM constructions are unquestionably recognized as most vulnerable to earthquake forces. Most of the existing old URM buildings tend to pose greater risk during an earthquake, as compared to earthquake resistant buildings, because of their inability to dissipate energy during an earthquake. In most cases, masonry structures are constructed without any consideration for seismic loading resulting in huge loss of life as experienced in the past earthquakes in the last three decades (Uttarkashi 1991, Killari 1993, Bhuj 2001 and Kashmir 2005; Sikkim, 2006 and 2011; Nepal-India, 2015). During an earthquake, buildings experience seismic loading both in-plane and out-of-plane. However, their relative magnitude depends on the type of diaphragm i.e., how the wall is connected to the roof.

The recent earthquakes have created a necessity to review the capability of existing structures during an earthquake, and to find a suitable strengthening technique to strengthen a newly constructed masonry structure or to retrofit an existing old structure. Various rehabilitation and retrofitting techniques are available to enhance the seismic performance of URM buildings. These techniques include the application of fiber reinforced polymers (FRP), ferrocement overlay (surface coating), shotcrete overlay, centre core technique, grout injection, application of steel elements, bed joint reinforcement, post-tensioning etc. A review of various rehabilitation and retrofitting methods and their advantages and disadvantages may be found in the literature as reported by many researchers (D'Ambrisi et al. (2013), Ashraf et al. (2012), Papanicolaou et al. (2011), Hamid et al. (1998), Kadam et al. (2015), Lourenço et al. (2000), El Gawady et al. (2004)). These well-established techniques need to be verified for local materials and building system commonly used in practice. Among all available options, ferrocement overlay is a technique which is easy in application, rapid in construction and very low in cost, especially in developing countries with no heavy machinery and high-level skilled workers. In this technique,

steel welded wire mesh (WWM) is connected or anchored to the surface of masonry through bolts/ screws/ steel rods subsequently covered with plaster coating.

Strengthening of masonry using FRP, steel cord, steel grid, polymer grid etc. has been widely in practice. In this study, an attempt has been made to strengthen URM using WWM and 1:3 coarse sand mortar. Ferrocement is a commonly used strengthening system. This is a cementitious composite layer laminated with metallic mesh and has advantages such as a high tensile strength-to-weight ratio and superior cracking behavior (Tan et al. (2004), Mosallam et al. (2007), Kadam et al. (2015), Bajpai et al. (2003), Bencardino et al. (2004), Galal et al. (2010), Papanicolaou et al. (2008)).

Kadam et al. (2015) has previously used ferrocement as a strengthening material in URM using different reinforcement percentage and various anchoring technique and found that WWM along with micro concrete increases the in-plane shear capacity of masonry effectively. Prawel et al. (1988) showed that ferrocement overlays increased the efficiency of diagonal tensile strength, stiffness and deformation capacity of masonry panels. Kabir et al. (1999) have studied the strength enhancement in brick masonry columns by encasing with precast ferrocement. Based on their investigations, the cracking and failure stresses of the column with precast ferrocement jackets have substantially been increased compared to control specimens while exhibiting much ductile response. Ferrocement is found to be an effective system in the out-of-plane strengthening of unreinforced two-way masonry walls.

Very few studies are available in the strengthening of masonry with ferrocement, but a considerable number of researches have been carried out in reinforced concrete structures with ferrocement. It is evident from the literature that ferrocement is an effective material for strengthening both masonry and concrete (Prawel et al. (1988), Kabir et al. (1999), Ong et al. (1992)). It is found to be most effective and economical, easy to use and like FRP reinforcement it does not require the application of epoxy.

External application of overlays, such as ECC (Engineered Cementitious Composites) (Lin et al. 2010) and steel reinforced grout (Borri et al. 2011) has also been explored as a retrofit solution for masonry walls. ECC is a type of strain-hardening cement-synthetic fibre composite that is directly sprayed onto URM walls. Strain hardening property is imparted in ECC through the formation of micro-cracks. The study of Lin et al. (2010) showed that use of ECC is effective in resisting in-plane stresses. In steel reinforced grout (SRG), high strength steel cords are embedded in a cementitious matrix to form a composite. The technique was effective in

enhancing the strength of masonry wallettes but it needs further research about the size of steel cords and bond of cords with the cementitious matrix and masonry.

Textile reinforced mortar is another promising technique for masonry retrofit which combines the advantages of both conventional and modern techniques (Papanicolaou et al. 2011). In this technique, textile grid of fibres is bonded to the surface of masonry using specially developed mortars. The grid form of the fibres has similarity with WWM and results in good bond with the masonry. The technique is currently under development to identify the optimum amount of fibres and composition of mortar.

2.2 RESEARCH SIGNIFICANCE

In the present study, experimental investigation of the in-plane behavior of masonry strengthened with various sizes of WWM available in local market and various mortar ratios has been studied as per the seismic retrofit technique presented in Indian standard IS 13935: 2009. The in-plane behavior of both URM and strengthened masonry was studied based on diagonal compression test according to ASTM E519/ E519M-10. The relative increase in strength, ductility, and stiffness has been estimated.

2.3 EXPERIMENTAL PROGRAM

2.3.1 Material Properties

Tests were performed to characterize the mechanical properties of the material used in this investigation. Two different type of mortar mixes H2 (1:4) and M2 (1:6) widely used in practice in the country has been chosen for this study. As per IS 4326: 2013, M2 mortar mix is permitted only for building category C in seismic zone II and III. This mortar is not permitted for use in seismic zone IV and V. However, use of this mortar is prevalent even in higher seismic zones. The test samples were constructed using brick size of 230 mm x 110 mm x 70 mm. The masonry test samples of set 1, 3, 4, 5 was constructed using 10 mm thick 1:4 mortar and sample set 2, 6, 7, 8 was constructed using 1:6 mortar as per conventional site construction practice with the help of a local mason. English bond with alternate header and stretcher was used to construct the masonry samples. Mechanical properties of the materials were studied as per ASTM standards. Compressive strength test of mortar cube was carried out as per ASTM C109/ C109M. The compressive strength of brick was tested in accordance with ASTM C67-11 and compressive strength of masonry was tested in accordance with ASTM C1314-11. The tensile strength of WWM was studied in accordance with ASTM A370-11. The test results are represented in Tables 2.1 and 2.2.

Table 2.1 : Mechanical properties of masonry

Mortar mix	f_b [MPa]	f_c [MPa]	f_m [MPa]
1:4	10	2.50	3.95
1:6	10	1.45	2.17

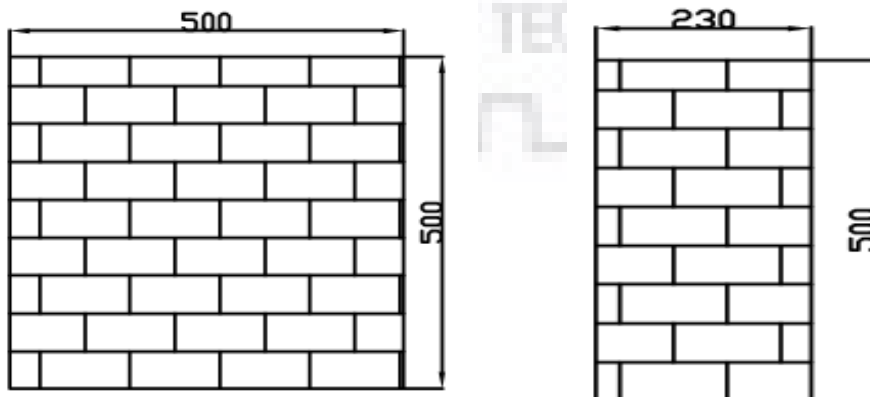
f_b = Compressive strength of brick; f_c = Compressive strength of mortar; f_m = Compressive strength of masonry

Table 2.2 : Mechanical properties of WWM reinforcement

WWM spacing	Diameter of wire (mm)	Elastic modulus [MPa]	Ultimate deformation [%]	Ultimate tensile strength [MPa]
1 inch	2.07	14905	14.76	873
1.5 inch	2.45	26750	7.89	936
2 inch	3.20	32790	8.50	1005

2.3.2 Mixing, Casting and Curing of Masonry Specimens

The in-plane shear behavior of URM panels of two types of mortar mixes (1:4, 1:6) and masonry panels strengthened with WWM (1 inch, 1.5 inch, 2 inch spacing) and 1:3 coarse sand mortar. The descriptions of test samples are given in Table 2.1. Eight unreinforced specimens and twenty four reinforced specimens were tested under in-plane shear. Different cement sand mortar ratio (1:4; 1:6) which is most commonly used in India has been chosen for this study. WWM of various sizes 1 inch, 1.5 inch, 2 inch spacing which is commonly available in the local market was chosen as reinforcement to strengthen URM. The WWM was reinforced in-between rich 1:3 coarse sand mortar. Anchorage was provided between WWM and the masonry with the help of 4 mm diameter mild steel rod as per IS 13935: 2009 recommendations.

**Figure 2.1 : Unreinforced specimen size details**

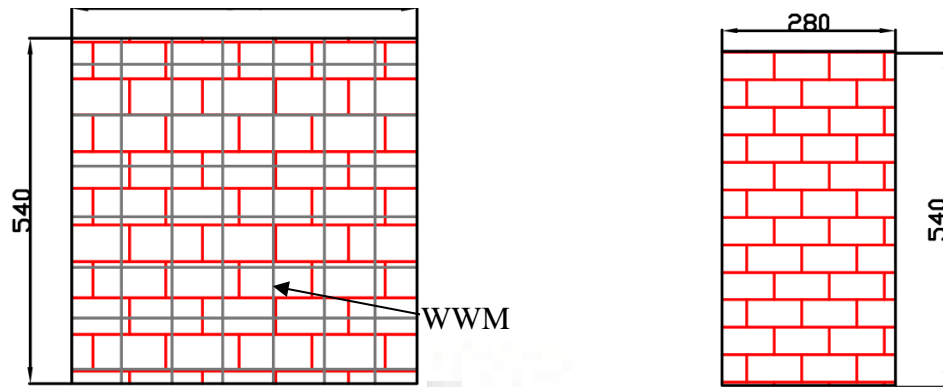


Figure 2. 2 : Specimen reinforcement and size details

The experimental program consisted of 8 sets of specimens out of which two sets were URM and 6 sets were of reinforced masonry specimen. All specimens were of two wythe thickness, as in practice all load bearing walls are constructed with two wythe thickness. The specimen size and details are given in Figures 2.1 and 2.2. All the test samples were constructed and cured as per site condition. The test samples to be strengthened were strengthened after 28 days of curing period.

Table 2. 3 : Specimen details

Set	Specimen	Mortar ratio	Strengthening
Set-1	UDSS-1	1:4	URM panel
	UDSS-2		
	UDSS-3		
Set-2	UDSS-4	1:6	URM panel
	UDSS-5		
	UDSS-6		
Set-3	RDSS-7	1:4	URM panel strengthened with 1 inch spacing WWM and 1:3 coarse sand mortar
	RDSS-8		
	RDSS-9		
Set-4	RDSS-10	1:4	URM panel strengthened with 1.5 inch spacing WWM and 1:3 coarse sand mortar
	RDSS-11		
	RDSS-12		
Set-5	RDSS-13	1:4	URM panel strengthened with 2 inch spacing WWM and 1:3 coarse sand mortar
	RDSS-14		
	RDSS-15		
Set-6	RDSS-16	1:6	URM panel strengthened with 1 inch spacing WWM and 1:3 coarse sand mortar
	RDSS-17		
	RDSS-18		
Set-7	RDSS-19	1:6	URM panel strengthened with 1.5 inch spacing WWM and 1:3 coarse sand mortar
	RDSS-20		
	RDSS-21		
Set-8	RDSS-22	1:6	URM panel strengthened with 2 inch spacing WWM and 1:3 coarse sand mortar
	RDSS-23		
	RDSS-24		

2.4 STRENGTHENING PROCEDURE

The test samples were strengthened as per IS 13935: 2009. Drill holes of 8 mm diameter were bored at an interval of 300 mm on the test samples for inserting 4 mm diameter mild steel rod for anchorage in the later stage of strengthening. These 4 mm rods pass through the bored holes and transfer the shear at the WWM masonry interface through dowel action. The samples to be strengthened were initially watered and cleaned with the help of a steel wire brush to remove dirt if any. Then a layer of cement grout slurry was applied with the help of a paint brush to provide better bond between the mortar and the masonry surface. Care was taken to close the drill holes with the help of wooden or steel rods to avoid its blockage during application of mortar. A layer of 10 mm thick 1:3 coarse sand mortar was applied above the cement slurry surface to level the uneven masonry surface as well as to provide better grip for the WWM and second layer of mortar. The mortar surface was roughened with the help of a steel wire brush ensuring better grip. The WWM was placed and anchored with the help of a 4 mm diameter mild steel rod, the rods were bent over the WWM on the two sides in opposite direction, the drill hole was grouted with the help of a high-pressure grout pump, to hold the rod in position. A layer of cement grout was applied above the WWM, over which a 10 mm thick layer of 1:3 coarse sand mortar was further applied and the surface was levelled. The sequential process of strengthening is shown in Figure 2.3. The strengthened panels were cured under normal site condition for another 28 days.



Figure 2. 3 : (a)-(b) Stages of strengthening unreinforced specimen with WWM (contd.)



Figure 2. 3 : Stages of strengthening unreinforced specimen with WWM

2.5 INSTRUMENTATION AND TEST SETUP

ASTM E519/ E519M-10 standard guidelines were used to investigate the in-plane diagonal shear strength of unreinforced and reinforced specimens. The diagonal compression load was applied on the diagonally opposite corners of the panels using a 250 ton capacity INSTRON closed loop UTM. The experimental test setup can be seen in Figure 2.4. Displacement controlled compression loading was applied to the test samples with the help of two steel shoes placed at the top and bottom of the specimen. The rate of loading was set such that the test is completed within 2 minutes

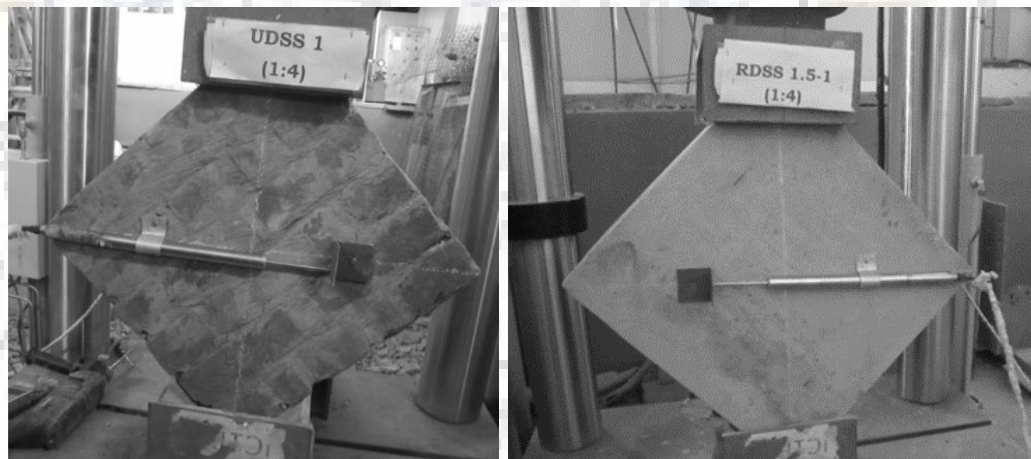


Figure 2. 4 : Test set up and arrangement of instruments on control specimen and on strengthened specimen

The specimens were transported and placed in position with the help of a hand operated crane. Two linear variable differential transducers (LVDT) were used to measure the displacement in both vertical and horizontal direction. The LVDTs were fixed on the test samples with the help of screw and clamp as shown in Figure 2.4 above. The LVDTs were connected to a data acquisition system facilitating synchronized measurement of load and deflection.

2.6 ANALYSIS AND DISCUSSION OF EXPERIMENTAL RESULTS

The global response of masonry is generally defined in terms of stress and strain. The shear stress can be obtained from the experimentally measured diagonal force taken by the masonry sample using the formula

$$\tau = \frac{0.707 p}{\frac{1}{2}t(L+H)}$$

where,

t = the thickness of the panel

L = length of the panel

H = height of the panel

P = diagonal force measured experimentally

The shear strain is calculated using the formula,

$$\gamma = \frac{\Delta V + \Delta H}{g}$$

where,

ΔV = diagonal shortening along the axis of applied force

ΔH = diagonal elongation measured perpendicular to the axis of applied force

g = gauge length, which is normally kept same for both the directions

The stress v/s strain graph plotted for selected samples can be seen in Figures 2.8 to 2.13

2.6.1 Test Observations and Failure Modes

A summary of experimental observation regarding crack pattern and failure modes of reinforced and unreinforced panels subjected to diagonal compression is discussed in the following section.

The unreinforced specimen showed a typical brittle failure (Figure 2.5). It showed cracks only in the mortar joints, whereas the reinforced specimen showed a ductile failure. The experimental observation showed that the reinforcement on both sides of the panel worked

effectively along with the anchorage provided. Cracks initiated in the diagonal region, indicating more stress concentration in that region, further the cracks either propagated towards the corner i.e., along the sides, propagation of cracked varied in each case (Figures 2.6 and 2.7). Spalling of external mortar cover was observed with increase in load. In case of all specimens (set 3, 4, 5, 6, 7, 8) wider cracks were seen along the thickness of the wall indicating complete failure of mortar joints, the bricks did not slide off indicating good anchorage due to the external reinforcement provided. Though the external mortar layer failed and debonding of mesh was observed in set 5, the mesh did not come off due to the anchorage provided. The mesh layer did not detach even after the masonry sample has completely failed, depicting a composite behavior. FEMA 356 says that if the reinforcement provided on either side of a masonry wall is connected through reinforcement (anchorage), it acts as a single composite material.



Figure 2. 5 : URM specimen after testing

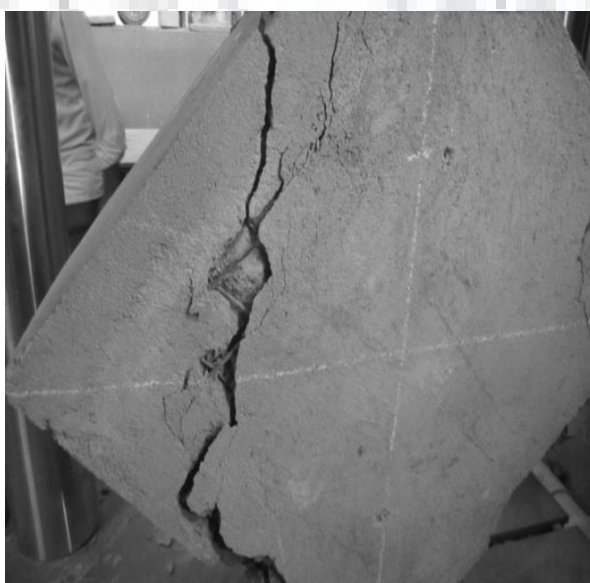


Figure 2. 6 : (a)-(b) High strength mortar retrofitted panel with 1 inch , 1.5 inch and 2 inch spacing WWM (contd.)

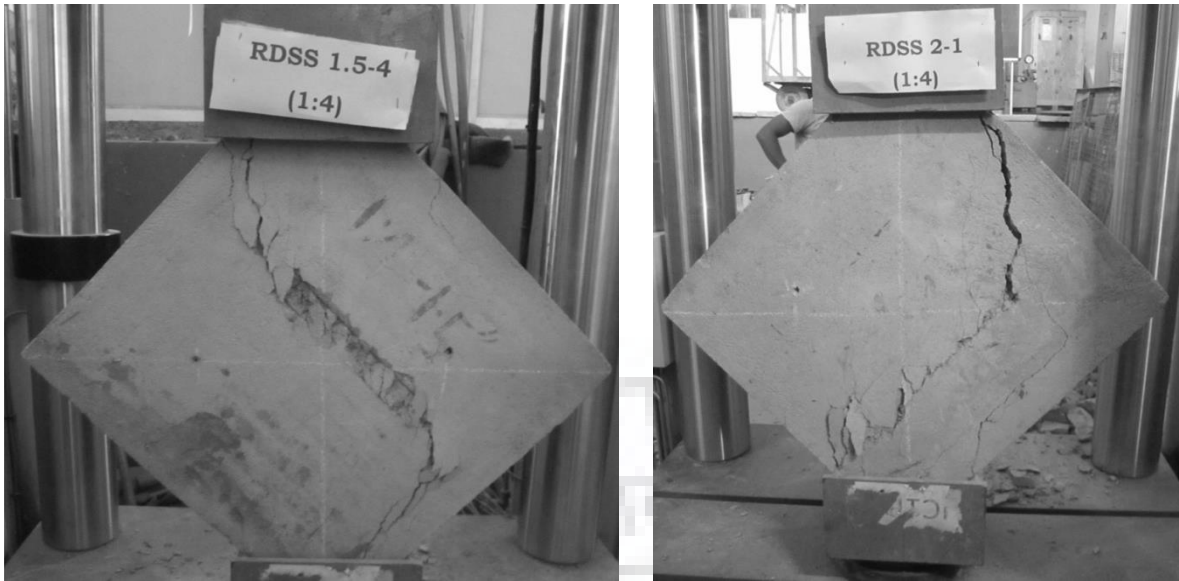


Figure 2. 6 : High strength mortar (1:4) retrofitted panel with 1 inch, 1.5 inch and 2 inch spacing WWM

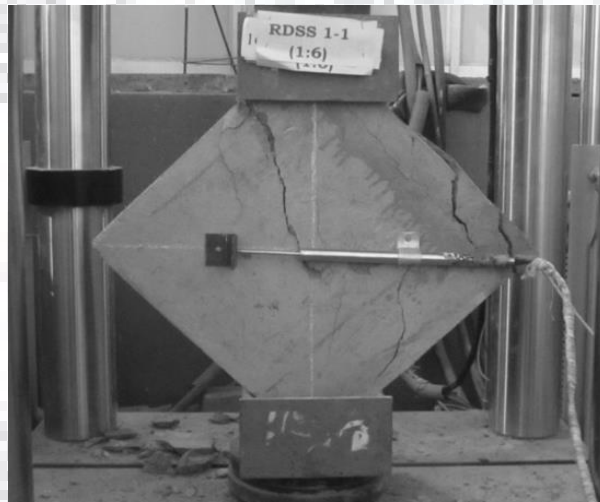


Figure 2. 7 : Low strength mortar (1:6) retrofitted panel with 1 inch, 1.5 inch and 2 inch spacing WWM

2.6.2 Influence on Strengthening

The average shear capacity of set 1 and set 2 specimens were 0.54 MPa and 0.07 MPa respectively, and that of sets 3, 4, 5, 6, 7 and 8 were 1.02 MPa, 1.27 MPa, 1.3 MPa, 0.80 MPa, 0.85 MPa, and 0.91 MPa respectively. The reinforced specimens showed a significant increase in strength compared to unreinforced specimens. The set 3, 4, 5 specimens were able to take more stress compared to other reinforced specimen (set 6, 7, 8). This was due to the high mechanical property of mortar used in set 3, 4, 5 but set 6, 7, 8 was able to withstand more stress compared to its control specimen i.e., set 2. Figures 2.5 to 2.7 show the failure modes of selected reinforced and unreinforced specimens. The effectiveness of reinforcement is clearer from this.

Figures 2.8 to 2.13 show the shear stress-strain curve obtained based on the experimental test data. It can be seen that the reinforced samples showed a linear elastic response initially and then gradually softened as the failure initiated.

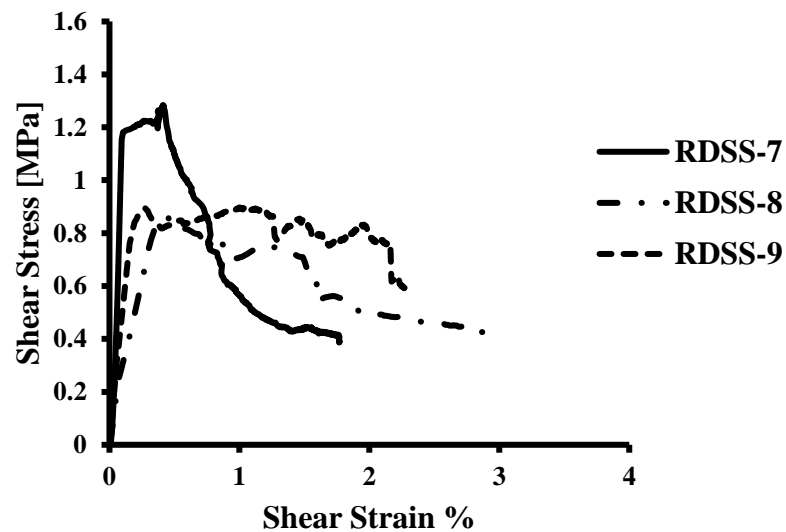


Figure 2. 8 : Specimen reinforced with 1 inch spacing WWM and coarse sand mortar 1:3

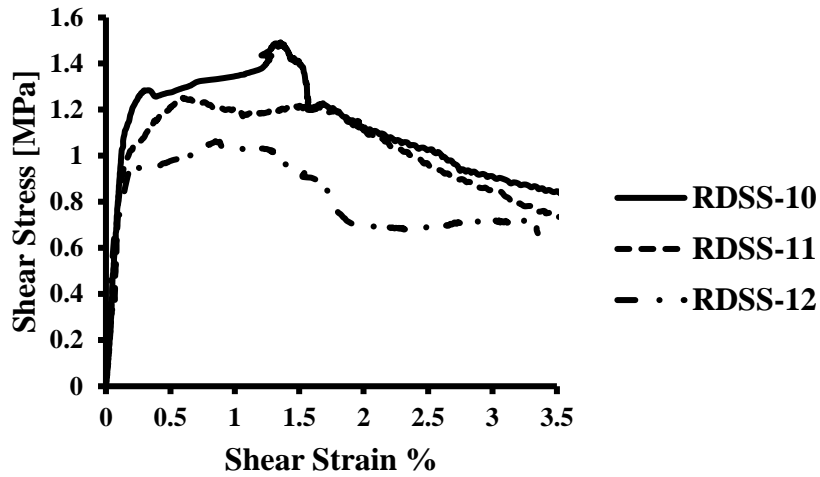


Figure 2. 9 : Specimen reinforced with 1.5 inch spacing WWM and coarse sand mortar 1:3

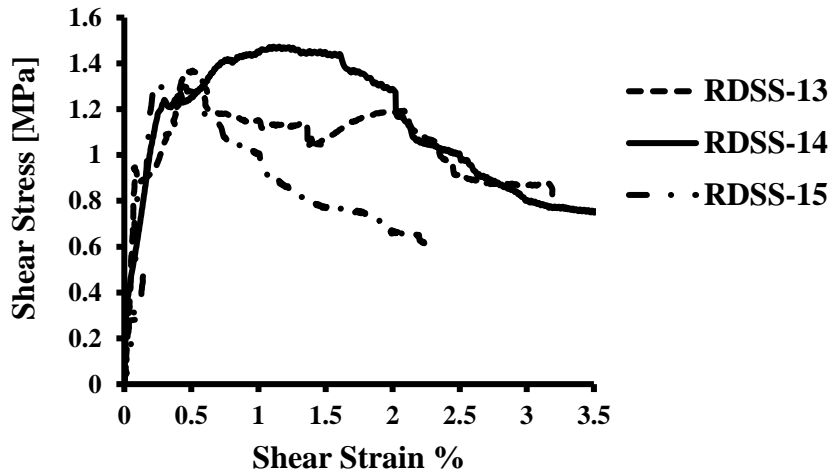


Figure 2. 10 : Specimen reinforced with 2 inch spacing WWM and coarse sand mortar 1:3

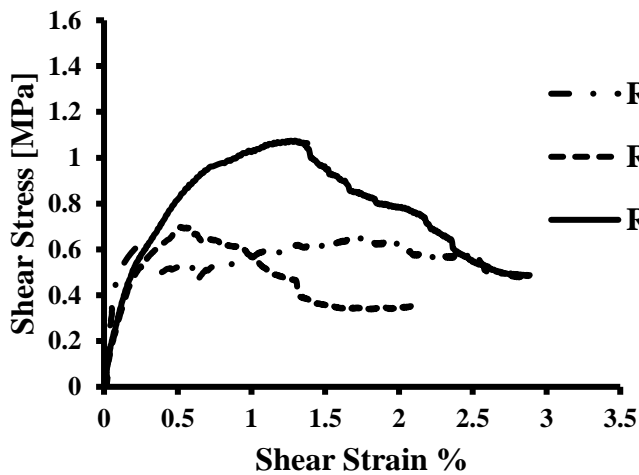


Figure 2. 11 : Specimen reinforced with 1 inch spacing WWM and coarse sand mortar 1:3

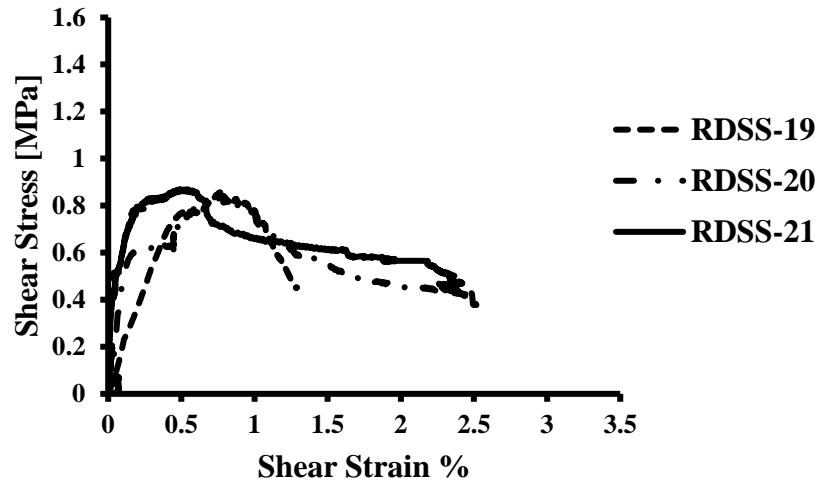


Figure 2. 12 : Specimen reinforced with 1.5 inch spacing WWM and coarse sand mortar 1:3

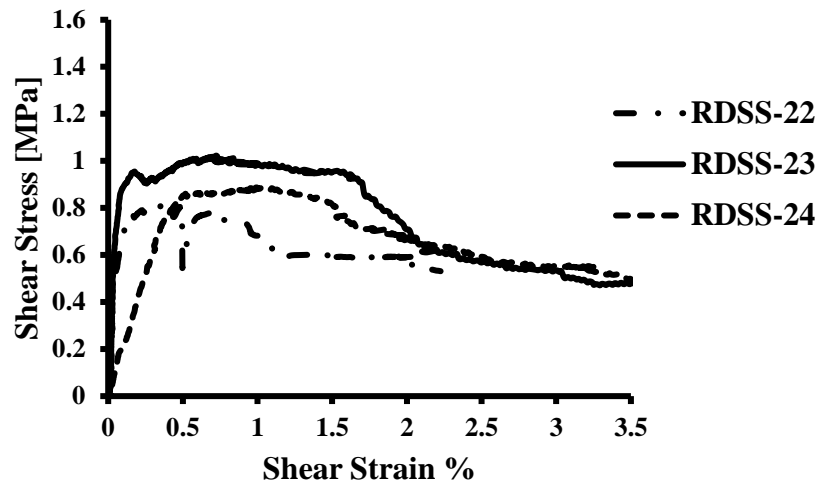


Figure 2. 13 : Specimen reinforced with 2 inch spacing WWM and coarse sand mortar 1:3

2.6.2.1 Bilinear idealization

Since masonry is highly nonlinear, in order to investigate the behavior of the masonry samples, the actual behavior is idealized with the help of a bilinear curve (Marcari et al. (2007)). Bi-linearization of curves is widely recommended by all codal provisions worldwide (Marcari et al. (2007)) to assess existing masonry structure by non-linear static procedure. In this study, the ultimate strength and ductility is evaluated for seismic design and assessment of masonry structures. The bilinear idealization has been obtained by ensuring that the areas below the actual and bilinear idealized curve were equal, and in agreement with the findings of Marcari et al. (2007) and Borri et al. (2011). For all the reinforced panels, an equivalent bilinear curve was defined with reference to Figure 2.14. The calculations are given in Table 2.4.

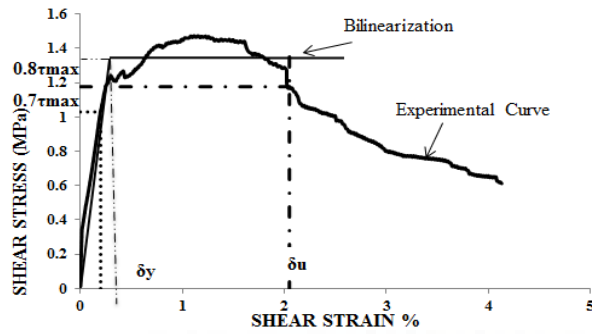


Figure 2. 14 : Bilinear curve

Table 2. 4 : Experimental results of shear-compression tests

Specimen	ρ_h (%)	ρ_v (%)	WWM spacing [Inch]	P_{max} [kN]	τ_{max} [MPa]	τ/τ_0	d_y	d_u	μ = d_u/d_y	Mean μ
UDSS-1				105.0	0.64	--	--	--	--	--
UDSS-2	0	0	--	121.0	0.74	--	--	--	--	--
UDSS-3				37.0	0.22	--	--	--	--	--
UDSS-4				11.5	0.07	--	--	--	--	--
UDSS-5	0	0	--	11.1	0.06	--	--	--	--	--
UDSS-6*				--	--	--	--	--	--	--
RDSS-7				276.9	1.28	2.38	2.20	4.48	2.03	
RDSS-8	0.10	0.10	1	184.9	0.86	1.60	0.36	1.54	4.27	5.90
RDSS-9				191.8	0.89	1.65	0.19	2.17	11.42	
RDSS-10				274.5	1.49	2.77	0.19	2.23	11.73	
RDSS-11	0.12	0.12	1.5	267.6	1.25	2.32	0.19	2.38	12.52	11.28
RDSS-12				227.4	1.06	1.97	0.18	1.73	9.61	
RDSS-13				292.0	1.47	2.74	0.17	2.22	13.05	
RDSS-14	0.11	0.11	2	315.0	1.30	2.42	0.22	0.74	3.38	12.14
RDSS-15				278.0	1.13	2.10	0.22	4.40	20.0	
RDSS-16				139.4	0.65	9.28	0.37	0.1	3.7	
RDSS-17	0.10	0.10	1	149.3	0.69	9.97	0.23	1.02	4.43	4.18
RDSS-18				229.8	1.07	15.2	0.38	1.68	4.42	
RDSS-19				184.1	0.86	12.2	0.42	1.1	2.62	
RDSS-20	0.11	0.11	1.5	180.4	0.84	12.0	0.19	1.18	6.05	4.48
RDSS-21				186.0	0.86	12.4	0.17	0.81	4.76	
RDSS-22				175.4	0.82	11.7	0.17	1.05	6.17	
RDSS-23	0.12	0.12	2	218.6	1.02	14.5	0.10	1.78	17.80	9.49
RDSS-24				189.6	0.88	12.6	0.39	1.76	4.5	

ρ_h =Horizontal reinforcement ratio; ρ_v =Vertical reinforcement ratio; p_{max} = Maximum applied load; τ_{max} = Maximum shear stress; d_y = Yield drift; d_u = Ultimate drift corresponding to 0.8τ ; μ = Ductility specimen damaged before testing*

2.6.3 Test Discussion

This experimental investigation was aimed at to find an alternate solution for strengthening the existing masonry structure using a cost effective economic material, which can be easily used in practice without any practical difficulty. The test was meant to study the effect of mortar type H2 and M2 (1:4 and 1:6) which are most commonly used in practice and then on reinforced masonry panel with same arrangement of reinforcement technique but with different sizes of reinforcement (1 inch, 1.5 inch, 2 inch spacing) which is commonly available in local market. The influence of various types of reinforcement has been studied. Based on the observations, following are the summary of test results.

- The unreinforced masonry when reinforced, has a significant effect on strength and ductility due to the reinforcing/ confining action of the reinforcement. The low strength masonry (1:6) showed good result compared to high strength masonry (1:4) when provided with reinforcement. The WWM reinforcement showed an average increase in strength ranging from 1.88, 2.35 and 2.42 times more compared to control specimen in case of 1:4 mortar masonry samples and 11.51, 12.24, 13.00 times more in case of 1:6 mortar masonry samples.
- When samples provided with the same percentage of reinforcement was compared it was observed that set 6 and 7 took more load compared to set 1 and 2 but less than set 3 and 4, as expected, set 5 took more load compared to set 8.
- The influence of reinforcement on high strength mortar sample is less compared to that of low strength mortar sample. It can be clearly observed from Figures 2.8 to 2.13 and Table 2.4.
- The ductility increased with increase in the size of mesh spacing in case of both high and low strength mortar masonry samples. The low strength masonry samples were lesser ductile compared to high strength masonry sample but much higher compared to their control specimens.

2.7 THE DIFFERENT MODELING APPROACHES FOR MASONRY

2.7.1 Modeling with FEM

The presence of vertical and horizontal mortar joints causes the masonry to be anisotropic. Basically, two different approaches have been adopted to model such anisotropy:

- i. The 'micro model', or 'two-material approach'

ii. The ‘macro model’ or ‘equivalent-material approach’

In the two-material model, the discretization follows the actual geometry of both the blocks and mortar joints, adopting different constitutive models for the two components. Particular attention must be paid to the modeling of joints since the sliding at a joint level often starts up the crack propagation. Although this approach may appear very straightforward, its major disadvantage comes from the extremely large number of elements to be generated as the structure increases in size and complexity. This renders unlikely the use of micro models for the global analysis of entire buildings, also considering the fact that the actual distribution of blocks and joints might be impossible to detect unless aggressive research is performed. The macro model assumes that the masonry structure is a homogeneous continuum to be discretized with a finite element mesh which does not copy the wall organism but obeys the method’s own criteria. The single element will thus have a constitutive model which must be capable of reproducing an average behavior. This assumption bypasses the physical characteristics of the problem. Nevertheless, the equivalent material models have proven to be able to grasp certain aspects of the global behavior without the number of parameters and the computing effort needed in the micro model.

2.7.2 Modeling with Interface Elements

In this approach, the blocks are modeled using conventional continuum elements, linear or non-linear, while mortar joints are simulated by interface elements, the ‘joint elements’, and are made up of two rows of superimposed nodes (Figure 2.16), with friction constitutive law.

The introduction of the joint is easy to implement in a software program, since the nodal unknowns are the same for continuum and joint elements, though for the latter the stress tensor must be expressed in terms of nodal displacements instead of deformation components. Two major concerns balance the apparent simplicity of this approach (Giordano et al. 2002)

- Block mesh and joint mesh must be connected together so that they have to be compatible, which is possible only if interface joints are identically located. This compatibility is very difficult to ensure when complex block arrangements are to be handled, like in 3D structures.
- The joint element is intrinsically able to model the contact only in the small displacement field. When large motion is to be dealt, it is not possible to provide easy remeshing in order to update existing contacts and/ or to create new ones.

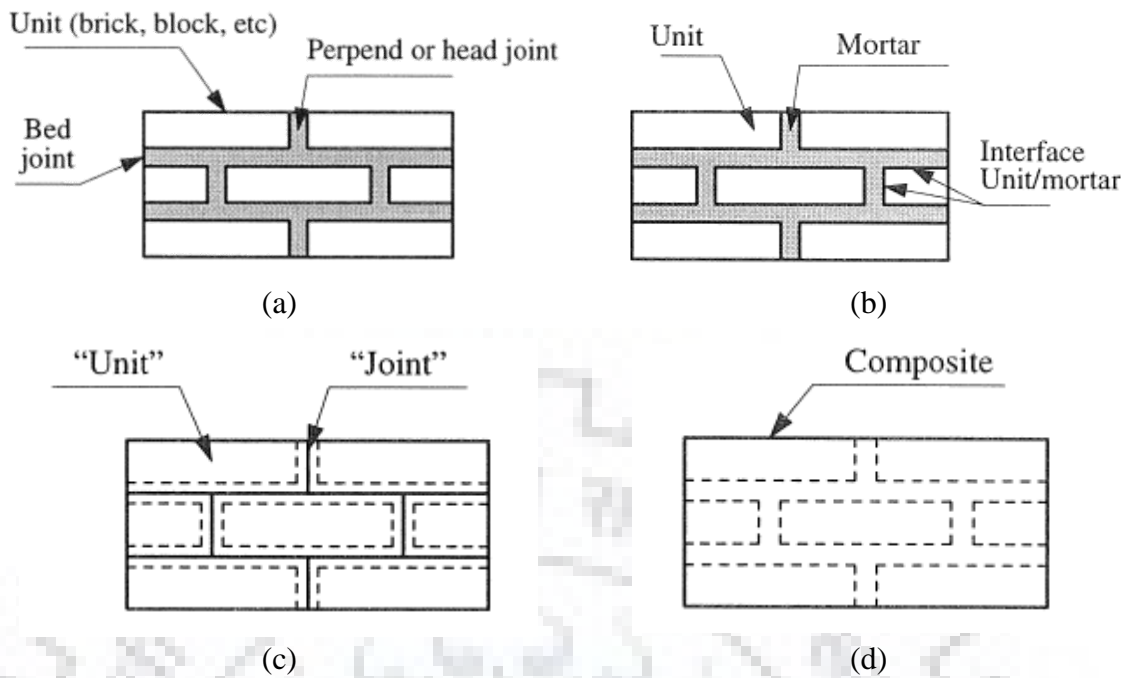


Figure 2.15 : Modeling strategies for masonry: (a) Masonry sample; (b) Detailed micro modeling (discrete crack); (c) Simplified micro-modeling (discrete crack); and (d) Micro modeling (smeared crack) (Lourenco et al. 1997)

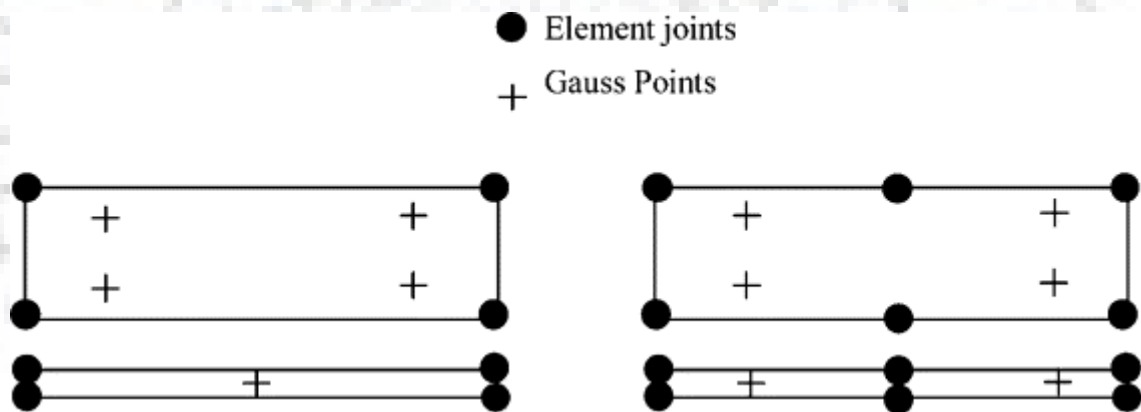


Figure 2.16 : Degeneration of continuum element into 'joint' element (Giordano 2002)

2.7.3 Modeling with DEM

The above-mentioned limitations are overcome by the DEM. In this approach, the structure is considered as an assembly of distinct blocks, rigid or deformable, interacting through unilateral elasto-plastic contact elements which follow a Coulomb slip criterion for simulating contact forces. The method is based on a formulation in large displacement (for the joints) and small deformations (for the blocks), and can correctly simulate collapse mechanisms due to sliding, rotations and impact. The contacts are not fixed, like in the FEMDE, so that during the analyses blocks can lose existing contacts and make new ones. Once every single block has been modeled both geometrically and mechanically, and the volume and surface forces are known, the

time history of the block's displacements is determined by explicitly solving the differential equations of motion. The main advantage of this approach is the possibility of following the displacements and determining the collapse mechanism of structures made up of virtually any number of blocks (Giordano et al. 2002). On the contrary, it must be considered that the finite elements used for the internal mesh of the blocks, when deformable, show poor performance, so the method is not accurate for the study of stress states within the blocks. For this purpose, other models are more suitable.

2.8 NON-LINEAR MATERIAL MODEL

The seismic response is a cyclic process on all type of materials. The earthquake load has a lot of influence on the material behavior. Masonry is a brittle material with very low tensile strength. In uni-axial compression or tension test, modulus of elasticity is constant (strain is directly proportional to stress) up to yield point i.e., the material is under elastic condition. The non-linear material properties help in understanding the material behavior beyond the elastic range. Dynamic behavior of masonry depends on the non-linear material properties. In this present study CDP constitutive model is used for masonry, mortar and concrete. The material property of all material (brick masonry, high strength mortar, concrete, WWM) involved this study has been elaborated in the following section. Modeling of masonry is a complex task due to heterogeneous and anisotropic nature of the material.

2.9 CONCRETE DAMAGE PLASTICITY (CDP)

The CDP model can be implemented on both Abaqus/Standard and Abaqus/Explicit. The CDP model is used for the analysis of concrete and other quasi-brittle material.

This constitutive theory can capture the irreversible effects of damage that occur in concrete under low confining pressure. To describe this behavior the following feature is considered:

- Different yield strengths in tension and compression (with the initial yield stress in compression is a factor of 10 or more higher than the initial yield stress in tension)
- Softening behavior in tension as opposed to initial hardening followed by softening in compression
- Different degradation of the elastic stiffness in tension and compression
- Stiffness recovery effects during cyclic loading and
- Rate sensitivity, especially an increase in the peak strength with strain rate

The main ingredients concrete damaged plasticity models are summarized below:

Strain rate decomposition: The rate independent model is governed by additive strain rate decomposition,

$$\dot{\varepsilon} = \dot{\varepsilon}^{el} + \dot{\varepsilon}^{pl}$$

where, strain rate total is represented by $\dot{\varepsilon}$ and the superscripts 'el' and 'pl' refer to the elastic and plastic of the strain rate respectively.

Stress-strain relations: The Stress-strain relations are governed by scalar damaged elasticity:

$$\sigma = D^{el}(\varepsilon - \varepsilon^{pl}) = (1 - d)D_0^{el}(\varepsilon - \varepsilon^{pl})$$

where, D_0^{el} is the initial undamaged elastic stiffness of the material $D^{el} = (1 - d)D_0^{el}$ is the degraded elastic stiffness and d is the scalar stiffness degradation variable (un-damaged material $d = 0$, fully damaged material $d = 1$). Damage associated with the failure mechanisms of the concrete therefore results in a reduction in the elastic stiffness. Hence in concrete damage plasticity theory the stiffness degradation is isotropic and characterized by a single degradation variable d . The effective stress is defined as:

$$\bar{\sigma}^{def} = D_0^{el}(\varepsilon - \varepsilon^{pl})$$

The Cauchy stress is related to the effective stress through the scalar degradation relation:

$$\sigma = (1 - d)\bar{\sigma}$$

For any given cross section of the material, the factor $(1-d)$ represents the ratio of the effective load carrying area to the overall section area. In the absence of damage $d=0$ the effective stress $\bar{\sigma}$ is equivalent to the Cauchy stress. When damage occurs, the effective stress is more representative than the Cauchy stress because it is the effective stress area that is resisting the external load. Thus, the plasticity problems are formulated in terms of effective stress. The degradation variable is governed by a set of hardening variables ε^{pl} , and the effective stress.

2.10 DAMAGE AND STIFFNESS DEGRADATION

The hardening variables $\dot{\varepsilon}_t^{pl}$ and $\dot{\varepsilon}_c^{pl}$ is based on the uni-axial loading conditions and then on the multi-axial condition

Uni-axial conditions

Under uni-axial condition, it means that the stress curves have the form

$$\sigma_t = \sigma_t(\tilde{\varepsilon}_t^{pl}, \dot{\tilde{\varepsilon}}_t^{pl}, \theta, f_i)$$

$$\sigma_c = \sigma_c(\tilde{\varepsilon}_c^{pl}, \dot{\tilde{\varepsilon}}_c^{pl}, \theta, f_i)$$

where, the subscript 't' and 'c' refer to tension and compression, respectively $\dot{\tilde{\varepsilon}}_t^{pl}$ and $\dot{\tilde{\varepsilon}}_c^{pl}$ are equivalent plastic strain rates, $\tilde{\varepsilon}_t^{pl} = \int_0^t \dot{\tilde{\varepsilon}}_t^{pl} dt$ and $\tilde{\varepsilon}_c^{pl} = \int_0^t \dot{\tilde{\varepsilon}}_c^{pl} dt$ are the equivalent plastic strain, θ is the temperature, and $f_i, (i = 1, 2, \dots)$ are the other predefined field variable.

Under uni-axial loading conditions, the effective plastic strain rates are given as

$$\dot{\tilde{\varepsilon}}_t^{pl} = \dot{\varepsilon}_{11}^{pl}. \text{ In uni-axial tension and}$$

$$\dot{\tilde{\varepsilon}}_c^{pl} = \dot{\varepsilon}_{11}^{pl}. \text{ In uni-axial compression}$$

Let σ_c be as positive quantities representing the magnitude of the uni-axial compression stress thus $\sigma_c = \sigma_{11}$

As shown in Figure 2.17 when the specimen is unloaded from any point on the strain softening branch of the stress-strain curves, the unloading response is observed to be weakened: the elastic stiffness of the material appears to be damaged (or degraded). The degradation of the elastic stiffness is significantly different between tension and compression tests but both the cases show considerable effect with the increase in plastic strain. The degraded response of concrete is characterized by two independent uni-axial damage variables, d_c and d_t which are assumed to be functions of the plastic strains, temperature, and field variables:

$$d_t = d_t(\tilde{\varepsilon}_t^{pl}, \theta, f_i), (0 \leq d_t \leq 1)$$

$$d_c = d_c(\tilde{\varepsilon}_c^{pl}, \theta, f_i), (0 \leq d_c \leq 1)$$

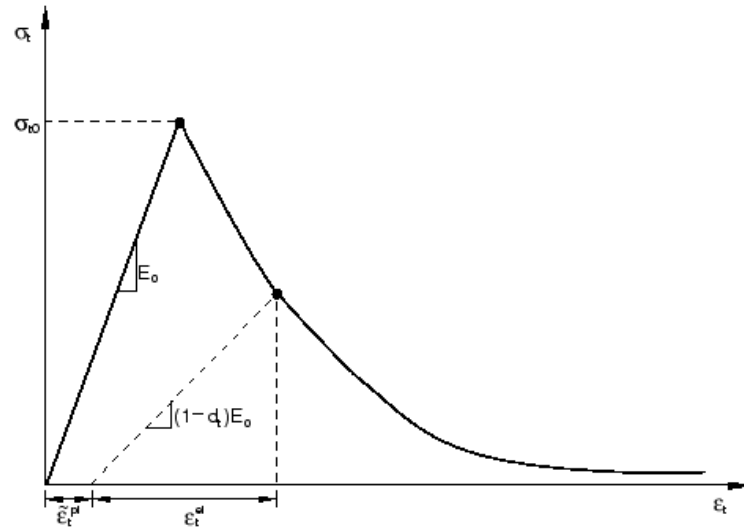


Figure 2.17 : Response of concrete to uni-axial loading in tension (Abaqus 2013)

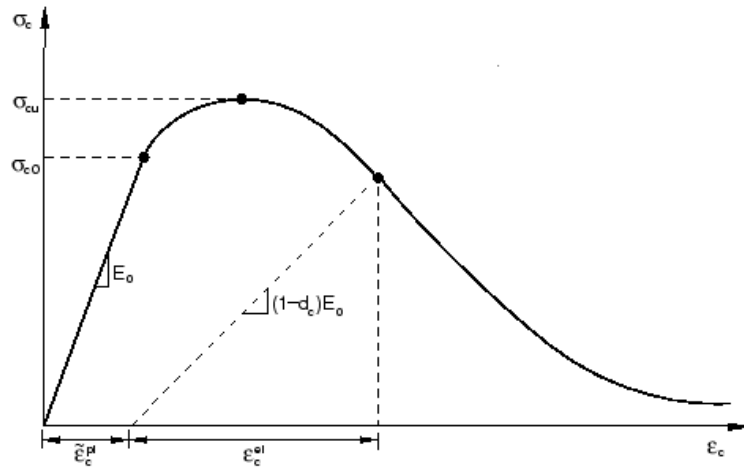


Figure 2.18 : Response of concrete to uni-axial loading in compression (Abaqus 2013)

The uni-axial degradation variables are increasing functions of the equivalent plastic strains. The values ranging from zero (undamaged material) to one (fully damaged material).

If E_0 is the initial (undamaged) elastic stiffness of the material, the stress-strain relations under uni-axial tension and compression loading are:

$$\sigma_t = (1 - d_t)E_0(\varepsilon_t - \tilde{\varepsilon}_t^{pl})$$

$$\sigma_c = (1 - d_c)E_0(\varepsilon_c - \tilde{\varepsilon}_c^{pl})$$

Under uni-axial loading, cracks propagate in a direction transverse to the stress. The formation and propagation of cracks, therefore, causes a reduction in available load-carrying area, which in turn leads to increase in the effective stress. The effect is less pronounced under compressive loading since cracks run parallel to the loading direction; however, after a significant amount of crushing, the effective load-carrying area is also significantly reduced. Thus the effective uni-axial cohesion stresses, $\bar{\sigma}_t$ and $\bar{\sigma}_c$ are given as

$$\bar{\sigma}_t = \frac{\sigma_t}{(1 - d_t)} = E_0(\varepsilon_t - \varepsilon_t^{pl})$$

$$\bar{\sigma}_c = \frac{\sigma_c}{(1 - d_c)} = E_0(\varepsilon_c - \varepsilon_c^{pl})$$

2.11 MATERIAL PROPERTIES OF MASONRY

In the present study, the basic material properties used for concrete damaged plasticity Modeling of masonry, have been taken from the actual laboratory tests conducted, whereas values of some of the constants which cannot be obtained from direct measurements have been referred from literature. The average values of compression strength of masonry prism for 1:4 and 1:6 mortar is 3.95 MPa and 2.17 MPa respectively. The density of masonry is considered according to IS 875 (Part 1): 1987. The breaking load on specimens has been utilized to compute the tensile strength (f_t) as per the procedure recommended in ASTM (ASTM 2010b). Being brittle material, the failure in bending test was too sudden and post peak stress-strain measurement is not reliable.

Therefore, to simulate the behavior of masonry in tension, the model suggested by Chen et al. (2008) has been used. For tensile stress-strain relationship was obtained from the following relationship

$$\sigma = \begin{cases} E_t \varepsilon & \varepsilon < \varepsilon_t \\ K_r f_t & \varepsilon > \varepsilon_t \end{cases}$$

where,

$$K_r = \left[1 + \left(C_1 \frac{\varepsilon - \varepsilon_t}{\varepsilon_v} \right)^3 \right] \exp \left(-C_2 \frac{\varepsilon - \varepsilon_t}{\varepsilon_v} \right) - \frac{\varepsilon - \varepsilon_t}{\varepsilon_v} (1 + C_1^3) \exp(-C_2).$$

E_t is the elastic modulus in tension that for simplicity is assumed to be equal to E_0 is compression.

$\varepsilon_t = \frac{f_t}{E_t}$, is the strain corresponding to the tensile strength. A small value of strain $\varepsilon_v = 0.0003$

and $C_1=3$, $C_2=6.93$ is used in the analysis

Under compression, the stress-strain curve for masonry was found to be linear for upto one-third of compressive strength of masonry (f_m) after which cracks began to form in the bricks introducing the nonlinearity (Kaushik et al. 2007)

Figure 2.19 shows the non-linear behavior of masonry under compression. The post yield tension behavior of masonry (Jankowiak et al. 2005) has been obtained from the assumed (Chen et al. 2008) stress-strain curve for the masonry in tension. Van der Pluijm (1992) found that the masonry behaved nearly linear right upto the peak tensile stress and then showed tension softening.

The compression damage and tension damage of masonry have been calculated based on numerical procedure available in the literature (Jankowiak and Lodygowski 2005, Yu et. al. 2010). In this procedure, the damage parameter is governed by stress to strength ratio in the considered (compression or tension) action. Using this procedure, the relation between damage and crushing/ cracking strain can be established as shown in Figures 2.19 to 2.23.

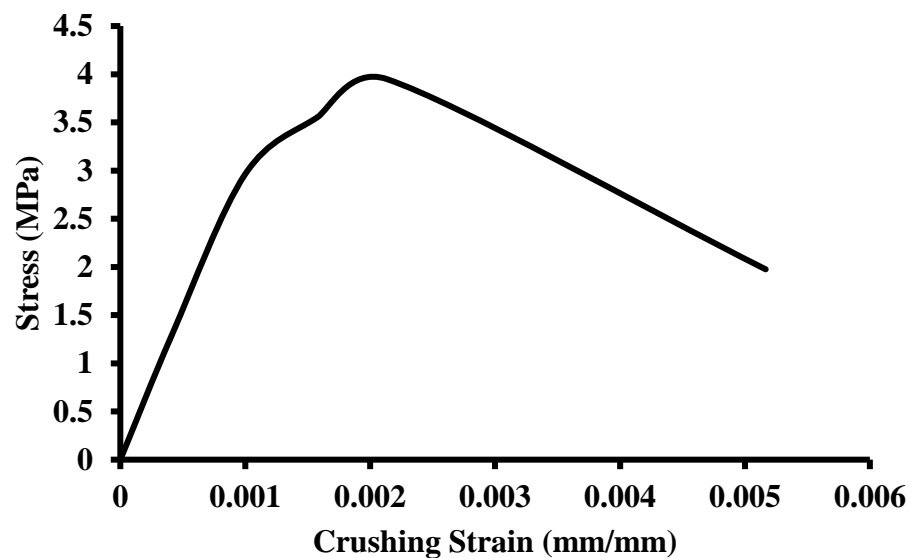


Figure 2. 19 : Compression behavior of 1:4 masonry in non-linear range

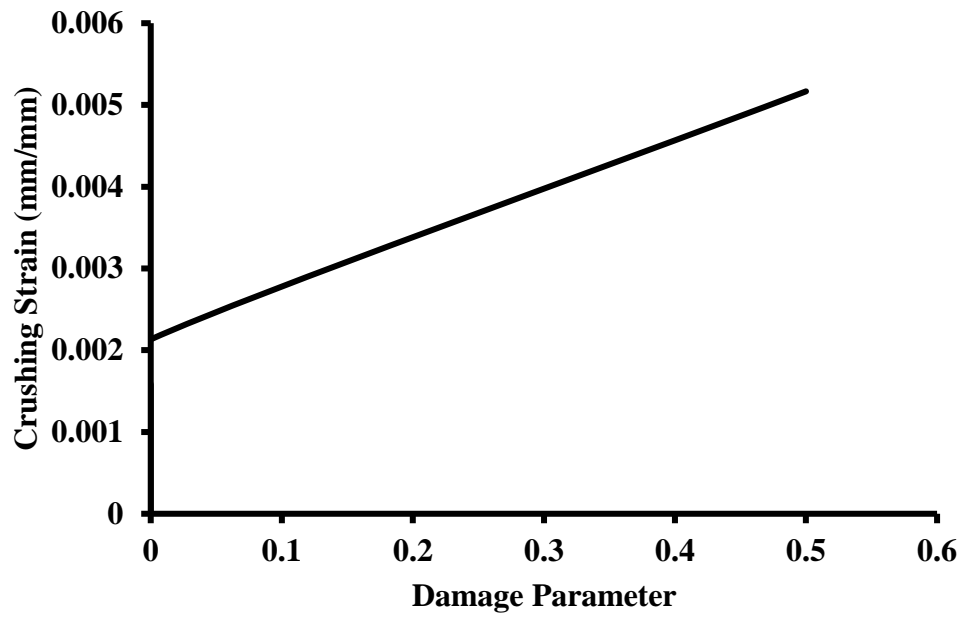


Figure 2. 20 : Compression damage of 1:4 masonry

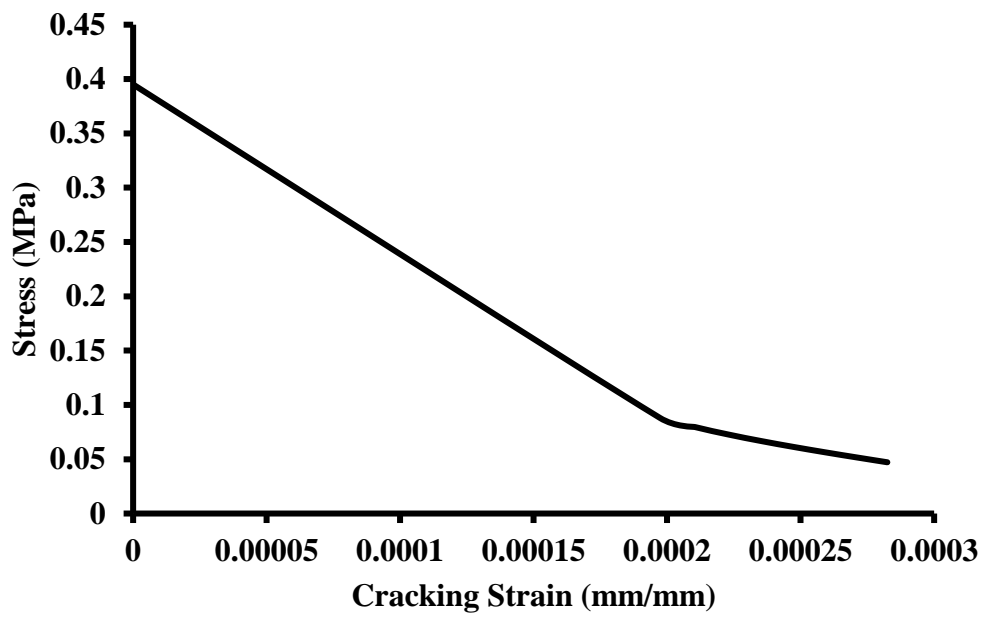


Figure 2. 21 : Tension behavior of 1:4 masonry in non-linear range

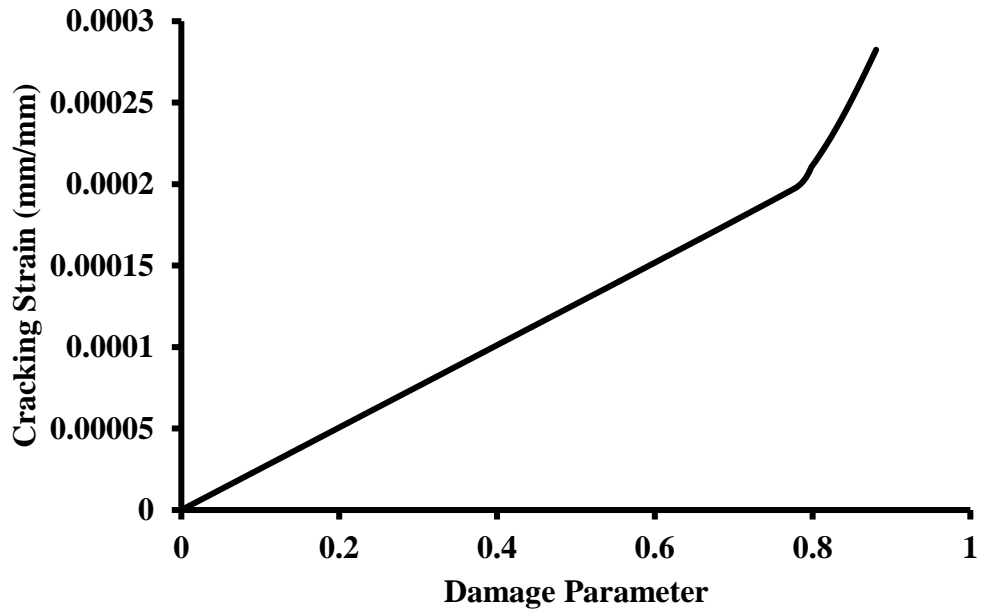


Figure 2.22 : Tension damage of 1:4 masonry

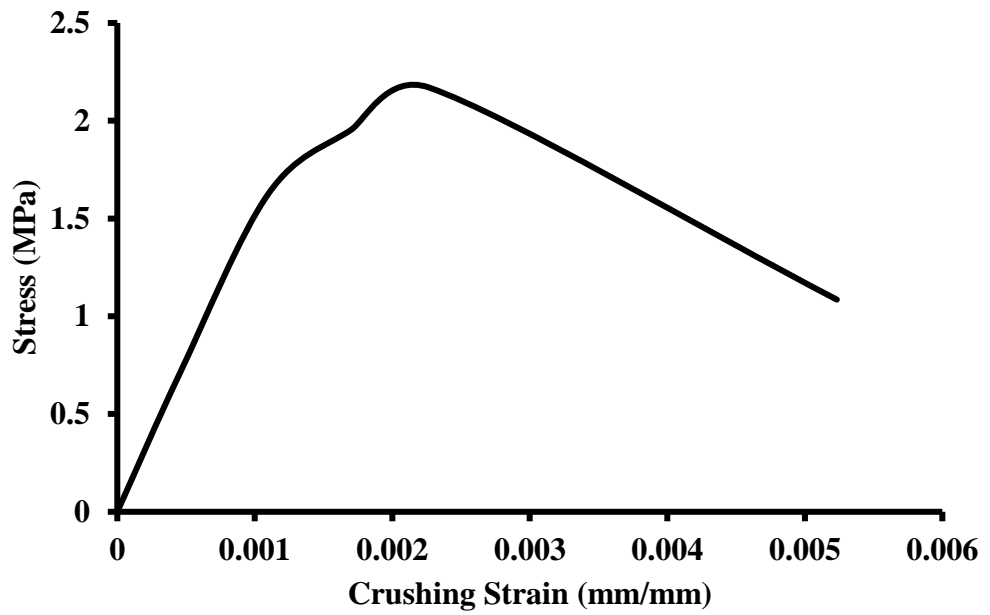


Figure 2.23 : Compression behavior of 1:6 masonry non-linear range

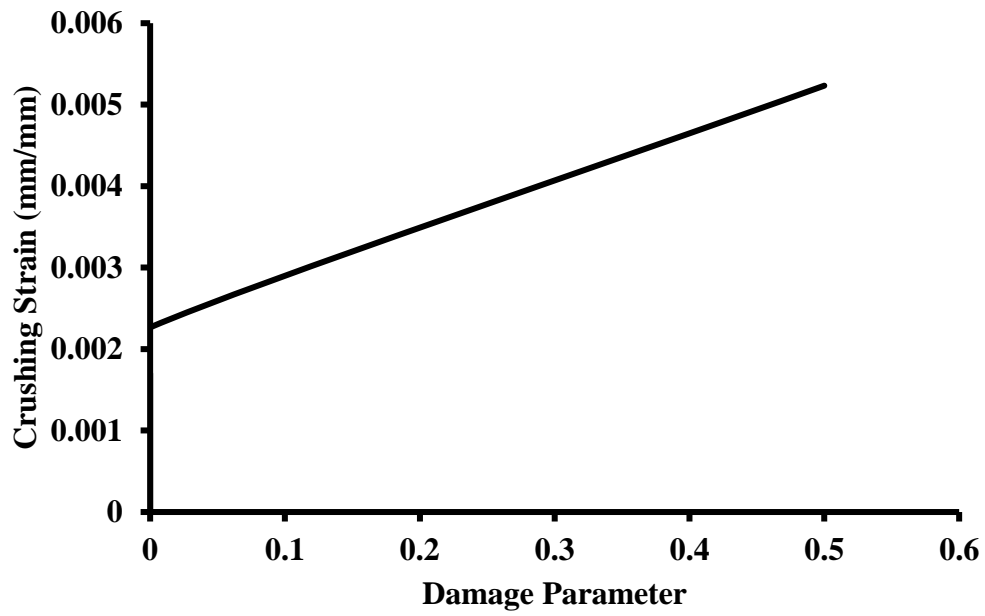


Figure 2. 24 : Compression damage of 1:6 masonry

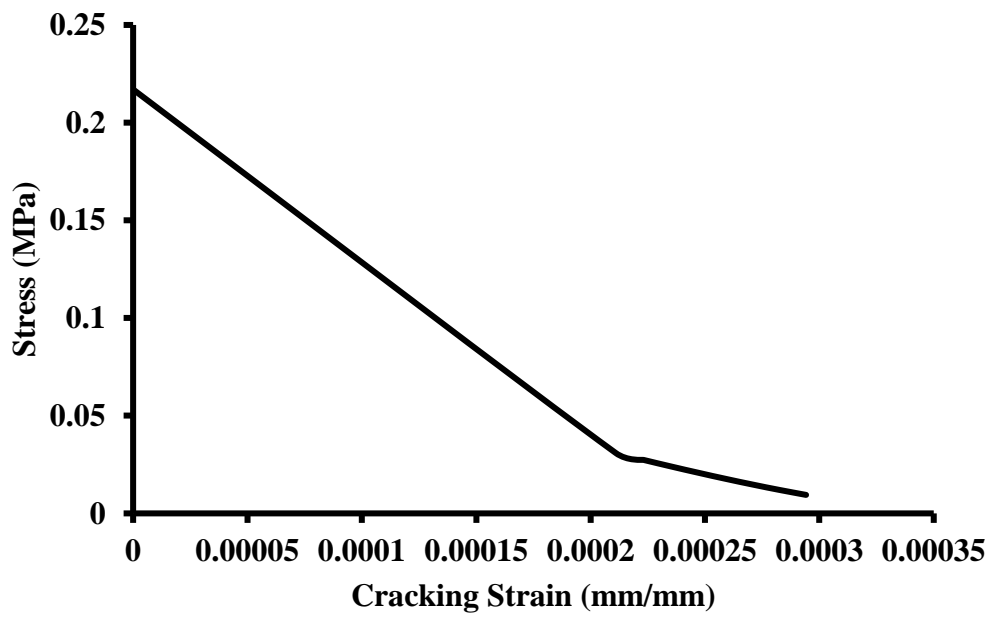


Figure 2. 25 : Tension behavior of 1:6 masonry in non-linear range

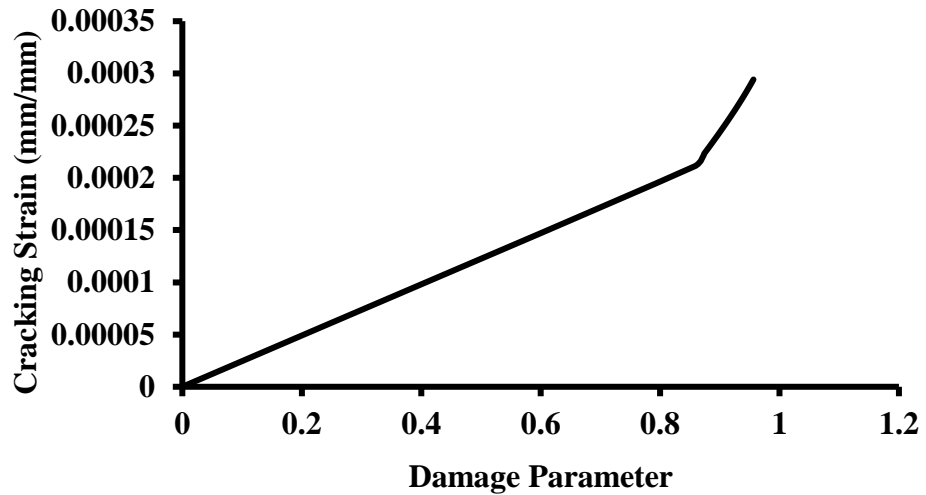


Figure 2. 26 : Tension damage of 1:6 masonry

As shown above, the basic parameters related to the material properties have been obtained directly from the experimental tests. Whereas, some of the parameters required in the modeling have been referred from the literature, as standard test procedures for obtaining these are not available. Other required material properties (Poisson's ratio=0.2, dilation angle = 30°, flow potential eccentricity = 0.1, ratio of initial equibiaxial compressive yield stress to initial uni-axial compressive yield stress = 1.16, ratio of second stress invariant = 0.667, viscosity parameter = 0.0) were taken from literature (Rai et al. 2011, Daniel 2012, Sousa et al. 2013, Choudhury et al. 2015, Kadam et al. 2015)

2.11.1 Material Properties of Coarse Sand Mortar

The same method used for obtaining CDP model of concrete has been used to derive the model for mortar.

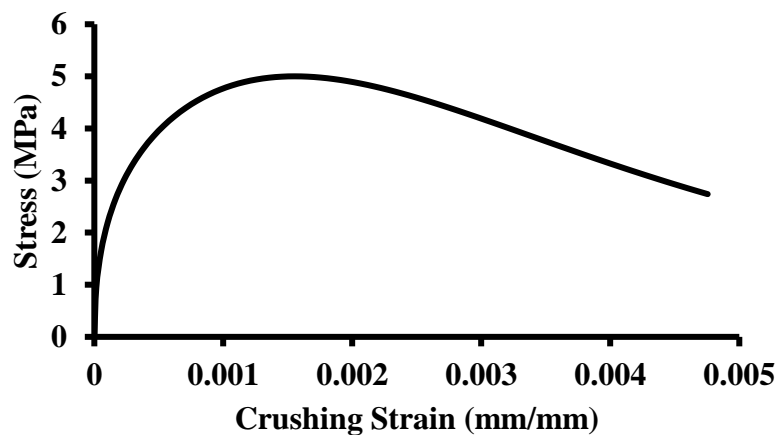


Figure 2. 27 : Compression behavior of coarse sand mortar in non-linear range expressed as a function of crushing

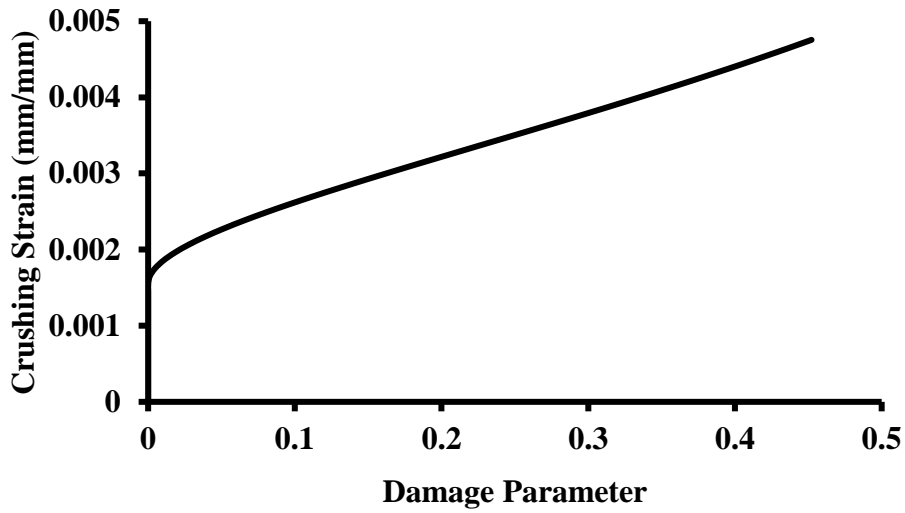


Figure 2.28 : Compression damage of coarse sand mortar

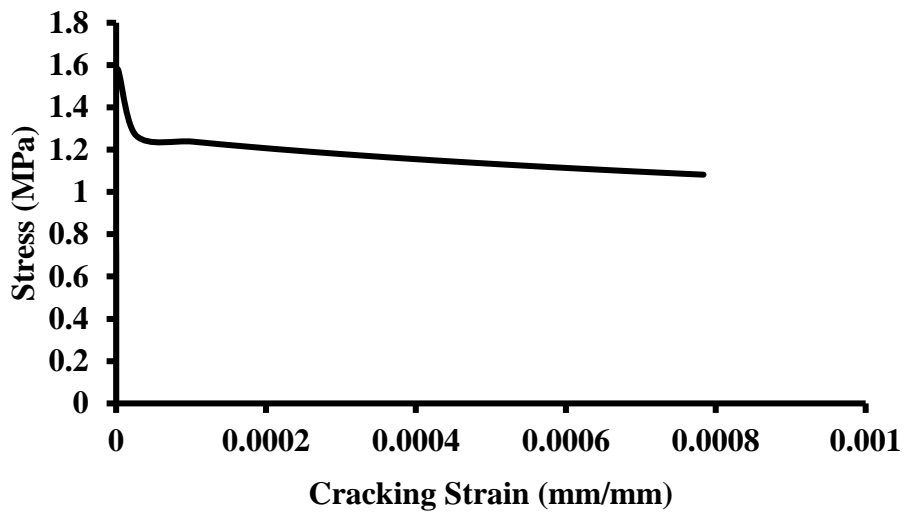


Figure 2.29 : Tension behavior of coarse sand mortar in non-linear range expressed as a function of crushing

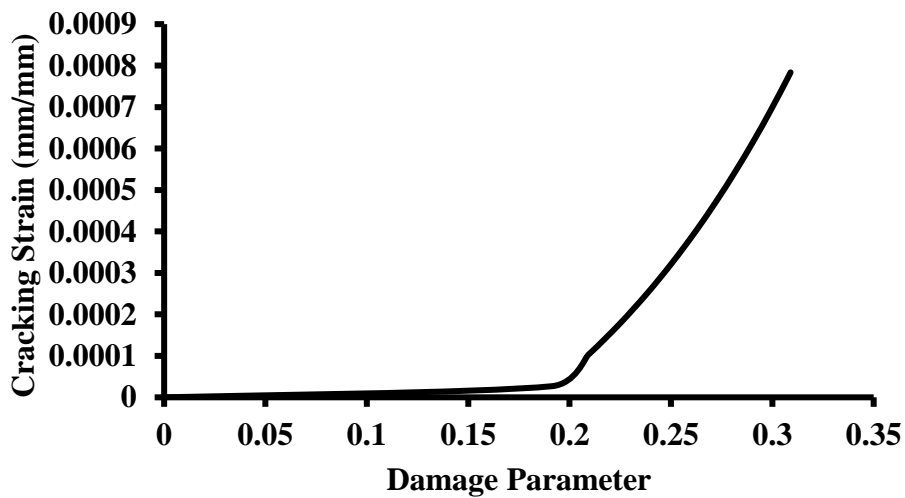


Figure 2.30 : Tension damage of coarse sand mortar

2.11.2 Welded Wire Mesh (WWM)

The WWM has been tested in the laboratory and the stress-strain plot is shown in Figure 2.31-2.33. It is observed from the curve that the WWM wire material has very low ductility and fails in an almost brittle manner. The Poisson's ratio of 0.3 and density of 7850 kg/m^3 (same as for steel, specified in IS 875 (Part I): 1987 and Pillai and Menon 2010) has been used for the WWM.

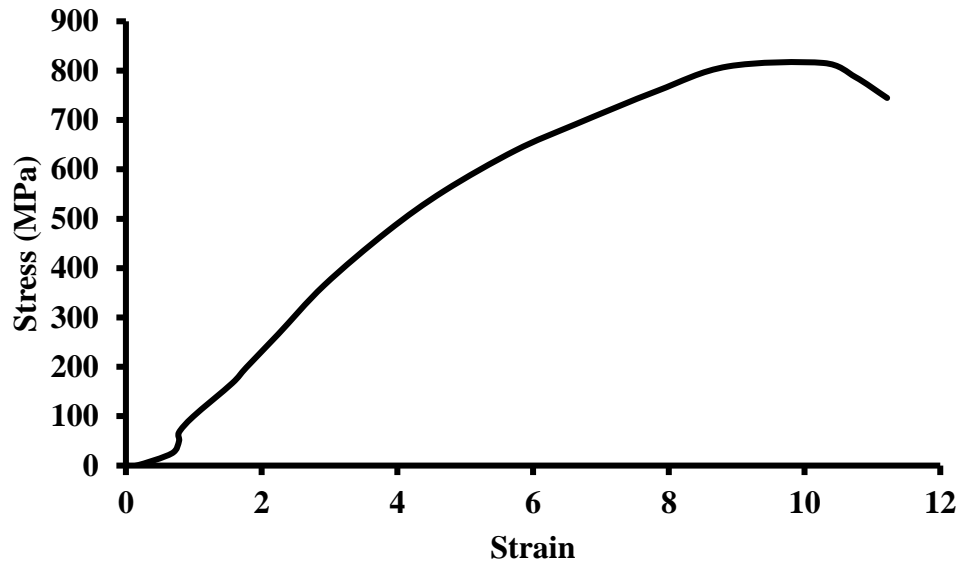


Figure 2. 31 : Stress-strain curve for 1 inch spacing WWM

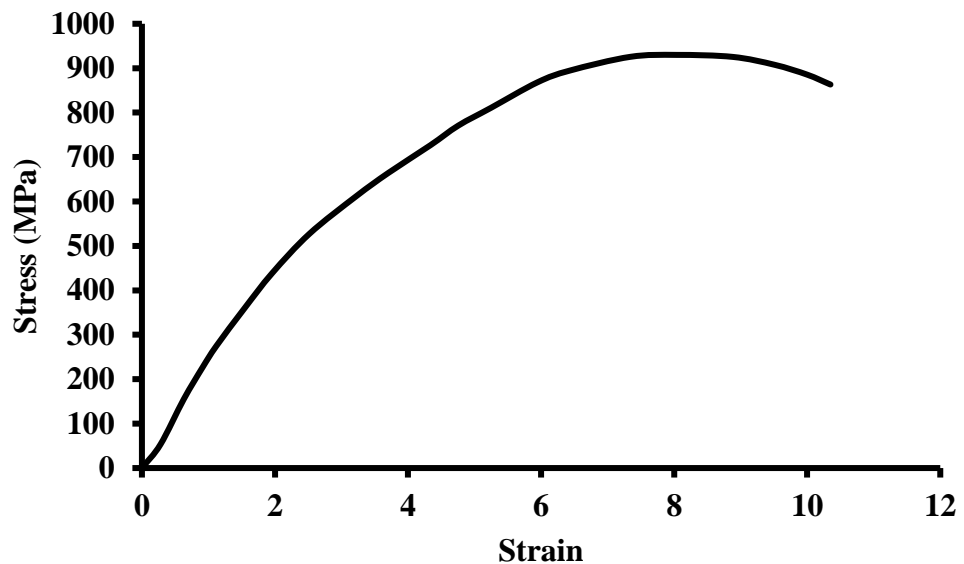


Figure 2. 32 : Stress-strain curve for 1.5 inch spacing WWM

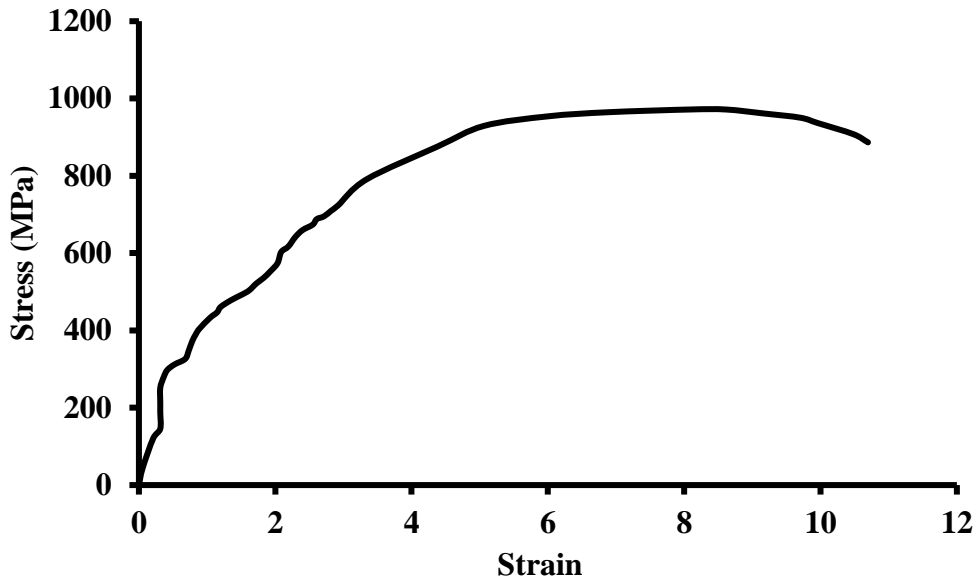


Figure 2. 33 : Stress-strain curve for 2 inch spacing WWM

2.12 FINITE ELEMENT MODELING OF STRENGTHENED MASONRY

Finite element simulation of the in-plane tests on strengthened and un-strengthened masonry has been carried out. The three constituent materials, masonry, mortar and WWM were modeled in different layers and interaction between them was considered assuming perfect bond. It was modeled using the “tie constraint” available in Abaqus/CAE as shown in Figure 2.34. This tie constraint ensures nodal connectivity by ensuring equal displacements of all connected nodes under the influence of externally applied load/displacement.

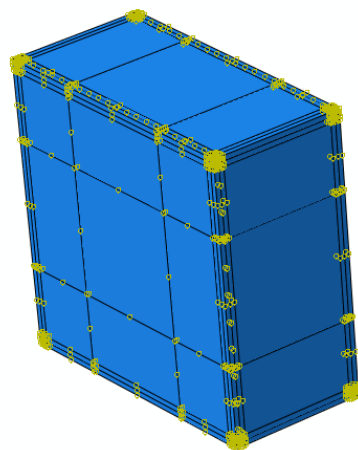


Figure 2. 34 : Diagonal compression test specimens with tie constraint used for simulating interaction between different materials

2.13 SIMULATION OF DIAGONAL COMPRESSION TEST ON RETROFITTED MASONRY PANEL

As discussed earlier, the three constituent materials used in strengthened specimens were modeled separately. Masonry was modeled using solid 8-noded linear hexahedral elements (C3D8). The two layers of the mortar used to cover the WWM reinforcement on the two sides of masonry panels were also modeled using 8-noded linear hexahedral elements (C3D8) as shown in Figure 2.36. The WWM reinforcement was modeled using 2-noded linear truss element (T3D2) (Rai and Goel 1996) as shown in Figure 2.35. This reinforcement was embedded inside mortar (Lee et al. 2008). The reinforcement was considered on two sides of masonry and the mortar was applied/ modeled as discussed in the strengthening procedure in Figure 2.3. Figure 2.36 depicts the FE meshing of composite of strengthened masonry panel.

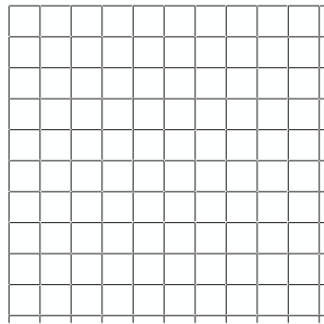


Figure 2. 35 : Linear 2-noded truss element (T3D2) used for modeling of WWM in simulation of diagonal shear test of strengthened masonry panel

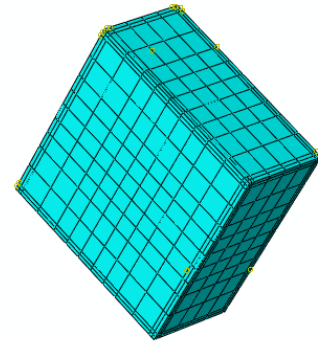


Figure 2. 36 : Meshing of composite masonry-WWM- coarse sand panel

Figure 2.37 depicts the loading and support conditions in modeling of strengthened masonry panel subjected to diagonal compression test. The numerical results of both high strength and low strength mortar strengthened panels in terms of distribution of minimum (tensile) principal stress and the corresponding global deformation has been shown in Figure 2.38 as the maximum compression load. In the experimental study, failure initiated in the form of diagonal cracks which were distributed within middle one third of the horizontal diagonal of the panels. These diagonal cracks developed into major cracks at the later stage and local crushing of masonry along the mortar took place near the loading and support shoes. Similar behavior was observed in this simulation and corresponding tension damage for both these specimens is shown in Figure 2.39.

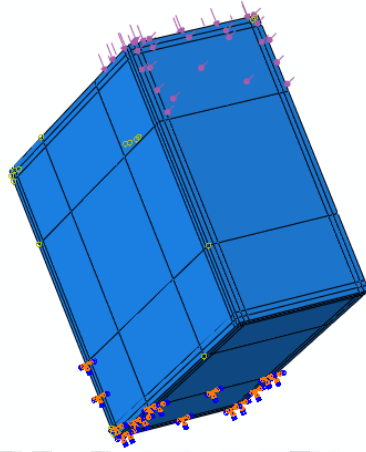
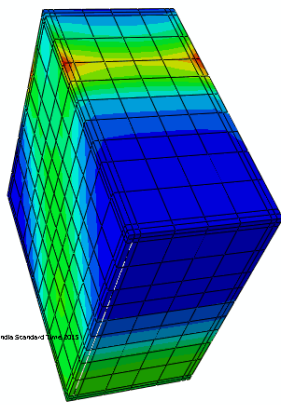
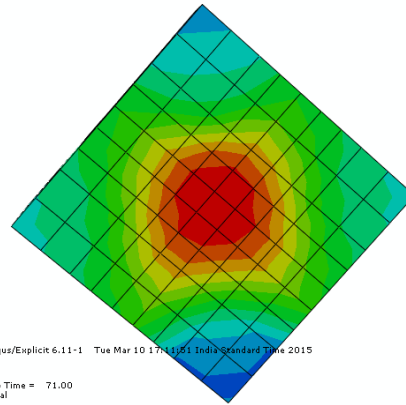


Figure 2. 37 : Modeling of loading and support condition in case of strengthened masonry panels



1:4



1:6

Figure 2. 38 : Minimum principal stress and deformation of 1:4 and 1:6 strengthened masonry panel

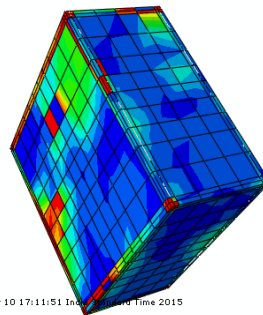
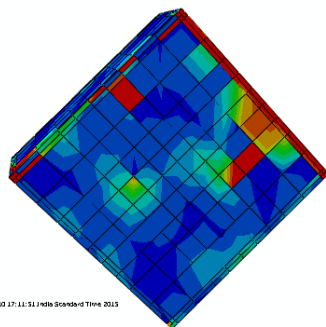


Figure 2. 39 : Tension damage of 1:4 strengthened masonry panel

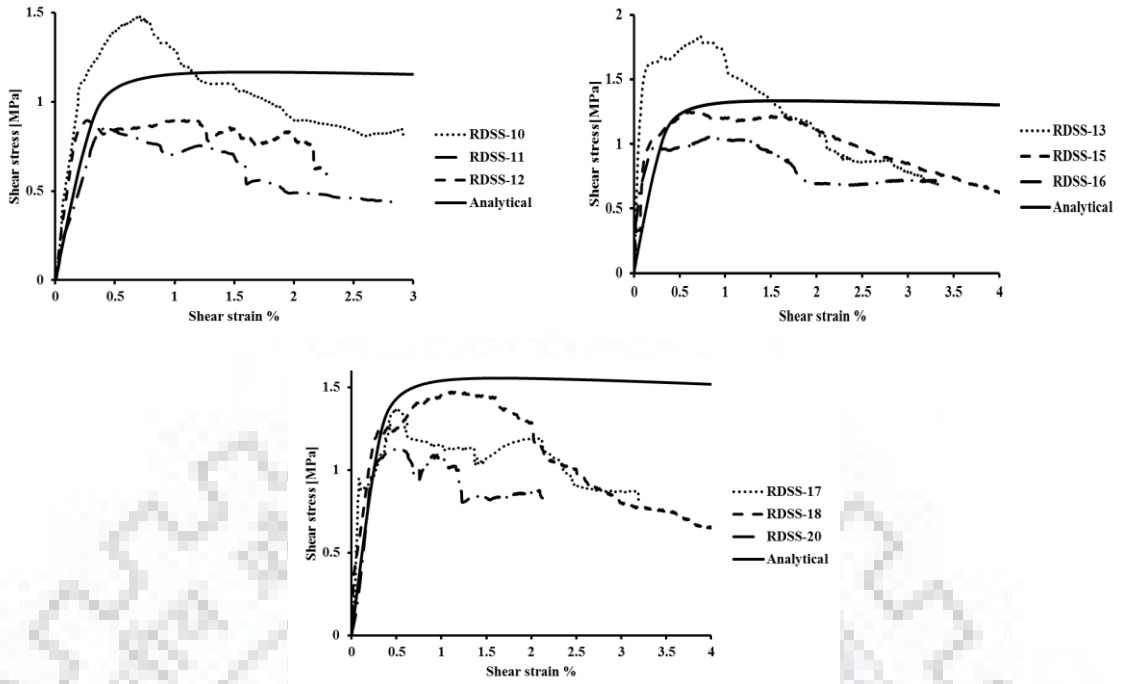


Figure 2.40 : Numerical and experimental shear stress vs shear strain curves for 1:4 strengthened masonry panel

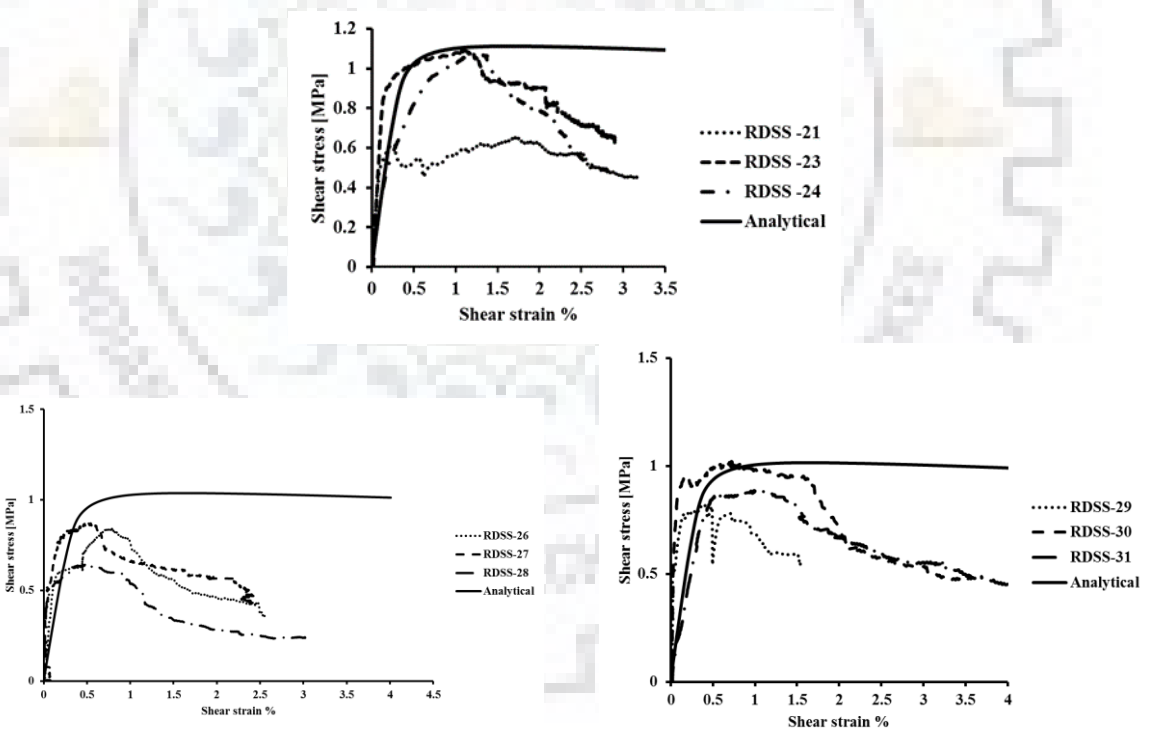


Figure 2.41 : Numerical and experimental shear stress vs shear strain curves for 1:6 strengthened masonry panel

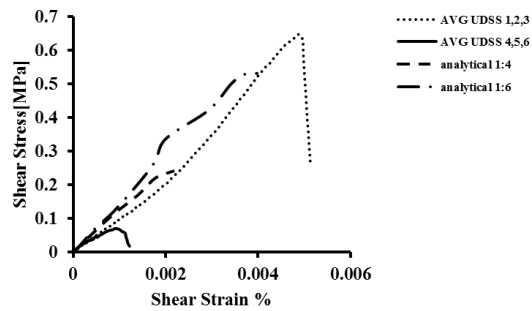


Figure 2. 42 : Numerical and experimental shear stress vs shear strain curves for unreinforced masonry panel

The numerically simulated shear stress-shear strain curves are compared with the experimental test results in Figures 2.40 and 2.41. The study showed that the numerical results are closely agreeing with the trend of experimental results. It is also noted that contours of tension damage, predicted numerically resemble with the crack pattern observed during the tests.

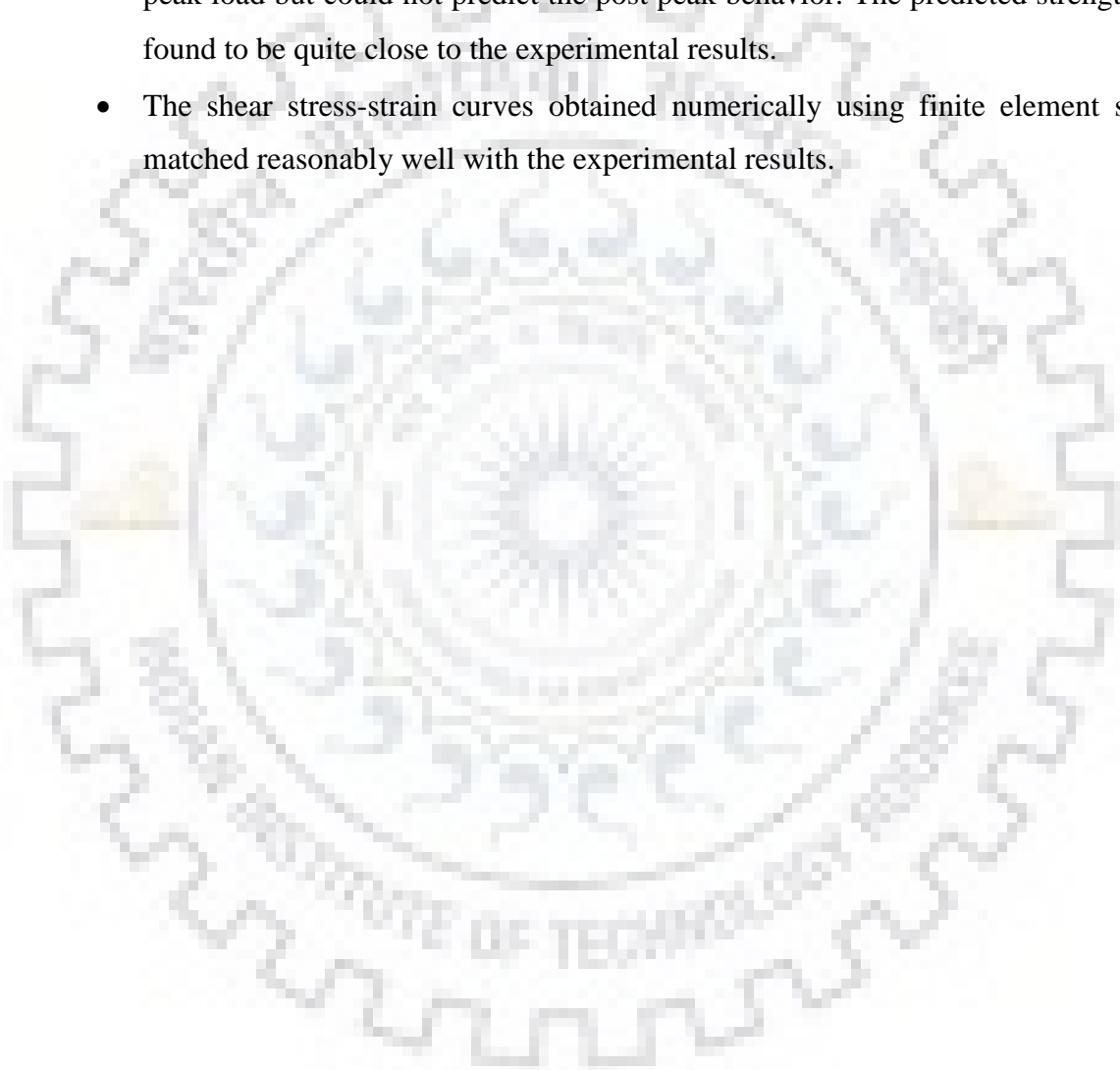
2.14 SUMMARY

In this study, the in-plane behavior of both URM and reinforced masonry is evaluated and studied according to ASTM guidelines, under displacement control loading. The test specimens were constructed using bricks and the dimensions of the specimens were chosen as per ASTM guidelines. The behavior of the test specimens was studied in terms of failure modes and shear stress vs shear strain plots.

The experimental behavior was simulated using finite element analysis. CDP model has been used to model the non-linear inelastic behavior of masonry, as it was successfully used in earlier studies by other researchers. The simulation has been used to evaluate shear stress-shear strain and load deflection curves under in-plane tests. The findings of this study are summarised as follows.

- The behavior of URM specimens in diagonal shear test has been observed as combination of diagonal failure and sliding shear failure modes. These URM specimens failed in a sudden brittle manner, by the formation of cracks along the loaded diagonal.
- The proposed reinforcement technique confines the masonry well intact between the WWM layers along with thin mortar layer. The shear strength of strengthened specimen has found to increase at an order of 4 when compared to URM specimens.
- The ductility ratio of URM specimen after strengthening increased up to 2 to 5 times.

- The relative increase in shear strength due to strengthening, observed in the present study, which was much higher compared to the other procedures used in earlier studies available in the literature. This is mainly due to the much lower shear strength of the original URM.
- The WWM reinforced samples showed significant increase in shear strength and ductility. Compared to unreinforced masonry specimen.
- It was observed that non-linear finite element simulation using CDP model could predict the behavior of URM specimens under in-plane shear loading quite reasonably up to the peak load but could not predict the post peak behavior. The predicted strength was also found to be quite close to the experimental results.
- The shear stress-strain curves obtained numerically using finite element simulation, matched reasonably well with the experimental results.





CHAPTER – 3

OUT-OF-PLANE BEHAVIOR OF UNREINFORCED AND REINFORCED MASONRY PANELS

3.1 INTRODUCTION

URM is the oldest building technique which is still commonly used in many developing countries either as load bearing structure or as infill in RCC structures. URM, which is less ductile, are subjected to severe damage during an earthquake. The earthquake damage history suggests that the most life loss has been due to collapse of masonry structures. Most of the historical monuments and most official government buildings are made of masonry which is at high risk during the earthquake and is in high demand to be preserved (D'Ambrisi et al. 2013). Recently grouting, FRP, RC jacket, ferrocement techniques are commonly used in restoration/strengthening of masonry buildings (Ashraf et al. 2012, Papanicolaou et al. 2011, Kadam et al. 2015)

In the past, it was observed that most of the masonry structure failed in out-of-plane action. During an earthquake, URM buildings experience seismic loading in both in-plane and out-of-plane. However, their relative magnitude depends on the type of diaphragm i.e., how the wall is connected to the roof. The structural wall perpendicular to seismic motion is subjected to out-of-plane bending which results in out-of-plane failure featuring vertical cracks at the corner and in the middle of the wall (Lourenço et al. 2000, Tomazevic 1996). Unreinforced masonry buildings are most vulnerable to out-of-plane failure. The causes of the out-of-plane failure of the wall are inadequate anchorage of the masonry wall into the roof diaphragm and limited tensile strength of the masonry and mortar. The resulting flexural stress apparently exceeds the tensile strength of the masonry leading to its rupture followed by collapse. Out-of-plane wall movement is characterized by the partial collapse of the exterior wall, by wythe separation or peeling off of the outer wythe or veneer units, and by cracks at lintel and top of slender piers near the opening. These types of failure were almost non-existent in lower storeys. It's found that the slenderer the wall the more it's prone to out-of-plane failure. Out-of-plane action can be resisted by intermediate support wall or buttress but it is not a proper solution. In case of a building which is to be newly constructed, seismic band can be provided at the lintel level in the wall to reduce the height, but there are limitations in case of existing structures. Nearly one third of the world

population is still living in masonry structure. The most crucial thing is that, in the past, the masonry buildings were constructed without any consideration of earthquake resistance. Though the codal provisions provide guidelines for earthquake resistant features, it has not been followed due to the ignorance of people or the additional cost involved.

In the past lot of studies has been carried out to study the out-of-plane behavior of masonry strengthened using various materials, a few of which has been selected and are discussed here. Kadam et al. (2015) have tested 6 URM panels and 12 panels strengthened with WWM and micro concrete under flexure. The results show that the URM panels exhibit sudden brittle failure whilst strengthened panels failed in a ductile fashion and exhibited a significant increase in the flexural strength. Bajpai et al. (2003) investigated the behavior of masonry beams strengthened using the (Near Surface Mounted) NSM technique. They named the beams with two layers of bricks as narrow beams and those with more than two layers as wide beams. FRP bars were inserted in pre-cut grooves between these layers. The technique was shown to be effective on both types of beams. Significant increase in flexural capacity and ductility of strengthened masonry is the common outcome of most of the experimental studies carried out using FRP as strengthening material (Bajpai et al. 2003, El Gawady et al. 2004, Bencardino et al. 2004, Khaled et al. 2010 Papanicolaou et al. 2008, Kadam et al. 2014)

Usage of polymeric grid is commonly used in practice for strengthening these days, the WWM is a commonly available material and is economical and easy to apply compared to other grid, and it is widely being used to strengthen existing masonry structures. (Papanicolaou et al. 2008, Kadam et al. 2014)

3.2 RESEARCH SIGNIFICANCE

In the present study, strengthening technique recommended by IS 13935: 2009 for masonry structures using WWM has been experimentally investigated. The guidelines of IS code has been followed in this study and the behavior of reinforced masonry strengthened with WWM (of various sizes 1 inch, 1.5 inch, 2 inch spacing) and mortar. Out-of-plane behavior of unreinforced masonry has also been evaluated experimentally. Both high (1:4) and low strength mortar (1:6) was chosen as both these types of mortars are commonly used in construction practice in India. The out-of-plane behavior of both URM and strengthened masonry was studied based on flexure test according to ASTM E518-10. The relative increase in strength, ductility, and stiffness has been estimated.

3.3 EXPERIMENTAL PROGRAM

This experimental program consisted of 8 sets of specimens out of which 2 sets were URM and 6 sets of reinforced masonry (RM) specimen. The details of the specimen are given in Table 3.1. All specimens were of two wythe thickness as in practice all load bearing walls are constructed with two wythe thickness. The URM specimens were 1000 mm long, 500 mm wide and 230 mm thick. All the test samples were constructed and cured as per site condition. The test samples were strengthened after its curing.

3.4 STRENGTHENING PROCEDURE

The test samples were strengthened as per IS 13935: 2009. Drill holes of 8 mm diameter were made at an interval of 300 mm on the test samples for inserting 4 mm diameter mild steel rod for anchorage in the later stage of strengthening. These 4 mm rods passing through the holes transferred the shear at the WWM masonry interface through dowel action. The samples to be strengthened were initially watered and cleaned with the help of a steel wire brush to remove dirt if any. Then a layer of cement grout slurry was applied with the help of a paint brush to provide better bond between the mortar and the masonry surface. Care was taken to close the drill holes with the help of wooden or steel rods to avoid its blockage during application of mortar. A layer of 10 mm thick 1:3 coarse sand mortar was applied above the cement slurry surface to level the uneven masonry surface as well as to provide better grip for the WWM and second layer of mortar, the mortar surface was roughened with the help of a steel wire brush. The WWM was placed and anchored with the help of a 4 mm diameter mild steel rod, the rods were bent over the WWM on the two sides in opposite direction, the hole was grouted with the help of a high pressure grout pump, to hold the rod in position. A layer of cement grout (1:3 coarse sand mortar) was applied above the WWM, and the surface was levelled. The sequential process of strengthening is shown in Figure 3.1. The strengthened panels were cured under normal site condition for another 28 days.



Figure 3. 1 : Stages strengthening unreinforced specimen with WWM

Table 3. 1 : Specimen details

Set	Specimen	Mortar ratio	Strengthening
Set-1	URMFST-1	1:4	URM panel
	URMFST -2		
	URMFST -3		
	URMFST -4		
Set-2	URMFST -5	1:6	URM panel
	URMFST -6		
	URMFST -7		
	URMFST -8		
Set-3	RMFST-9	1:4	URM panel strengthened with 1 inch spacing WWM and 1:3 coarse sand mortar
	RMFST-10		
	RMFST-11		
	RMFST-12		
Set-4	RMFST-13	1:4	URM panel strengthened with 1.5 inch spacing WWM and 1:3 coarse sand mortar
	RMFST-14		
	RMFST-15		
	RMFST-16		

Set-5	RMFST-17 RMFST-18 RMFST-19 RMFST-20	1:4	URM panel strengthened with 2 inch spacing WWM and 1:3 coarse sand mortar
Set-6	RMFST-21 RMFST-22 RMFST-23 RMFST-24	1:6	URM panel strengthened with 1 inch spacing WWM and 1:3 coarse sand mortar
Set-7	RMFST-25 RMFST-26 RMFST-27 RMFST-28	1:6	URM panel strengthened with 1.5 inch spacing WWM and 1:3 coarse sand mortar
Set-8	RMFST-29 RMFST-30 RMFST-31 RMFST-32	1:6	URM panel strengthened with 2 inch spacing WWM and 1:3 coarse sand mortar

3.5 INSTRUMENTATION AND TEST SETUP

Testing of both RM and URM samples were carried out as per ASTM E518-10 standard guidelines to study their out-of-plane behavior. The specimens were tested under four-point loading condition as shown in Figure 3.2. The experimental test setup can be seen in Figure 3.2. As masonry is very brittle, much care was taken while transporting the samples from casting yard until it was placed on the machine for testing. Load controlled loading was applied such that the test completes approximately in 2-3 minutes. Four linear variable displacement transducers (LVDT) were used to measure the displacement, two at the mid span in either direction and two at 100 mm from the support in both directions to measure the deflection at that point. The instrumentation setup can be clearly seen in Figure 3.2. The LVDT was connected to the inbuilt data acquisition system.

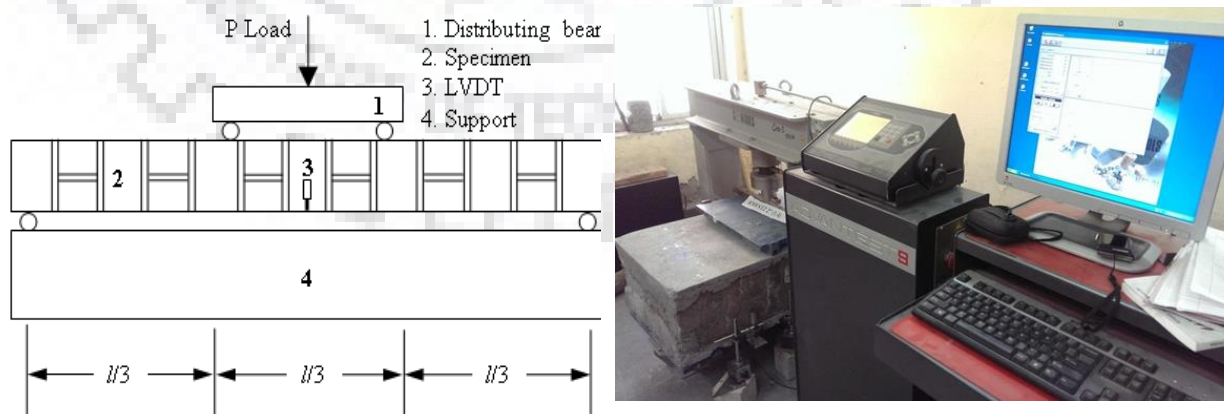


Figure 3. 2 : Test set up

3.6 TEST OBSERVATION AND FAILURE MODES

The failure pattern and test observations are summarised in Table 3.4. In case of set 1 and 2 specimens, a typical bed joint failure parallel to the mortar joint was observed. In most of the reinforced masonry specimen, i.e., set 3-8 diagonal shear failure was predominant in most except in a few specimens (RMFST-21, 23, 24). In the set 3 and 6 i.e., in specimen reinforced with 1 inch spacing WWM, rupture of reinforcement was observed in tension zone. In set 4 and 7 the failure initiated as shear crack (Table 3.4) failure of reinforcement (WWM) was not experienced, breaking noise was heard during testing, reinforcement yielded and failure of anchorage was also observed in few cases (RMFST-10). Slight debonding was observed in samples reinforced with 1.5 inch spacing WWM. In set 5 and 10, shear crack was observed, except RMFST-19. In no other cases, reinforcement failure was observed. Though failure initiated near loading point, it ended up near support resulting in slight debonding, which was not permitted by the provided anchorage.

The observed strength of strengthened panels was independent of the grade of mortar used in masonry, as the contribution of masonry in bending tension was negligible and being under reinforced sections, the bending strength was governed by tension reinforcement. Hence there was not much remarkable variation as such in the strength gained by strengthened masonry specimens as the grade of mortar used for strengthening was same in all specimens.

3.6.1 Strength, Stiffness and Deformation Characteristics

The performances of both the reinforced and URM samples were assessed through the load-deflection curves Figures 3.4 to 3.9; the ultimate load capacity, stiffness and ductility were also assessed. The load-deflection curves shown in Figures 3.4 to 3.9 and results are summarized in Tables 3.2 and 3.3. The yield load P_y was the applied load at which the yield starts and P_u , ultimate load. The ductility indexes can be defined as,

Deflection ductility, $\mu_\Delta = \Delta_u / \Delta_y$

Energy ductility, $\mu_E = E_u / E_y$

where,

Δ_u = mid span deflection at ultimate load

Δ_y = mid span deflection at tension steel yielding

E_u = area under the load-deflection diagram at ultimate load

E_y = area under the load-deflection diagram up to yielding of tension steel

The secant stiffness is given by the ratio of ultimate measured load to the deflection corresponding to peak. The energy dissipation is usually defined as the area under the load-deflection curve. The energy capacity values were calculated up to the P_{umax} on the load-deflection curve. The ductility of structural members is considered one of the most critical parameters for evaluating its performance. Based on the load-deflection response of the samples, ductility can be measured in terms of deflection ductility, energy ductility or the energy absorption capacity of the sample. Ductility characterizes the deformation capacity of members (structures) after yielding, or their ability to dissipate energy. In general, ductility is a structural property which is governed by fracture of the structural member.

In this study, the ductility, stiffness, strength is compared to the low strength mortar sample (1:6) and high strength masonry samples (1:4) strengthened with various reinforcement ratios. With reference to Figures 3.4 to 3.9 and Tables 3.2 and 3.3, it is observed that the reinforced low strength mortar specimen behaved in more ductile manner as compared to strengthened high strength mortar specimen. The performance of 1.5 inch spacing reinforced specimen was much better (in terms of ductility) as compared to specimen reinforced with 1 inch and 2 inch spacing WWM. From the graph, it is observed that all the strengthened flexure specimen behaves in a non-linear manner and the post peak behavior showed gradual strain softening in the case of high strength mortar specimen and steep slope was observed in case of low strength mortar specimen.

The flexural load carrying capacity of masonry has significantly increased in the order of 4 in case of strengthened specimen compared to that of conventional masonry. This shows the effectiveness of the strengthening technique which can be clearly seen in Table 3.2.

The effect of strengthening in case of moment capacity is given in Table 3.2. It is observed that the moment carrying capacity has increased in the order of 2 compared to conventional masonry. It is observed that the strengthening technique adopted has enhanced the ductility and strength of masonry but however, it is much lower than that of RC beam. This was due to lower ductility of WWM compared to reinforcing steel used in conventional RC structure

The initial stiffness of both reinforced high strength mortar specimen and low strength mortar specimen were same except in 2 inch spacing WWM reinforced specimen. The secant stiffness, i.e., stiffness after achieving yield point, was more in case of reinforced high strength mortar specimens compared to that of low strength mortar specimens.

Further investigations are required to study the strain distribution in WWM and masonry and to exactly understand the failure mechanism of strengthened masonry panels.

Table 3.2 : Test results

Specimen	ρ_v (%)	ρ_h (%)	p_{max}	Avg. p_{max}	Δ_{max}	Avg. Δ_{max}	R	R/R _o	Avg. R/R _o
URMFST-1	0	0	5	4	0.7	0.47	0.54		
URMFST -2	0	0	3		0.3		0.33		
URMFST -3	0	0	4		0.4		0.44		
URMFST -4*	0	0	-	-	-	-	-	-	-
URMFST -5	0	0	2.5	2.2	1.4	0.86	0.28		
URMFST -6	0	0	1.6		.9		0.18		
URMFST -7	0	0	2.5		.3		0.28		
URMFST -8*	0	0	-	-	-	-	-	-	-
RMFST-9	0.10	0.10	73.25	78.54	3.62	6.59	9.93	22.57	24.20
RMFST-10	0.10	0.10	73.14		6.19		9.91	22.54	
RMFST-11	0.10	0.10	78.6		9.39		10.65	24.22	
RMFST-12	0.10	0.10	89.2		7.16		12.09	27.47	
RMFST-13	0.12	0.13	89	83.66	4.69	8.59	12.06	27.41	25.77
RMFST-14	0.12	0.13	86		12.73		11.65	26.49	
RMFST-15	0.12	0.13	76		8.3		10.30	23.42	
RMFST-16*	0.12	0.13	-	-	-	-	-	-	-
RMFST-17	0.12	0.11	58	65	4.69	5.64	7.87	17.89	22.27
RMFST-18*	0.12	0.11	94	-	-	-	-	-	-
RMFST-19	0.12	0.11	68		6.37		9.22	20.96	
RMFST-20	0.12	0.11	69		5.88		9.35	21.27	
RMFST-21	0.10	0.10	77	74.3	3.943	5.62	10.44	41.76	37.30
RMFST-22	0.10	0.10	91		8.47		12.33	49.33	
RMFST-23*	0.10	0.10	52	-	-	-	-	-	-
RMFST-24	0.10	0.10	55		4.46		7.46	29.86	
RMFST-25	0.12	0.13	51	62.25	8.5	9.24	6.92	27.70	33.78
RMFST-26	0.12	0.13	75		10.03		10.17	40.68	
RMFST-27	0.12	0.13	63		8.03		8.54	34.19	
RMFST-28	0.12	0.13	60		10.4		8.14	32.57	
RMFST-29	0.12	0.11	31	40	2.84	9.04	4.22	16.89	21.75
RMFST-30	0.12	0.11	54		3.96		7.33	29.32	
RMFST-31	0.12	0.11	35		2.24		4.76	19.05	
RMFST-32*	0.12	0.11	-	-	-	-	-	-	-





Damaged specimen, irrelevant data*

Table 3.3 : Stiffness and ductility

Specimen	Yield		Ultimate		Ductility factor Δ_u/Δ_y	Stiffness		E_u	E_y	Energy ductility $\mu_E=E_u/E_y$
	P_y (kN)	Δ_y (mm)	P_u (kN)	Δ_u (mm)		Initial	Secant			
RMFST-9	72	3.2	63.5	5.1	1.60	22.71	12.48	254	121	2.09
RMFST-10	71	4.4	73.1	6.19	1.39	15.98	11.81	280	153	1.83
RMFST-11	68	3.7	73.7	10.7	2.89	16.75	6.88	606	109	5.59
RMFST-12	82	6.3	85	7.2	1.13	12.8	11.78	322	234	1.37
RMFST-13	85	4.4	81.1	5.15	1.17	19.43	15.75	232	171	1.35
RMFST-14	58	5	82.6	13.2	2.65	11.6	6.22	799	174	4.59
RMFST-15	44	2.6	67.5	10.2	3.84	16.79	6.61	545	63	8.65
RMFST-16*	-	-	-	-	-	-	-	-	-	-
RMFST-17	55	4.4	49.1	6.2	1.4	12.6	7.39	216	119	1.81
RMFST-18*	-	-	-	-	-	-	-	-	-	-
RMFST-19	66	5.9	59.5	8.08	1.36	11.14	7.36	344	204	1.68
RMFST-20	60	4.4	64.4	6.61	1.48	13.51	9.75	287	144	1.99
RMFST-21	74	3.0	69.9	4.9	1.59	24.05	14.26	263	127	2.07
RMFST-22	81	5.4	84.6	10.9	2.01	15	7.67	691	280	2.47
RMFST-23*	-	-	-	-	-	-	-	-	-	-
RMFST-24	54	4.2	46.8	6.19	1.47	12.9	7.55	213	108	1.97
RMFST-25	46	2.6	41.7	13.4	5.17	17.6	3.09	587	59	9.94
RMFST-26	64	4.1	66.7	11.2	2.75	15.6	5.91	622	139	4.47
RMFST-27	55	4.1	53	10.0	2.46	13.6	5.25	464	138	3.36
RMFST-28	54	3.8	58.4	9.47	2.49	14.2	6.17	459	109	4.21
RMFST-29	30	1.8	24.7	4.16	2.25	16.4	5.95	95	29	3.27
RMFST-30	51	1.7	47.3	6.34	3.62	29.1	7.46	280	70	4
RMFST-31	34	2.1	27.1	3.6	1.65	15.6	7.56	87	40	2.17
RMFST-32*	-	-	-	-	-	-	-	-	-	-

Damaged specimen, irrelevant data *

Table 3. 4 : Test observations and failure pattern

Specimen	Failure pattern	Remarks/observation
URMFST-1		✓ Cracking (Debonding) along the bed joint
URMFST -2		✓ Cracking (Debonding) along the bed joint
URMFST -3		✓ Cracking (Debonding) along the bed joint
URMFST -4*	-	-
URMFST -5		✓ Cracking (Debonding) along the bed joint

URMFST -6



- ✓ Cracking (Debonding) along the bed joint

URMFST -7



- ✓ Cracking (Debonding) along the bed joint

URMFST -8



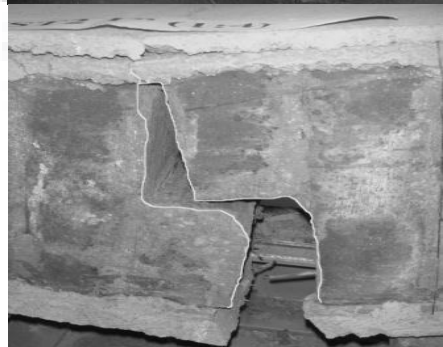
- ✓ Cracking (Debonding) along the bed joint

RMFST-9



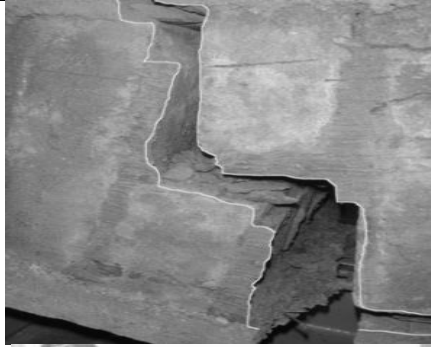
- ✓ Shear failure
- ✓ No reinforcement failure

RMFST-10



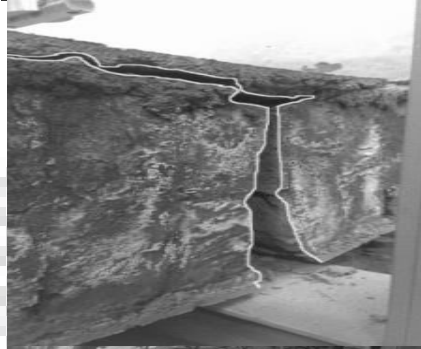
- ✓ Reinforcement ruptured
- ✓ Shear failure
- ✓ Anchorage failure was observed

RMFST-11



- ✓ Reinforcement failure in tension zone
- ✓ Ductile shear failure
- ✓ Cracks were observed in compression zone

RMFST-12



- ✓ Flexure failure at centre
- ✓ Reinforcement failed in tension

RMFST-13



- ✓ Brittle shear failure
- ✓ No reinforcement damage
- ✓ Mortar joint failure

RMFST-14



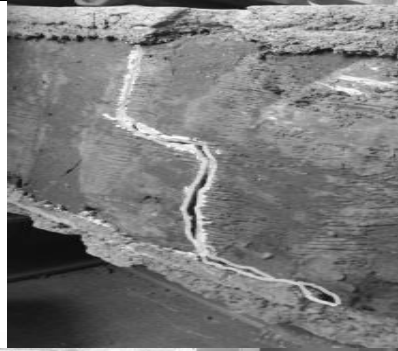
- ✓ Failure was experienced at both loading point
- ✓ Shear failure
- ✓ Cracks in compression zone
- ✓ Spalling of mortar was observed in tension zone

RMFST-15



- ✓ slight debonding was observed
- ✓ poor workmanship

RMFST-16



- ✓ shear crack
- ✓ crack in tension zone

RMFST-17



- ✓ both shear and parallel head joint failure was observed
- ✓ No crack in comp zone
- ✓ Cracks in tension zone

RMFST-18



- ✓ No crack in compression zone
- ✓ Cracks were observed in tension zone
- ✓ Complete failure was not experienced till 95 kN
- ✓ Shear crack

RMFST-19



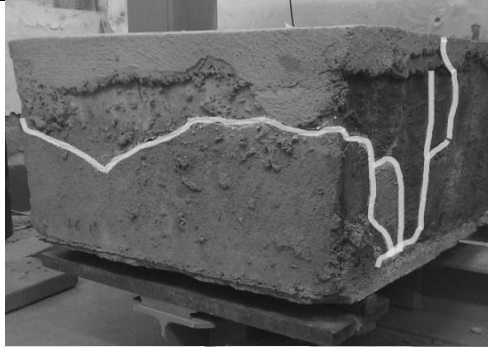
- ✓ Tension failure
- ✓ Reinf failed only in tension zone
- ✓ Shear failure

RMFST-20



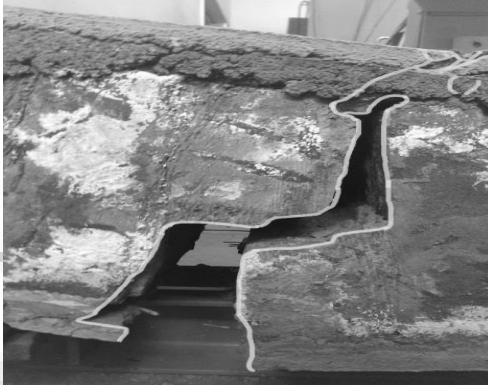
- ✓ Shear brittle failure
- ✓ No crack in compression zone
- ✓ No reinforcement failure

RMFST-21



- ✓ Head joint cum toothed failure
- ✓ No reinforcement failure

RMFST-22



- ✓ Shear failure
- ✓ Reinf rupture completely in tension zone
- ✓ Cracks in compression zone

RMFST-23



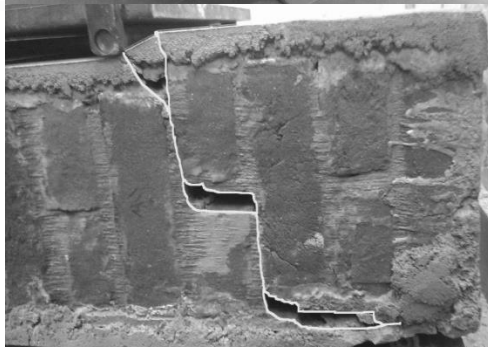
- ✓ Toothed shear failure
- ✓ Cracks in comp zone
- ✓ Brick failure was observed

RMFST-24



- ✓ Toothed shear failure

RMFST-25



- ✓ Crack in compression zone
- ✓ Debonding in tension zone
- ✓ Failure of anchorage
- ✓ Weld failed at few location in WWM
- ✓ No failure of mesh reinf

RMFST-26



- ✓ Shear failure
- ✓ Reinf yielded
- ✓ Crack in compression zone
- ✓ Mesh weld failed
- ✓ Anchorage failed

RMFST-27



- ✓ Shear crack
- ✓ Debonding in tension zone
- ✓ Cracks in compression zone

RMFST-28



- ✓ Shear failure near both loading point
- ✓ Reinf yielded
- ✓ Crack in both tension and comp zone

RMFST-29



- ✓ Shear crack
- ✓ No crack in comp zone

RMFST-30



- ✓ Shear crack
- ✓ Debonding in tension zone
- ✓ Cracks in compression zone

RMFST-31



- ✓ Shear crack
- ✓ No Cracks in compression zone
- ✓ Failure near support

Specimen damaged before testing *

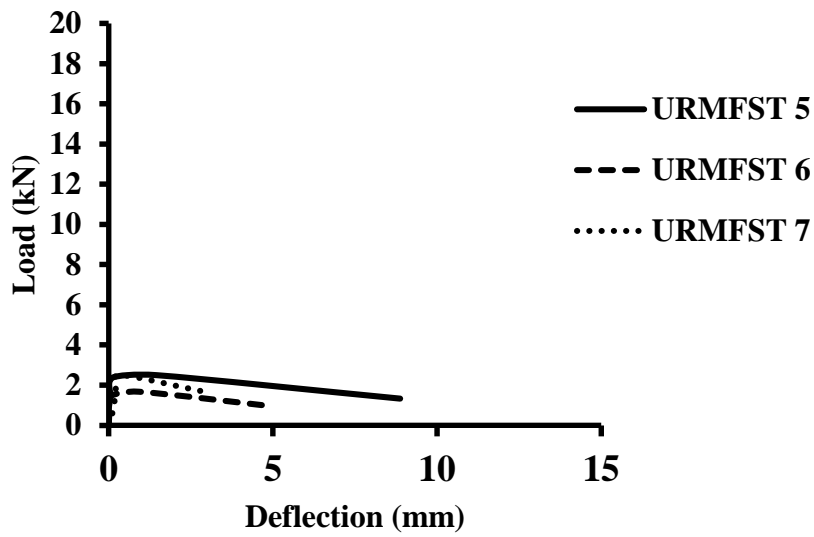


Figure 3. 3 : Load-deflection behavior of low strength URM sample

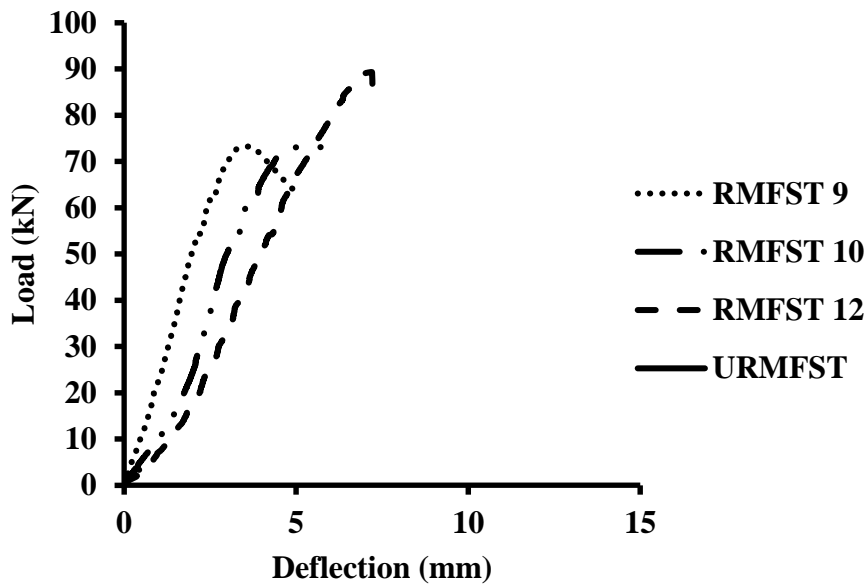


Figure 3. 4 : Load-deflection behavior of high strength masonry reinforced with 1 inch spacing WWM and 1:3 mortar

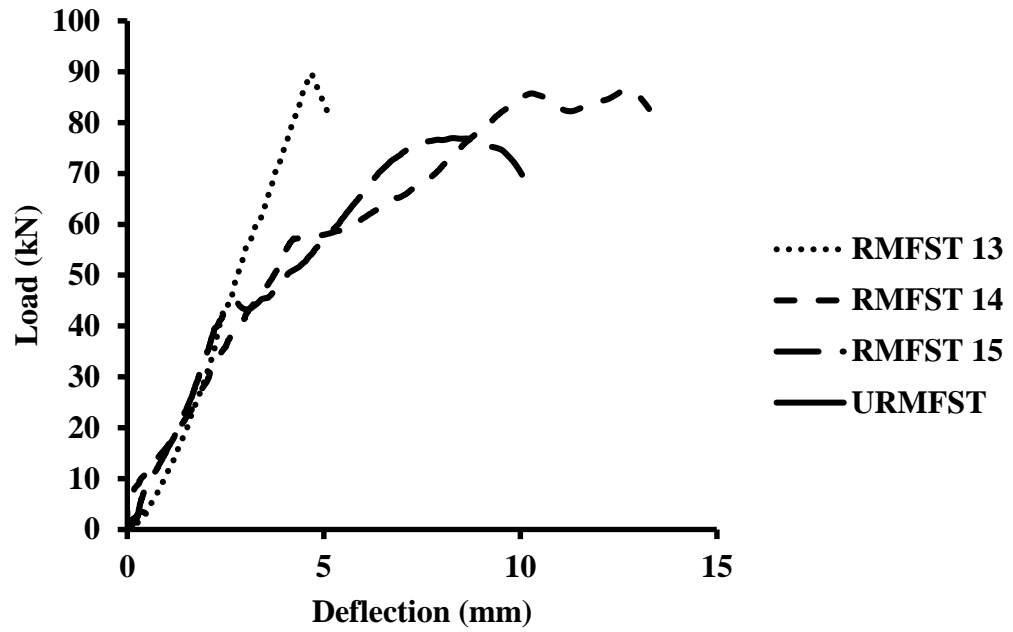


Figure 3. 5 : Load-deflection behavior of high strength masonry reinforced with 1.5 inch spacing WWM and 1:3 mortar

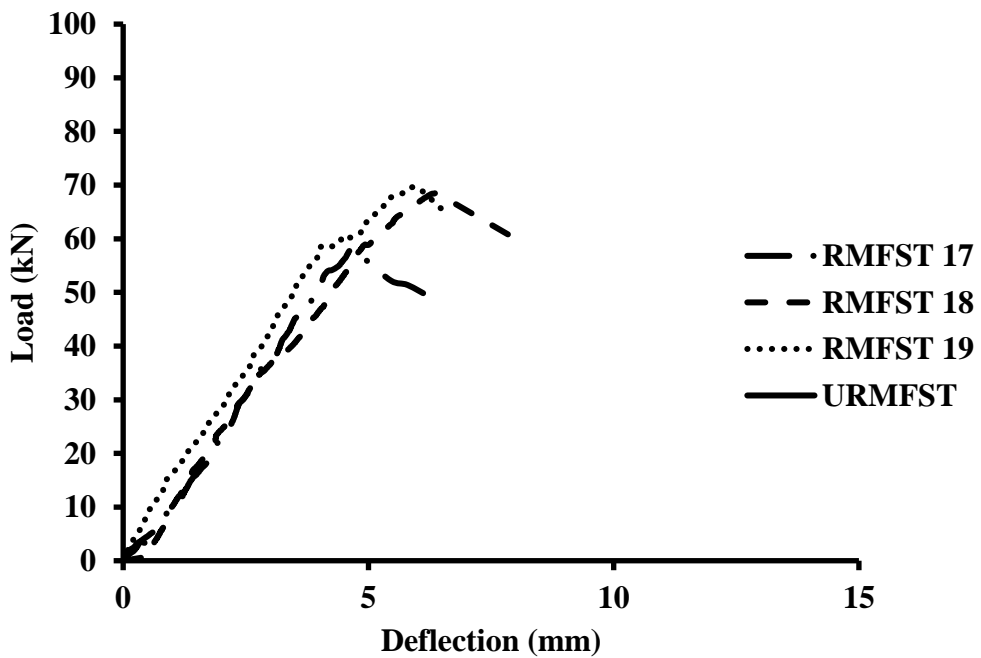


Figure 3.6: Load-deflection behavior of high strength masonry reinforced with 2 inch spacing WWM and 1:3 mortar

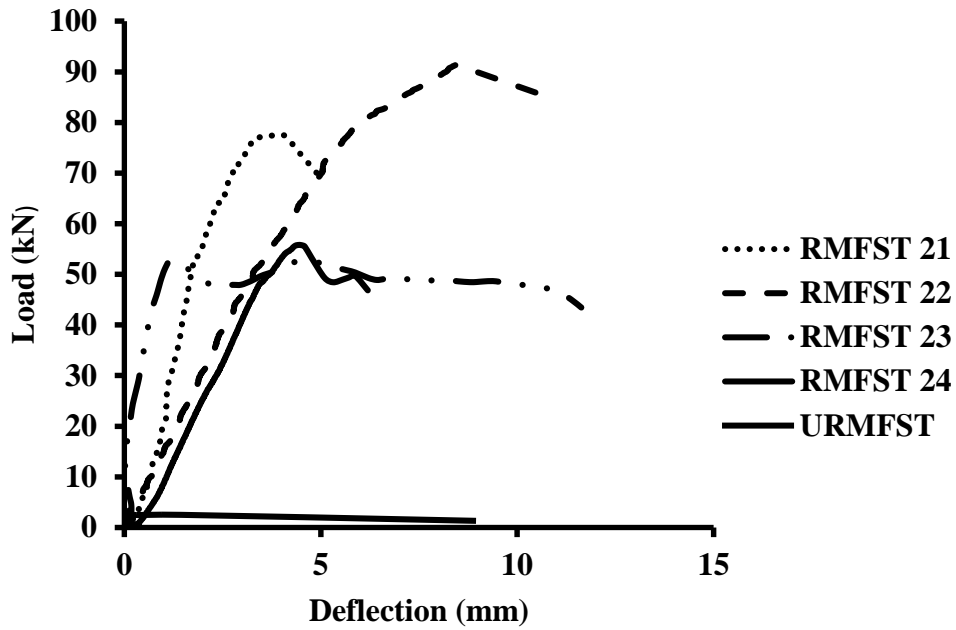


Figure 3.7 : Load-deflection behavior of low strength masonry reinforced with 1 inch spacing WWM and 1:3 mortar

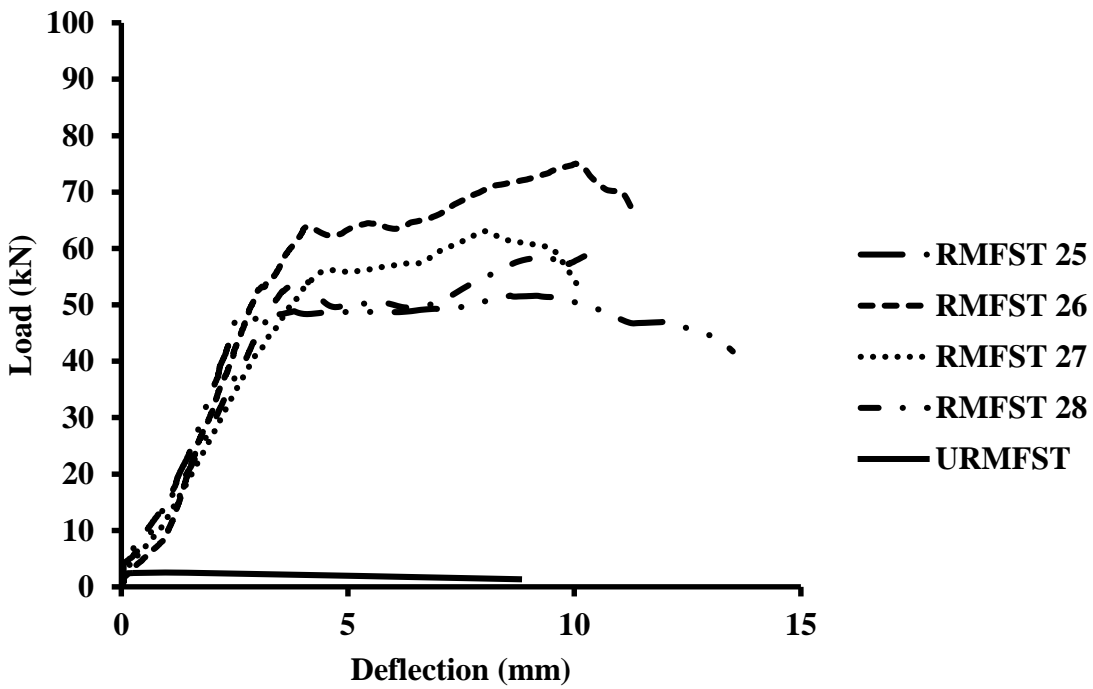


Figure 3.8 : Load-deflection behavior of low strength masonry reinforced with 1.5 inch spacing WWM and 1:3 mortar

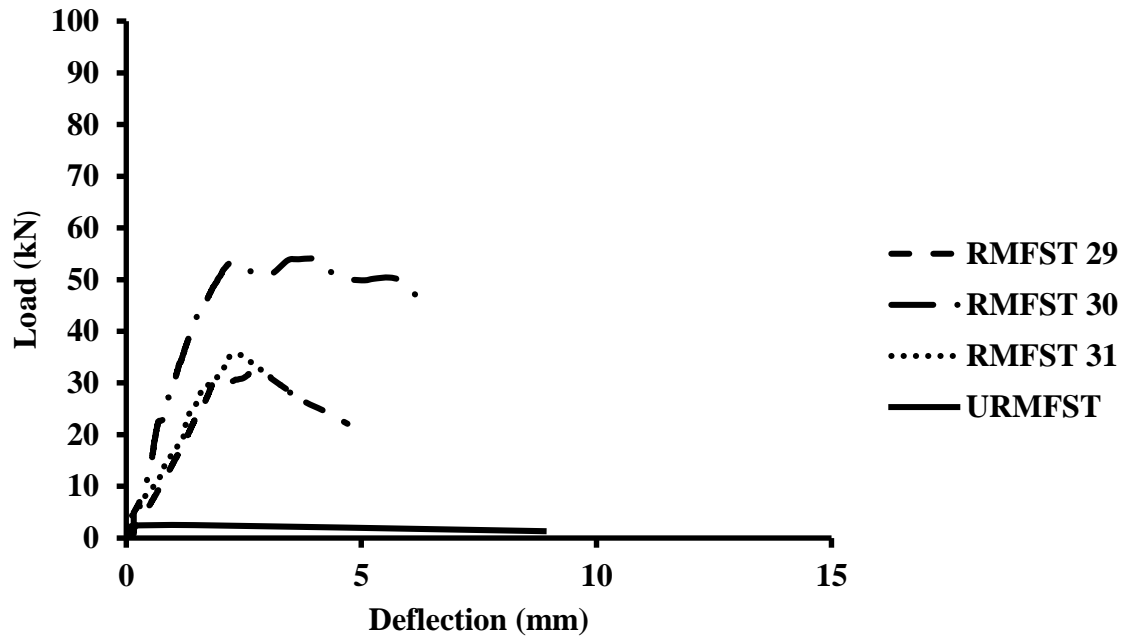


Figure 3. 9 : Load-deflection behavior of low strength masonry reinforced with 2 inch spacing WWM and 1:3 mortar

3.7 SIMULATION OF FLEXURE TEST ON RETROFITTED PANELS

The same micro modeling technique as discussed in the previous chapter for the diagonal compression test has been used to simulate the flexural behavior of strengthened masonry panels. The masonry and coarse sand mortar have been modeled using 8-noded linear hexahedral elements (C3D8) as shown in Figure 3.10, and the reinforcement grid has been modeled as 2-noded, linear truss elements (T2D2) as shown in Figure 3.11. Figure 3.12 depicts the mesh of composite strengthened panels and Figure 3.13 shows the loading and support conditions in modeling of strengthened panels subjected to flexure test.

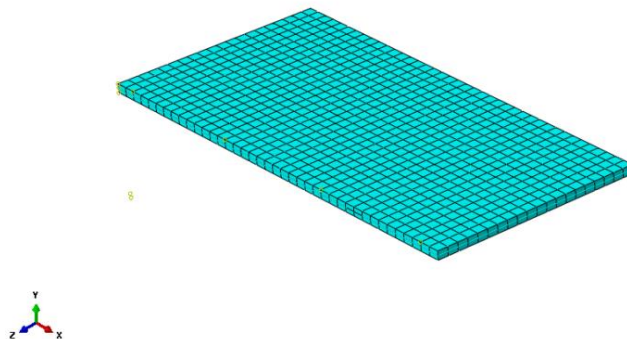


Figure 3. 10 : Solid 8-noded brick elements used for modeling of coarse sand mortar in flexure test simulation of strengthened panels

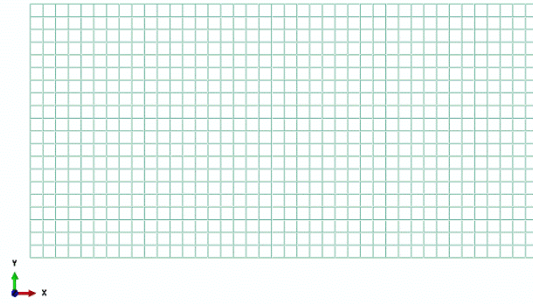


Figure 3. 11 : Linear 2-noded truss elements used for modeling of WWM

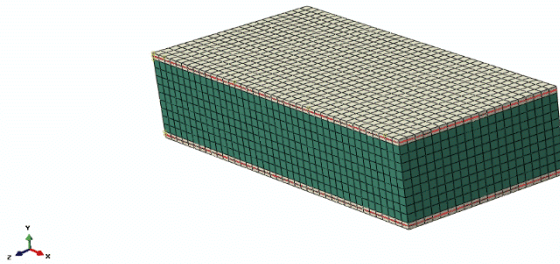


Figure 3. 12 : Meshing of composite masonry WWM-coarse sand panel in flexure test simulation of strengthened panels

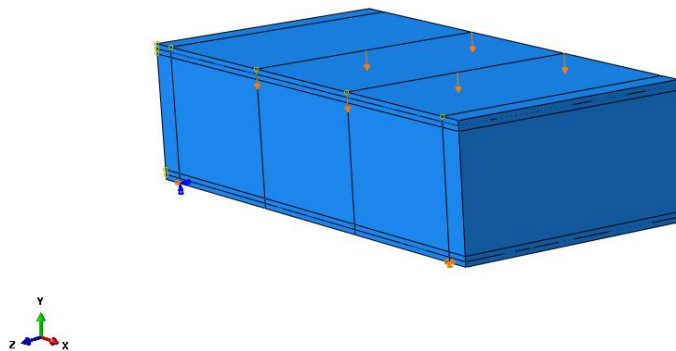


Figure 3. 13 : Modeling of loading and support conditions in flexure test simulation of strengthened panels

The numerical results of strengthened panels are shown in Figures 3.14 and 3.15, in terms of distribution of minimum principal stress and corresponding global deformation at the maximum flexure load. The tension damage for both the cases is shown in Figures 3.16 and 3.17. It has been noted that the pattern of tension damage in the numerical simulation resembles with the crack initiation and propagation in the experimental testing of the panels.

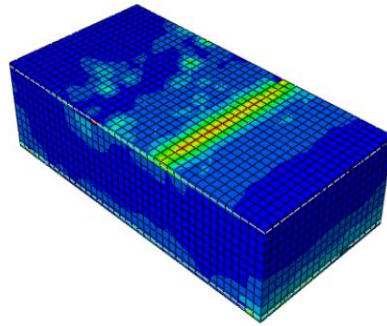


Figure 3. 14 : Minimum principal stress and deformation of strengthened masonry panel (1:4 masonry)

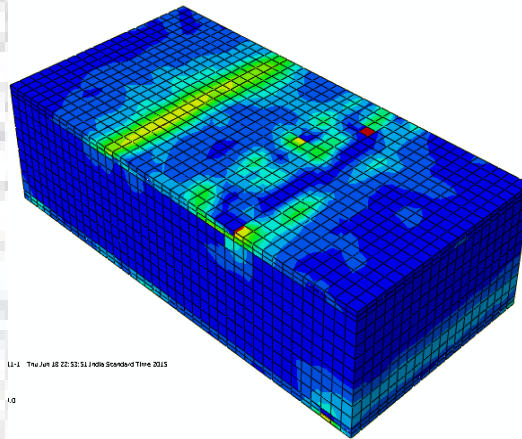


Figure 3. 15 : Minimum principal stress and deformation of strengthened masonry panel (1:6 masonry)

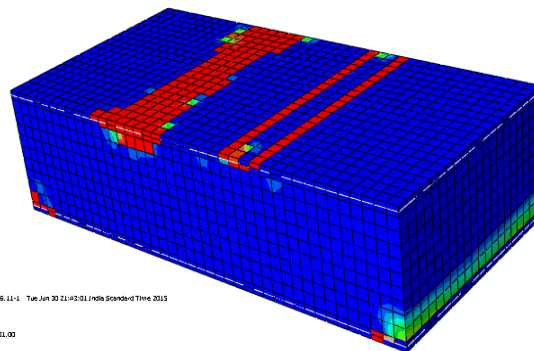


Figure 3. 16 : Tension damage of strengthened panel (1:4 masonry)

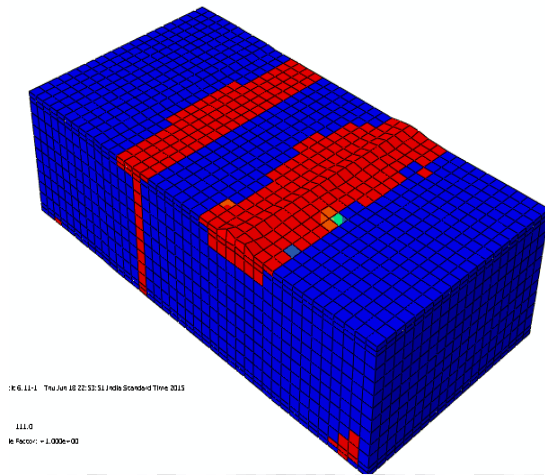


Figure 3. 17 : Tension damage of strengthened panel (1:6 masonry)

The numerical and experimental load-deflection curves for the flexure test on the strengthened panels are compared in Figures 3.20 to 3.25. It was observed that the strength of strengthened masonry panel is governed by reinforcement. The final failure took place due to rupture of wire mesh. The load-deflection curves show that the numerical results are closely agreeing with the trend of experimental results.

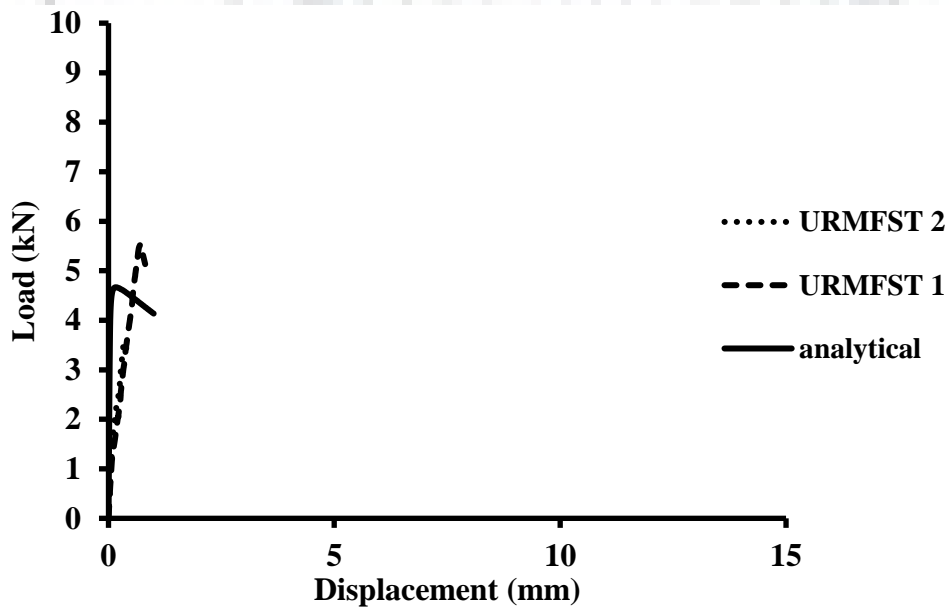


Figure 3. 18 : Numerical and experimental load-deflection curves for 1:4 masonry panel

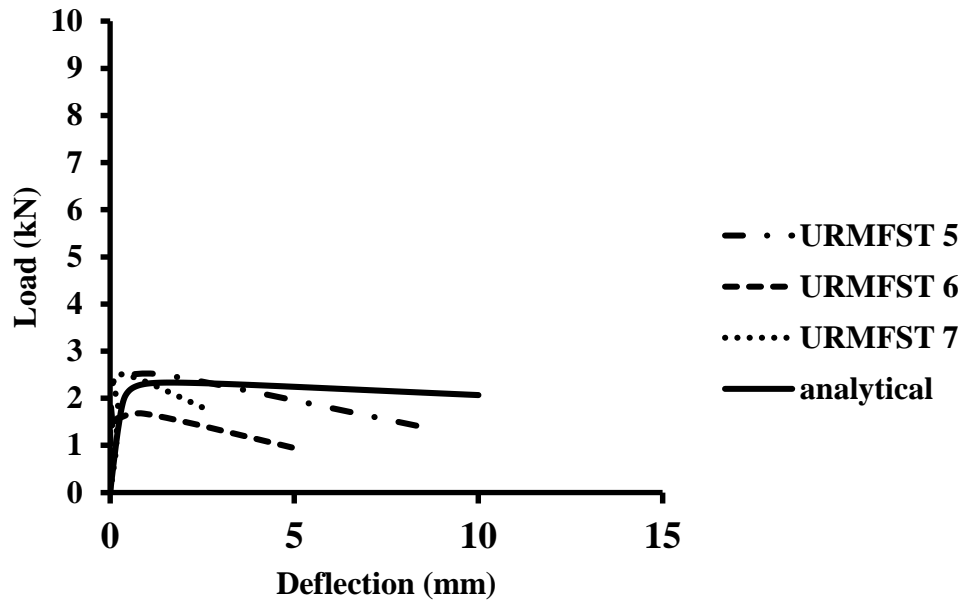


Figure 3. 19 : Numerical and experimental load-deflection curves for 1:6 masonry panel

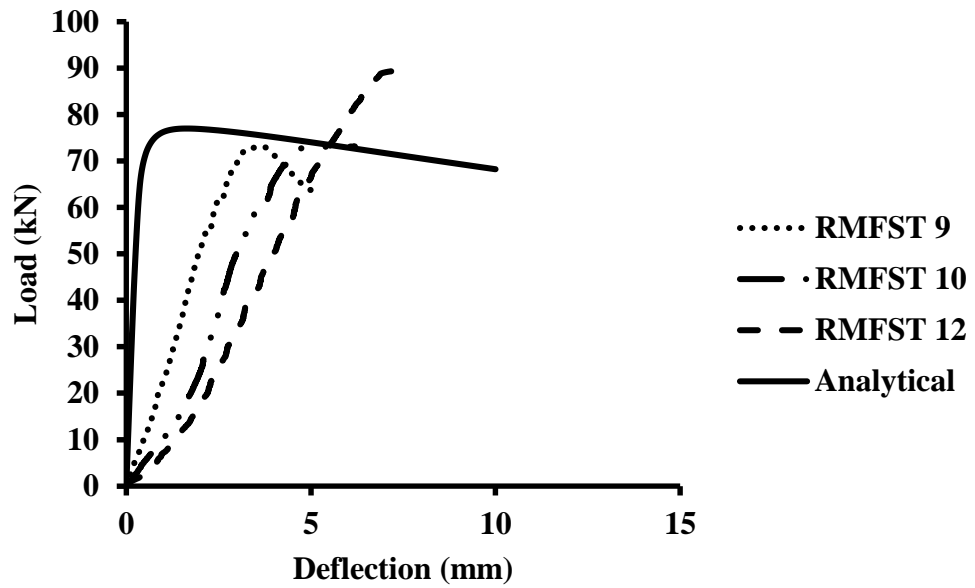


Figure 3. 20 : Numerical and experimental load-deflection curves for 1 inch spacing 1:4 strengthened masonry panel

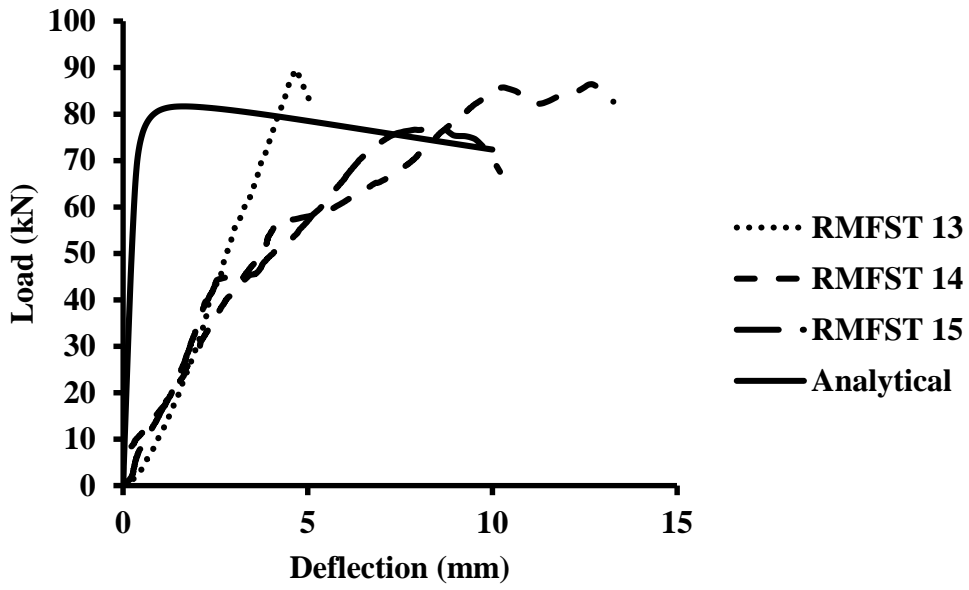


Figure 3. 21 : Numerical and experimental load-deflection curves for 1.5 inch spacing 1:4 strengthened masonry panel

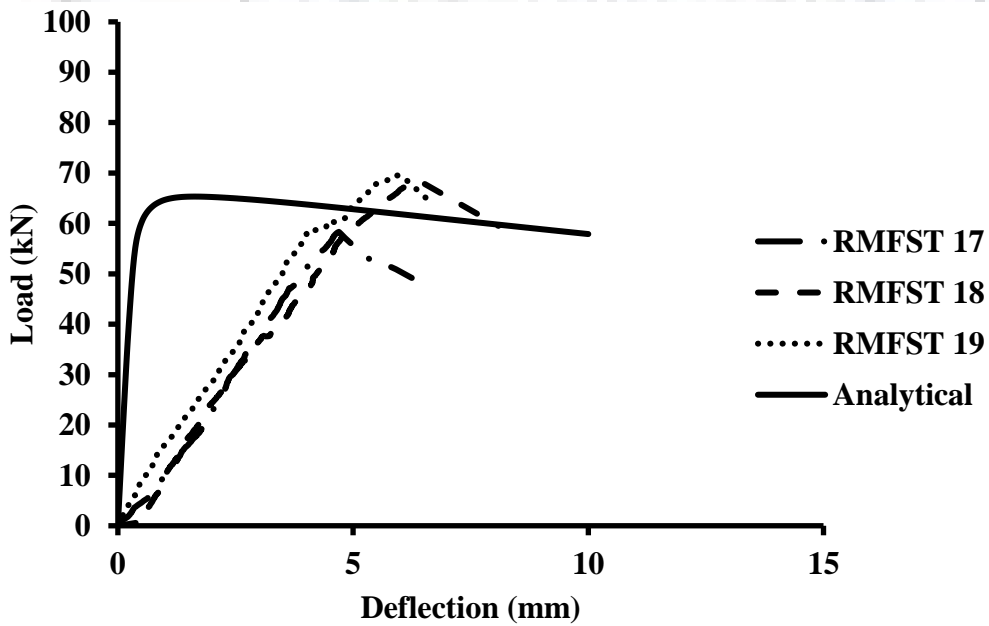


Figure 3. 22 : Numerical and experimental load-deflection curves for 2 inch spacing 1:4 strengthened masonry panel

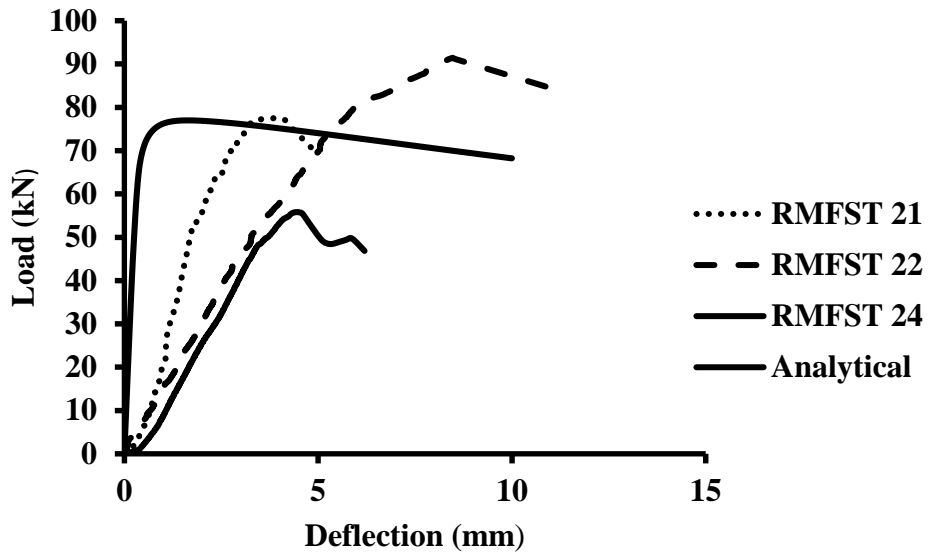


Figure 3.23 : Numerical and experimental load-deflection curves for 1 inch spacing 1:6 strengthened masonry panel

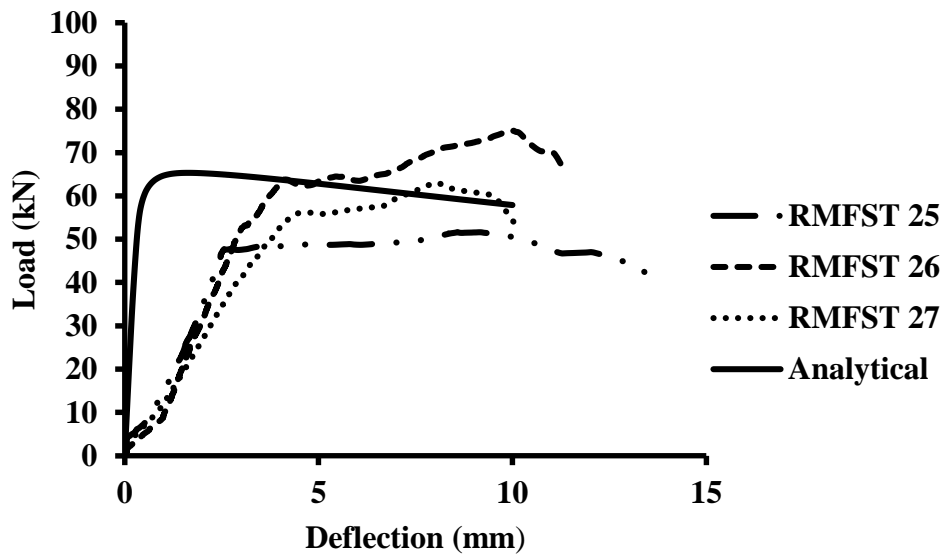


Figure 3.24 : Numerical and experimental load-deflection curves for 1.5 inch spacing 1:6 strengthened masonry panel

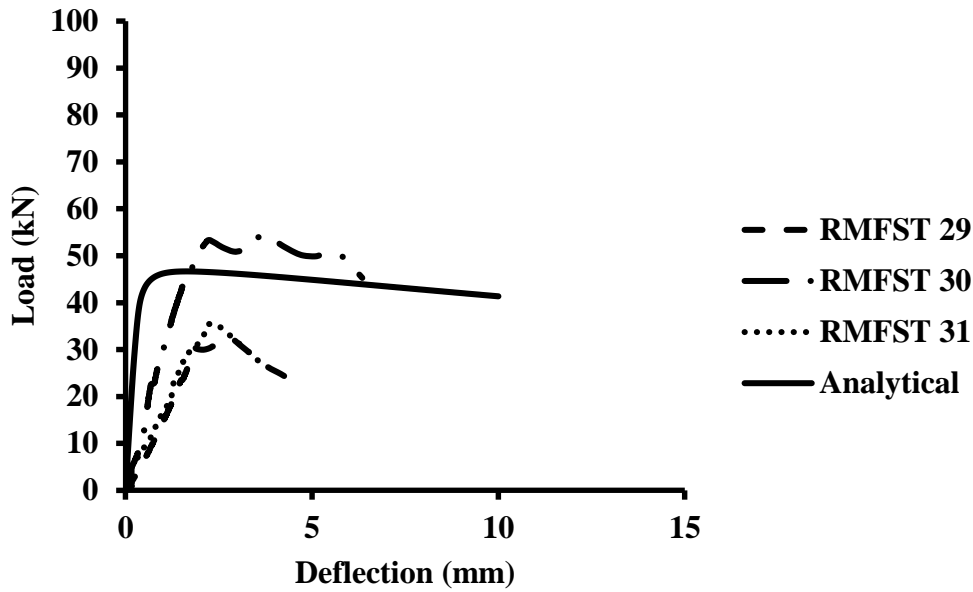


Figure 3. 25 : Numerical and experimental load-deflection curves for 2 inch spacing 1:6 strengthened masonry panel

3.8 SUMMARY

A study on the efficacy of the adopted strengthening technique at component level has been presented in this chapter. The out-of-plane behavior of the URM panels strengthened with ferrocement has been compared with the behavior of URM panels. The specimens have been tested under out-of-plane bending action according to ASTM E518-10 procedure and relative increase in strength and ductility has been estimated.

The behavior of the strengthened and unstrengthened specimen has been simulated using finite element analyses. Concrete damaged plasticity model has been utilized to model the non-linear plastic behavior of masonry and concrete as it was successfully used in earlier studies by other researchers. The major conclusions are summarised as follows.

- The WWM mortar strengthening technique is easy to use, and it can be used for both existing structure which has to be strengthened and for structure which is to be newly constructed, anchorage can be provided at a certain interval for better performance.
- The reinforced flexural specimens were able to show better performance compared to URM specimens without any end anchorage.
- In case of set 4 and 6 specimens, slight debonding was observed, though it was taken care by the 4 mm diameter anchorage, it was not adequate enough to prevent debonding. The specimens would have performed better if some end anchorage was provided. The test

results show that WWM mortar strengthening technique can effectively be used in URM for better performance.

- The ductility of strengthened specimen increased up to 3 times of that of URM specimen. The out-of-plane flexural capacity of strengthened specimen increased at an order of 4 when compared to that of URM specimen.
- In case of strengthened specimen subjected to out-of-plane loading, the failure initiated in the form of flexural cracks near mid span, which were restrained by the WWM reinforcement, resulting in a relatively ductile failure i.e., the initial failure pattern was much influenced by the masonry strength, but the final failure was influenced by the reinforcement provided.
- At large displacements, there was crushing of mortar and masonry in compression zone and final failure occurred due to rupture of wires.
- The results of finite element analyses were in good agreement with the experimental results in predicting the load carrying capacity and damage pattern of strengthened and URM panels.



CHAPTER – 4

DYNAMIC TESTING AND SIMULATION OF HALF-SCALE URM AND RM MODELS

4.1 INTRODUCTION

In the previous chapters, the behavior of masonry with and without reinforcement has been studied, though the reinforced masonry shows an enhanced behavior in static testing, it is equally important to study the dynamic behavior of masonry as well. So far, many tests have been conducted on half-scale masonry models with various reinforcing/ strengthening techniques. Based on the availability of test facilities, the models have been tested either on the shock table testing facility and/ or shake table testing facility.

Almost half of the Indian houses are made up of unreinforced masonry and their performance in the past earthquakes (Bihar, 1988; Uttarkashi, 1991; Killari, 1993; Jabalpur, 1997; Chamoli, 1999; Bhuj, 2001; Sumatra, 2004; Kashmir, 2005; Sikkim, 2006; Sikkim, 2011) have created a necessity to review the capability of existing structures during future earthquake, and to find a suitable strengthening technique to strengthen either newly constructed masonry structures or to retrofit existing structures. Due to low cost and less skilled labour, masonry buildings are still in use. There is a number of research carried out on strengthening/ retrofitting of masonry structures both in India and across the globe.

Strengthening using FRP, polymeric meshes, textile reinforcement and reinforcing steel wires (D'Ambrisi et al. (2013), Ashraf et al. (2012), Papanicolaou et al. (2011), ElGawady et al. (2004), Tan et al. (2004), Mosallam et al. (2007), Galal et al. (2010), Papanicolaou et al. (2008), Saleem et al. (2016), Shermi et al. (2017)) have been reported by many researchers.

Small scale and full-scale brick masonry and stone masonry structures have been tested on shake table testing facility in the past including both reinforced masonry and unreinforced masonry (Koutromanos et al. (2012), Lourenço et al. (2013), Saleem et al. (2016), Stavridis et al. (2016), Candeias et al. (2017)). These tests were conducted to evaluate the performance of masonry to study the influence of opening, wall aspect ratio, different types of the diaphragm, reinforcement etc. Nevertheless, no shake table test has been carried out to evaluate the seismic behavior of masonry strengthened with WWM and coarse sand mortar externally.

In this present study, an attempt has been made to compare the behavior of conventional unreinforced masonry and masonry strengthened with WWM and coarse sand mortar by subjecting both the models to a series of ground motions separately. The strengthened model was subjected to more intense ground motion as compared to unstrengthened model.

4.2 EXPERIMENTAL PROGRAM

In order to contribute in enhancing the knowledge about strengthening technique studied in the previous chapters, an experimental dynamic testing was carried out on half-scale masonry models subjected to acceleration time history similar to Indian standard code response spectra for seismic zone V on hard soil. The masonry model was constructed as per the common construction practice followed in the state of Uttarakhand, India.

4.3 CONSTRUCTION OF MASONRY MODEL

4.3.1 Unreinforced Masonry Model

A half-scale 2.25 m x 2.25 m unreinforced masonry model (URM) with 2.0 m height was built on a steel platform. This was later bolted to the shake table before testing. Figures 4.1 and 4.2 show the plan and section of the masonry model. Bricks of size 115 mm x 57 mm x 35 mm were used for making the model. A mortar mix of 1:4 (cement : sand) was used for constructing these models. Both the models were of a single room size, constructed as per the common construction practice followed in the state of Uttarakhand, India. Normally in case of load bearing structures, one full-scale brick wall having thickness of 230 mm is constructed. For half-scale models to be tested on the shake table facility, thickness of the wall was kept as 115 mm. The same mason was used for constructing the half-scale models throughout so that quality of masonry is not varied due to workmanship. Companion mortar cubes were cast every time, a mortar mix was prepared, to check the quality of mortar. The north and south wall have a standard door opening of size 1.50 m x 0.75 m. The east wall has a window opening of size 0.75 m x 0.75 m, while the west wall was a solid wall without any opening.

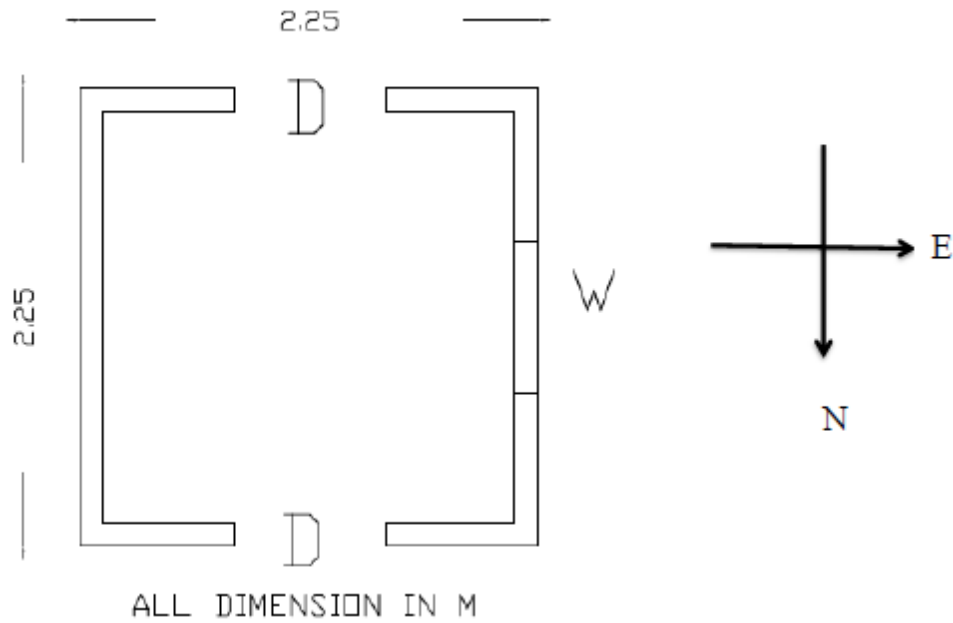


Figure 4. 1 : Plan

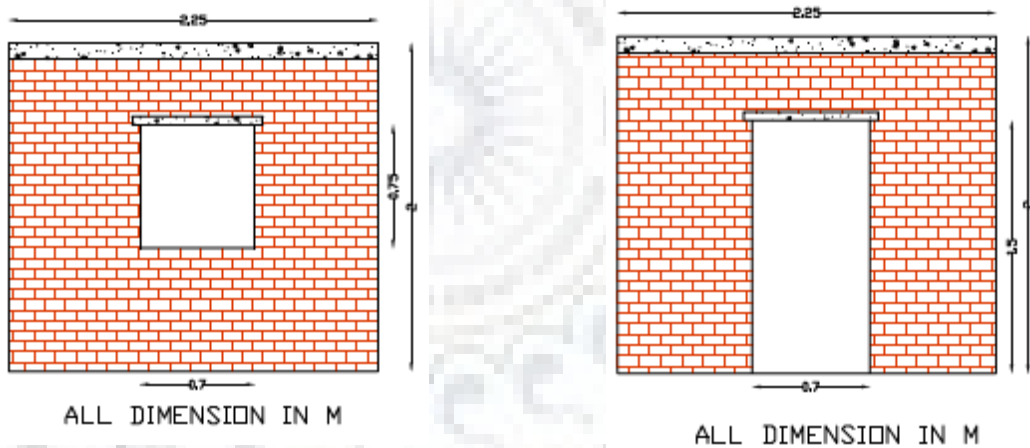


Figure 4. 2 : Window side section and front door section

The platform for the construction of models was made up of flat steel plate. For providing grip between the foundation and the model, shear keys were provided with the help of angle iron (25 mm x 25 mm x 3 mm) at the outer and inner periphery. Further, a steel strip (25 mm wide and 3 mm thick) was welded at the center of the outer and inner periphery on the plate. A 75 mm thick foundation was laid with 1:2:4 concrete mix representing the fixed base of the model. This arrangement was done for holding the foundation of the model from shearing/ sliding from the platform during testing. This was equivalent to a rigid foundation constructed in actual practice. In the absence of the shear keys, the model may slip or slide because of the flat steel platform. Proper precautions were taken to weld the shear keys to the platform. The surface of the

foundation was roughened to ensure better grip between foundation and brick work. Before laying the bricks, a layer of thick grout was applied above the foundation surface and then the brick work was laid on top of 75 mm thick foundation. The sequence of construction was similar to that of the conventional construction procedures followed in the northern part of India. Cut lintel beams were provided above the door and window openings. The roof slab was cast at the end. The construction procedure of the unreinforced masonry model can be seen in Figures 4.3 to 4.9. The model was cured for 28 days from the date of casting of slab.



Figure 4.3 : Angle section welded on plate



Figure 4.4 : Casting of foundation



Figure 4.5 : Laying of bricks above foundation



Figure 4.6 : URM model up to roof



Figure 4.7 : Casting of roof slab



Figure 4.8 : Front facing URM building model



Figure 4.9 : Fully completed model N-E

4.3.2 Reinforced Masonry Model

The traditional building constructed as per the above-mentioned procedure (section 4.3.1) is a common construction practice in many parts of India. These structures are highly damaged during earthquake hence it is necessary to retrofit the structures with suitable material. So far, many retrofitting techniques (FRP confinement, reinforcing with steel rod, shotcrete, bamboo reinforcement, reinforcing with steel strip) are in practice.

The retrofitted model has the same dimension of the unreinforced masonry building. The detailed section of the retrofitted model is shown in Figure 4.10.

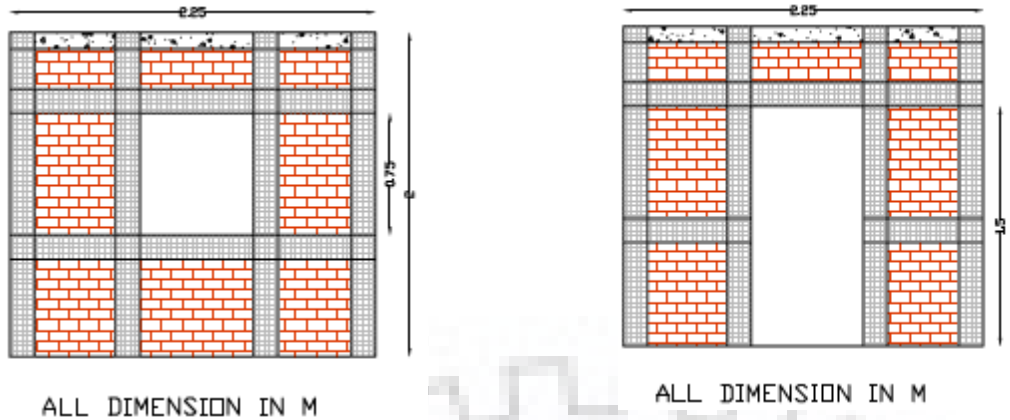


Figure 4.10 : Retrofitted window side section and door side section of RM model

The main cause of failure of masonry building is loss of integral box action due to cracking of corners resulting in separation of walls. Therefore, the most important step in retrofitting of masonry building is to ensure integral box action. The integral box action can be ensured by providing vertical and horizontal band along the door and window openings, vertical and horizontal bands are constructed using WWM with rich cement mortar of 1:3 (cement: coarse sand) as per IS 13935: 2009 was provided on both sides of the wall. 4 mm diameter steel rod was used to connect the two layers of WWM. These steel rods transfer the shear between the WWM mortar layer and the masonry through dowel action. The spacing of steel rod is provided as per IS 13935: 2009.

The construction of reinforced masonry model is similar to that of reinforced model, other than the additional anchoring of the WWM to the foundation base. Along with the shear key, steel sheets were also welded to the base plate to ensure proper anchorage of WWM to the foundation.

The retrofitting /strengthening work was carried out as per Indian standard code of practice IS 13935: 2009 after the complete construction and curing of the conventional model. The model was cleaned with the help of a steel wire brush to remove dirt if any. Then a layer of cement slurry was applied with the help of a paint brush to provide better bond between the mortar and the masonry surface. A layer of 10 mm thick 1:3 coarse sand mortar was applied above the cement slurry surface to level the uneven masonry surface as well as to provide better grip for the WWM and second layer of mortar. The mortar surface was roughened with the help of a steel wire brush to ensure better grip. The WWM was placed and anchored with the help of a 4 mm diameter mild steel wire. The wires were bent over the WWM on the two sides in opposite

direction as shown in Figure 4.12. These 4 mm wires transfer the shear at the WWM masonry interface through dowel action. A layer of cement slurry was spread above the WWM and 10 mm thick 1:3 coarse sand mortar was applied above the WWM and the surfaces were levelled. The strengthening process can be seen in Figures 4.11 and 4.12. The strengthened model was cured under normal site condition for another 28 days.

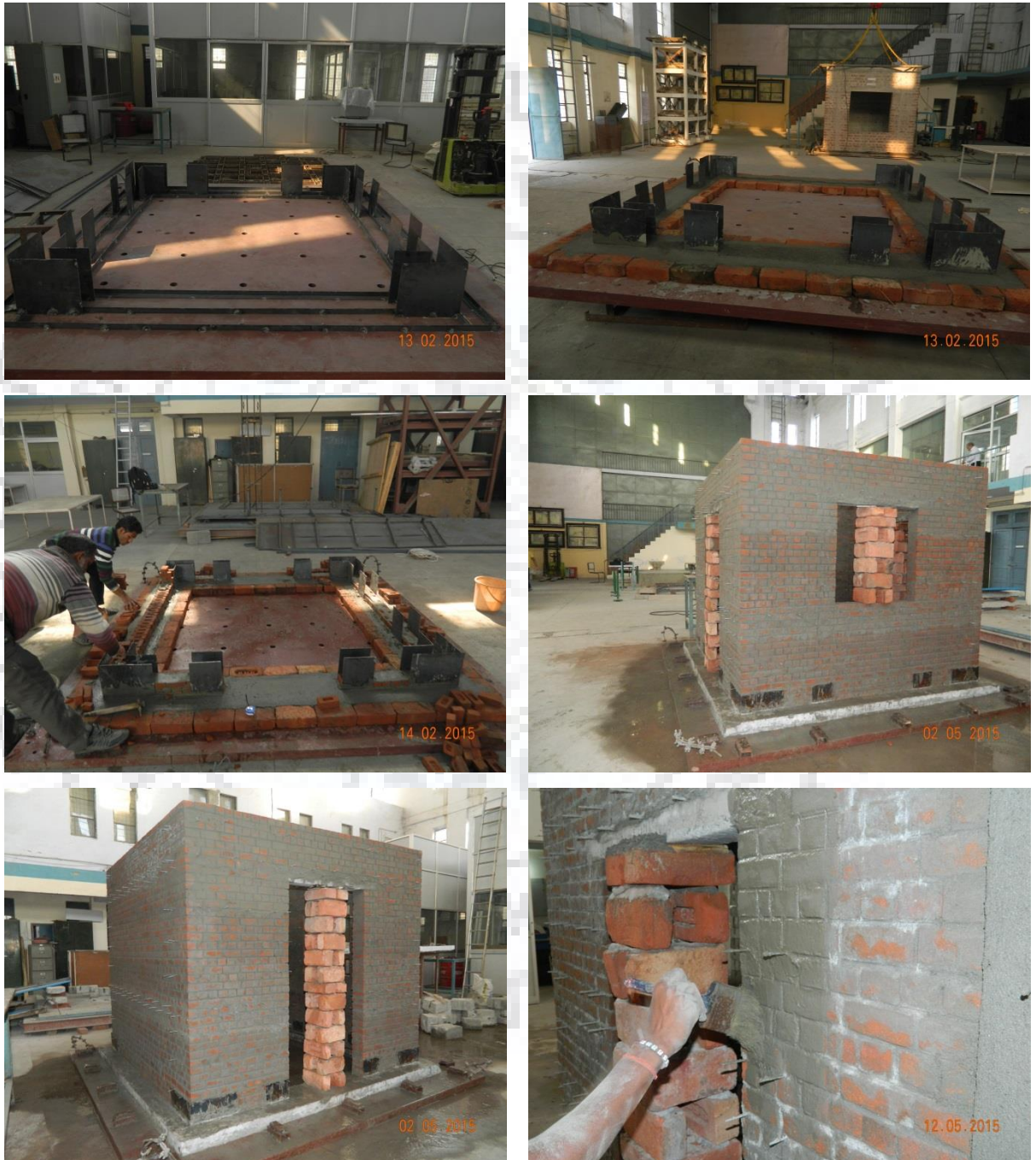


Figure 4. 11 : RM model construction process



Figure 4. 12 : Model strengthening process



Figure 4. 13 : RM model after completion

4.4 TESTING PROCEDURE

The models were shifted to the shake table with the help of a 20 ton capacity mechanically operated crane. The model was bolted to the shake table with the help of bolts. The required test setup was made. Initially, a free vibration test was carried out for the model to find the natural frequency of the structure.

4.4.1 Free Vibration Test

Free vibration test was conducted to determine the frequency of the model. For acquiring the free vibration data two ranger seismometer were placed on the roof of the models (Figure 4.14), one in the longitudinal direction (E-W) and other in the transverse direction (N-S). The models were excited with mild impact by a hammer. The data were recorded with the help of a data acquisition system.



Figure 4. 14 : Free vibration setup for URM model and RM model

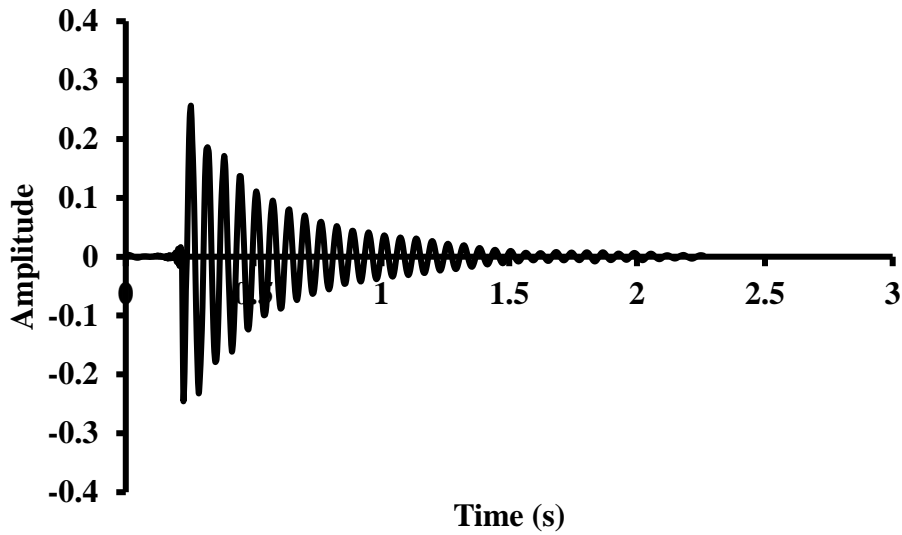


Figure 4.15 : Free vibration data of URM model

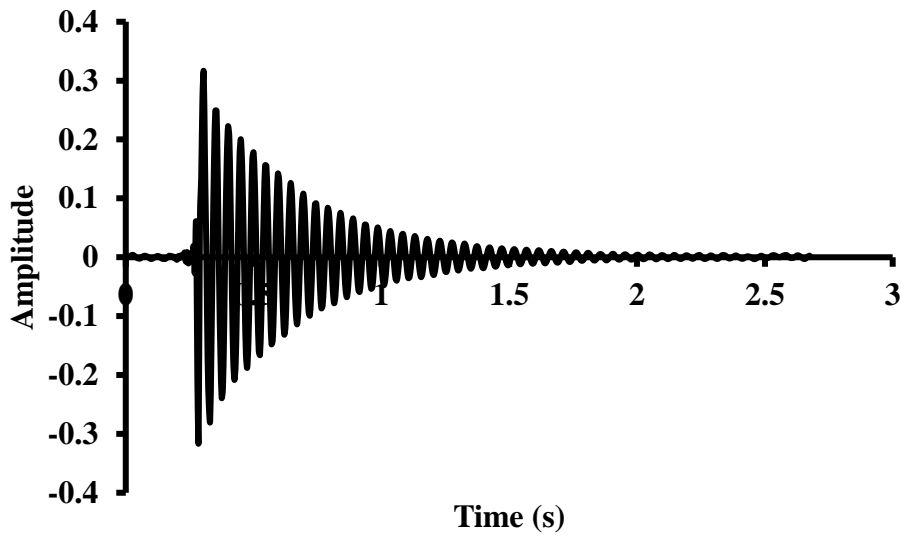


Figure 4.16 : Free vibration data of RM model

4.5 ANALYSIS OF FREE VIBRATION DATA

After free vibration testing, vibration records were downloaded and processed. The natural frequency of the model was computed from the recorded data. The time period of URM and RM model is obtained as 0.056 sec and 0.050 sec respectively.

From the above-mentioned data, it is concluded that the time history acceleration having frequency content in this range should be used during the dynamic testing of the model with the help of shake table testing facility.

4.6 SHAKE TABLE TESTING

4.6.1 Shake Table Specification

The masonry model will be tested on a digitally controlled shake table facility, capable of reproducing specified real earthquake accelerogram or simulated synthetic accelerogram compatible with a specified design for testing structures, available in the Department of Earthquake Engineering, Indian Institute of Technology Roorkee. The driving mechanism of the table is of servo-hydraulic type with hydraulic power supply of 750 lpm. The running current is 400 amp. The size of the shake table is 3.5 m x 3.5 m with geometry truncated pyramidal welded plate structures. This table can give motion in a plane containing vertical and one horizontal direction. The table is driven by three actuators, two vertical and one horizontal. A square grid pattern of bushes of special alloy steel is provided at 400 mm c/c on the top plate of the shake table platform for mounting model on the table. The shake table can support a pay load of 200 kN. The zero-period acceleration (ZPA) can be up to 3 g depending on payload. The fundamental frequency is 49.5 Hz. The table is controlled by monitoring the desired acceleration in a closed loop system by the computer, the input motion to the shake table can be given either that of an earlier recorded real earthquake or it can be an artificial earthquake motion compatible to a given response spectra. Other types of excitations that may be given are sine wave and sine sweep.

The specification of the actuators of the shake table is as follows:

Characteristics	Horizontal actuator	Vertical actuator
Static Thrust (kN)	250	125
Dynamic Thrust (kN)	200	100
Stroke (mm)	300	300
Velocity (mm/sec)	1200	1500
Oil flow at maximum velocity (L/min)	750	400

The URM model was subjected to two-time history accelerations similar to that of artificial time history record compatible to IS code zone V hard soil spectra.

4.6.2 Sensors and Data Acquisition

The data acquisition consists of 128 voltage channels. The sensors used were single channel force-balanced accelerometers having natural frequency of about 100 Hz and damping of 70%. Accelerometers provide voltage output, which is proportional to acceleration of points where these are mounted. This analog acceleration time history is then fed to data acquisition system. The data acquisition system first conditions the analog signal to its requirement through amplifier and anti-aliasing filter and then this conditioned analog signal is fed to ADC where digitization at prescribed sampling rate takes place. The digital data is then stored in hard disks of the computer.

In order to obtain complete data about the excitation of the models, they were instrumented with two accelerometers and Linear Variable Displacement Transducers (LVDT). Accelerometers were mounted on the roof of the model at two different locations (in the centre of the roof in the middle and other at the base plate). The LVDT will be fixed diagonally near the corner of openings to measure the local displacement and crack openings. The entire instrumentation setup can be seen in Figure 4.14.

4.6.3 Input Acceleration

The URM model was subjected to two different horizontal ground motions similar to that of artificial time history record compatible with IS code seismic zone V hard soil spectra (Figure 4.19). Whereas, the RM model was subjected to four different horizontal ground motion records.

Sl. No.	Unreinforced Model	Reinforced Model
1	DBE	DBE
2	2 DBE	2 DBE
3	-	3 DBE
4	-	4 DBE

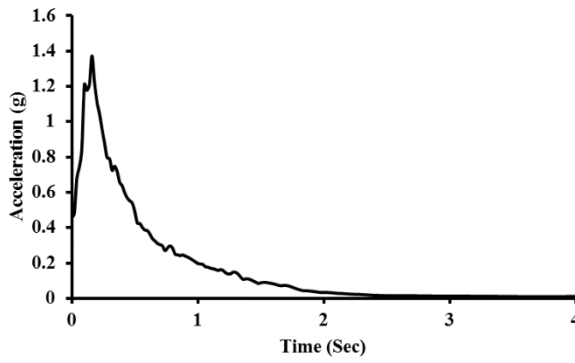


Figure 4.17 : Response spectra of input acceleration time history -DBE

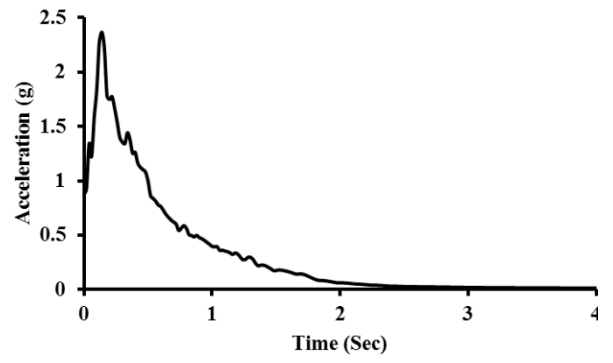
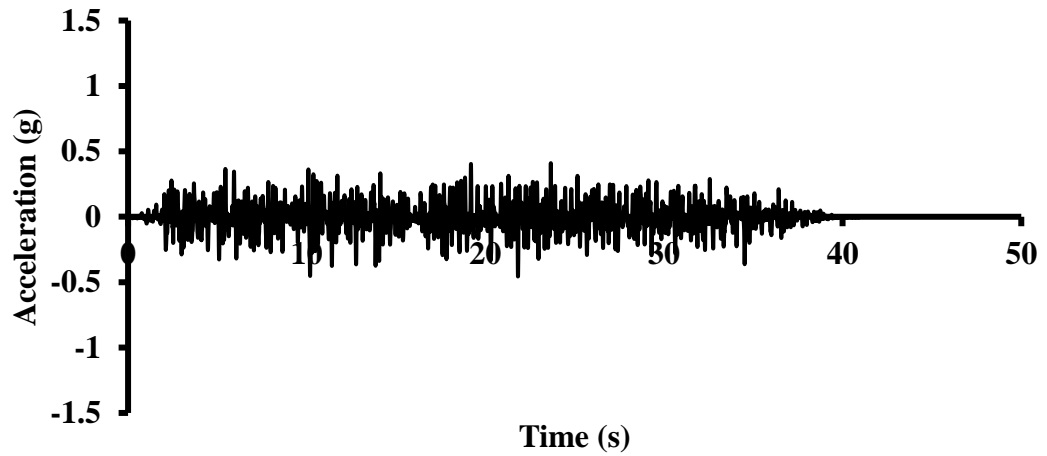


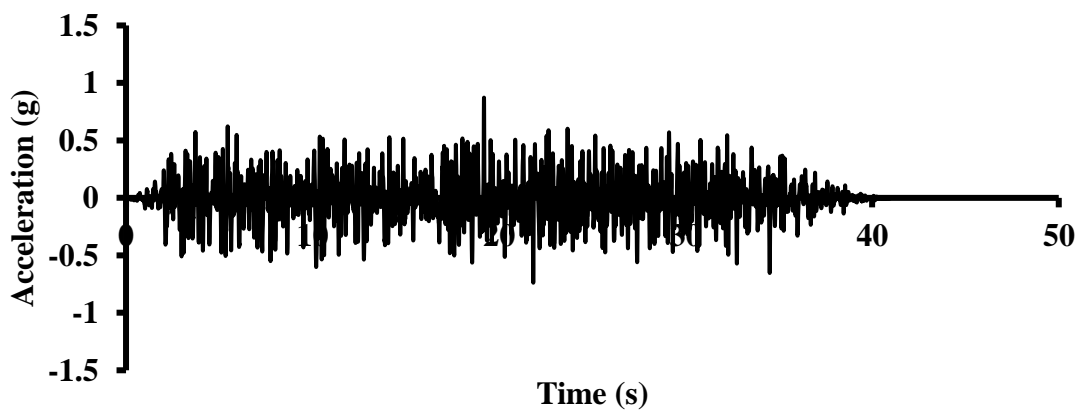
Figure 4.18 : Response spectra of input acceleration time history -MCE

DBE



(a) Input acceleration time history -DBE

MCE



(b) Input acceleration time history -MCE

Figure 4.19 : (a)-(b) Input acceleration time history

4.7 BEHAVIOR OF URM MODEL

4.7.1 First Shake

The global behavior of the unreinforced masonry model was analysed in terms of deformation and damage patterns for all the seismic inputs. Time history acceleration similar to IS code spectra for DBE specified under input section was applied to the base of the model. Care was taken at the time of testing by holding the roof with the help of a crane to avoid damage to the table in case the model collapse at the time of testing.

Minor cracks were observed after the first shake to the URM model, which can be seen in Figure 4.18. It was observed that the given ground motion was not intense enough to create any severe damage to the model. The maximum roof acceleration observed at the top in the direction of the applied motion (X direction) was 0.61 g. The plot of the acceleration time history at the roof in X direction can be seen in Figure 4.21.



Figure 4. 20 : Failure pattern after first shake

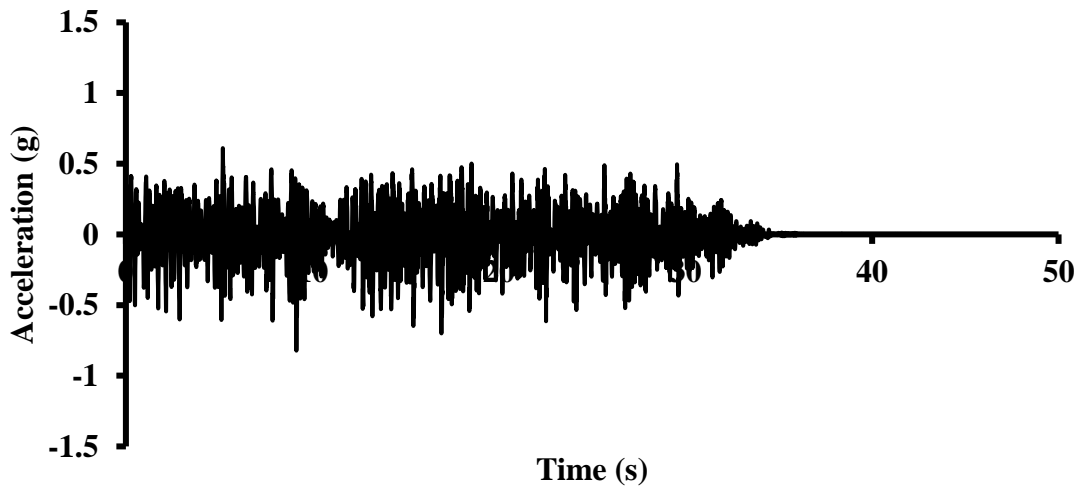


Figure 4. 21 : Acceleration at roof level in X direction of URM model - DBE

4.7.2 Second Shake

The second ground motion applied to the URM model was equivalent MCE. It was observed that the minor cracks formed in the first shake started to widen further. Severe cracks in the form of shift/ displacements in the walls at different locations in URM model (Figure 4.20) were also observed. In north facing wall, a shift of 7 cm was observed at the lintel level (Figure 4.22). Further, this wall also displaced by 4.8 cm at the right top corner and by 8.1 cm shift in first brick layer just below the roof level. In the west facing wall cracks were observed at the corners of the window opening. A shift of 3.5 cm was observed in the brick layer below roof at the right top corner of the wall. In the south facing wall with a door opening, displacement of the wall of about 10 cm was observed at the left and right lintel corners with a 5.0 cm wide crack. In the east facing wall (solid wall), a 7 cm shift was observed at the fourth brick layer below roof. The maximum roof acceleration observed at the top in the direction of the applied motion (X direction) was 0.91 g. The plot of the horizontal component of acceleration time history at the roof level in URM model is shown in Figure 4.23 in the direction of the applied motion (X direction). Further shake was not applied to the model since it would result in collapse leading to damage of the shake table.



Figure 4. 22 : Failure pattern after second shake

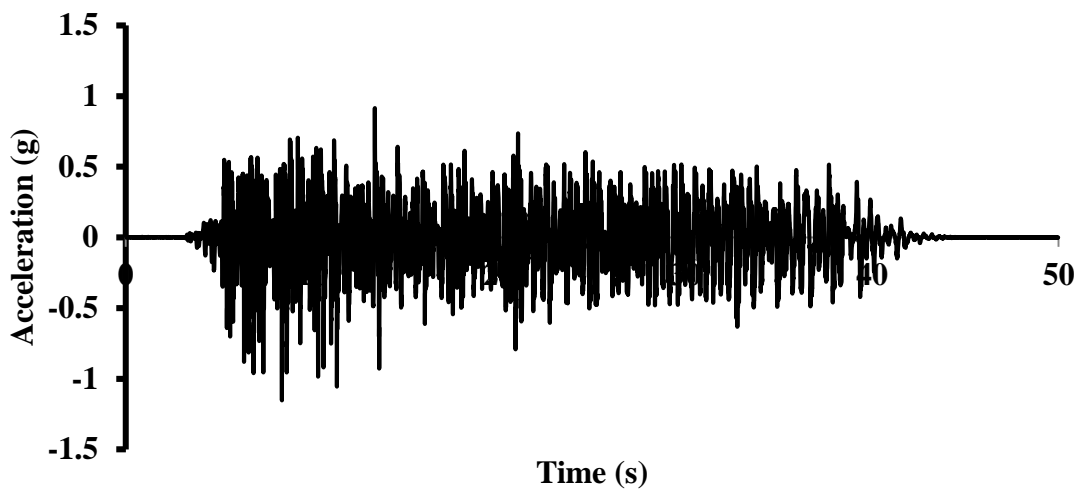


Figure 4. 23: Acceleration at roof level in the X direction in URM model - MCE

4.8 BEHAVIOR OF RM MODEL

4.8.1 First Shake

During the first shake, the maximum roof acceleration observed at the roof in the X direction was 0.60 g. From the recorded acceleration data, the velocity and displacements at the roof were computed with the help of Seismosignal software. The maximum velocity observed at the roof level in X directions was 18.61 cm/s. The maximum roof displacement in the X direction was 9.11 cm. The horizontal component of acceleration time history at the roof (X direction) is plotted and can be seen in Figure 4.24.

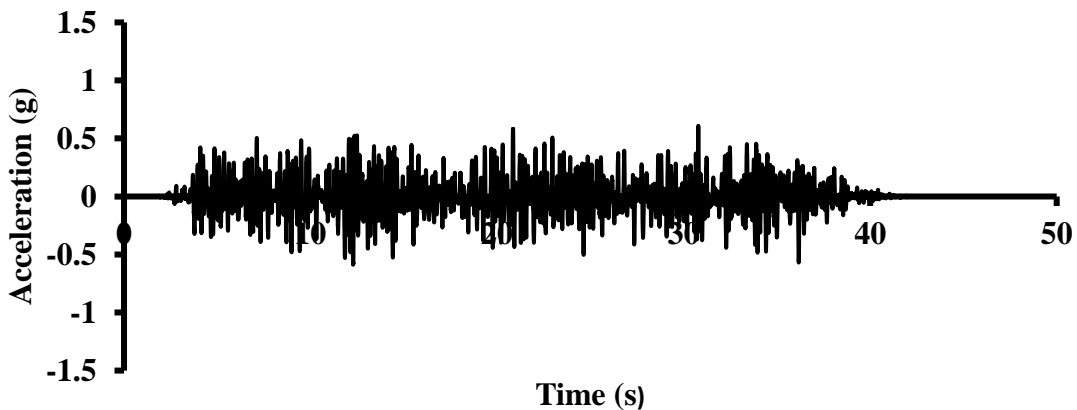


Figure 4. 24: Acceleration at roof level in the X direction in RM model - DBE

4.8.2 Second Shake

During the second shake, the maximum roof acceleration observed at the top in X direction was 0.77 g. The maximum roof velocity and displacement computed at the roof level in X direction were 26.89 cm/s and 9.42 cm respectively. Figure 4.25 shows the acceleration time history recorded at the roof in the X direction.

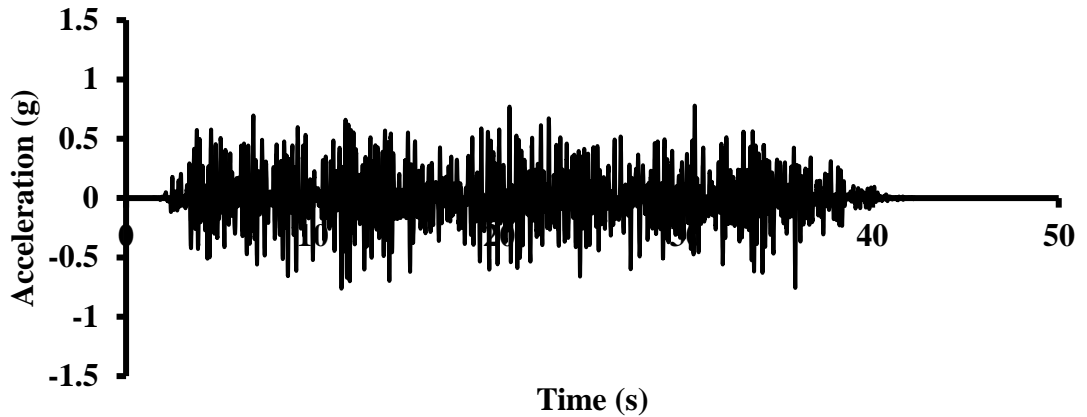


Figure 4. 25 : Acceleration at roof level in the X direction in RM model - 2 DBE

4.8.3 Third Shake

During the third shake, the maximum roof acceleration observed at the roof in the X direction was 0.79 g. The maximum roof velocity observed in X direction was 17.20 cm/s and maximum roof displacement in X direction was 17 cm. Figure 4.26 shows the plot of acceleration time history at the roof in the X direction.

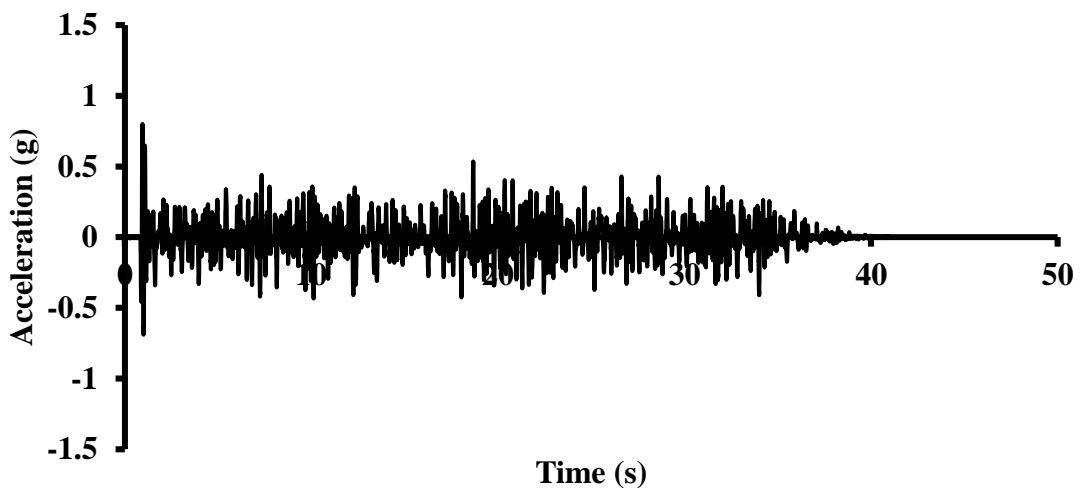


Figure 4. 26 : Acceleration at roof level in the X direction in RM model – 3 DBE

4.8.4 Fourth Shake

During the fourth shake, the maximum roof acceleration observed at the roof in the X direction was 0.80 g. The maximum roof velocity observed at the roof level in the X direction was 26.05 cm/s. The maximum roof displacement in the X direction was 10.19 cm. The plotted graph of acceleration time history at the roof in the X direction can be seen in Figure 4.27.

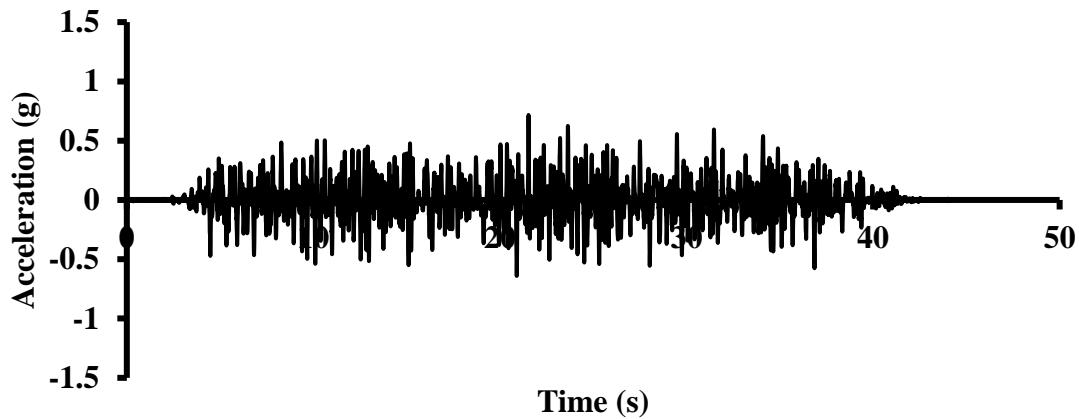


Figure 4. 27 : Acceleration at roof level in the X direction in RM model – 4 DBE

4.9 CLASSIFICATION OF DAMAGE

The extent of the damage depends upon intensity and duration of the ground motion, the nature of the supporting soil, construction material, type of construction, quality of construction, frequency of vibration and damping in the structure. The grade of damage, its severity and the damage descriptions are based on the experience in the past earthquake. The grades of damage range from 1 to 5 according to Tomazevic (1999). The category of damage is clearly elaborated in Table 4.1.

Table 4. 1 : Categories of damage

Grade of damage	Severity of damage	Damage description
1	Slight non-structural damage	Thin cracks in plaster, falling of plaster in bits
2	Slight structural damage	Small cracks in walls, fall of fairly large pieces of plaster, pantiles slip off, cracks in chimneys, parts of chimney fall down
3	Heavy damage	Large and deep cracks in walls, fall of chimneys

4	Destruction	Gaps in walls, parts of buildings may collapse, separate parts of buildings lose their cohesion, and inner walls collapse
5	Total damage	Total collapse of buildings

4.9.1 Structural Failure Mechanism

The conventional building model considered in the present study may be treated as a typical box system in which the walls parallel to loading direction are called in-plane walls or shear walls, whereas the walls perpendicular to the loading direction are termed as out-of-plane walls or cross walls. The in-plane walls develop a shear resisting mechanism while the out-of-plane walls develop a flexure one. The in-plane walls provide lateral resistance by means of membrane action. They resist inertia force due to their own mass as well as that of the roof, and they also resist the forces transmitted by out-of-plane walls during shaking. Bending moment induced in the in-plane walls during shaking is maximum at its extreme ends producing vertical cracks at the corners. The diagonal cracks in the in-plane walls leading to shear failure are due to the principal tensile stresses developed in the walls because of vertical and lateral loads. Due to the window and door opening, the unsupported length of the shear wall is reduced accordingly its shear strength is also reduced. The shear forces become critical in the in-plane walls with openings and the failure occurs in the form of diagonal cracks.

In URM model, cracks initiated at the plinth level propagated towards top of the model. During the second shake, the URM model was severely damaged causing widespread gaps in walls and the model was almost on the verge of collapse. In case of RM model, no cracks were observed because of the presence of sill band, lintel band and vertical band (in form of WWM) due to the additional tensile and bending strength developed in the model. Thus, the failure of conventional brick masonry can be greatly minimized by incorporating the adequate earthquake resistant features.

4.10 SIMULATION OF DYNAMIC TESTING OF URM AND STRENGTHENED MASONRY BUILDING MODELS

4.10.1 Material Properties of Concrete

The compressive stress-strain curve for concrete, as proposed by Desai and Krishnan (1964) has been adopted in the present study. The parameters of this stress-strain curve have been presented numerically by Hu et al. (2004) and the same has been used.

$$\sigma_c = \frac{E_c \varepsilon_c}{1 + (R + R_E - 2) \left(\frac{\varepsilon_c}{\varepsilon_0}\right) - (2R - 1) \left(\frac{\varepsilon_c}{\varepsilon_0}\right)^2 + R \left(\frac{\varepsilon_c}{\varepsilon_0}\right)^3}$$

where,

$$R = \frac{R_E(R_\sigma - 1)}{(R_E - 1)^2} - \frac{1}{R_\varepsilon}, R_E = \frac{E_c}{E_0}, E_0 = \frac{f'_c}{\varepsilon_0}$$

Where, $R_\sigma = 4, R_\varepsilon = 4$ are used.

For concrete in tension, the following stress-strain relationship used by Vecchio (1990) has been adopted. As per his relationship, the concrete follows a linear relationship prior to cracking, given as

$$f_{c1} = E_c \varepsilon_{c1}, 0 \leq \varepsilon_{c1} \leq \varepsilon_{cr}$$

where,

$$E_c = \frac{2f'_c}{\varepsilon_0}$$

$$\varepsilon_{cr} = \frac{f_{cr}}{E_c}$$

After cracking, concrete in tension is made to reflect tension stiffening effects through the following relation

$$f_{c1} = \frac{f_{cr}}{1 + \sqrt{200\varepsilon_{c1}}}$$

Here f_{c1} and ε_{c1} are the average principal tensile stress and strain of the concrete. The limiting tensile strain of concrete has been considered as 0.0001 (Pillai and Menon 2010). The flexural; tensile strength of concrete (f_{cr}) was estimated based on IS 456: 2000. The tension stress-strain curve for concrete, constructed using these relationships is considered in the present study.

The basic modeling parameters related to the material properties have been obtained directly from the experimental tests conducted. Other parameters like (dilation angle = 38° , flow potential eccentricity = 0.1, ratio of initial equibiaxial compressive yield stress to initial uni-axial compressive yield stress = 1.16, ratio of second stress invariant = 0.667, viscosity parameter = 0.0) were taken from Jankowiak and Lodygowski (2005).

The post yield compression and tension behavior of concrete are shown in Figure 4.28 and 4.29 respectively (Jankowiak and Lodygowski 2005). The compression and tension damage curves for concrete have been obtained using the same procedure as discussed in the previous section.

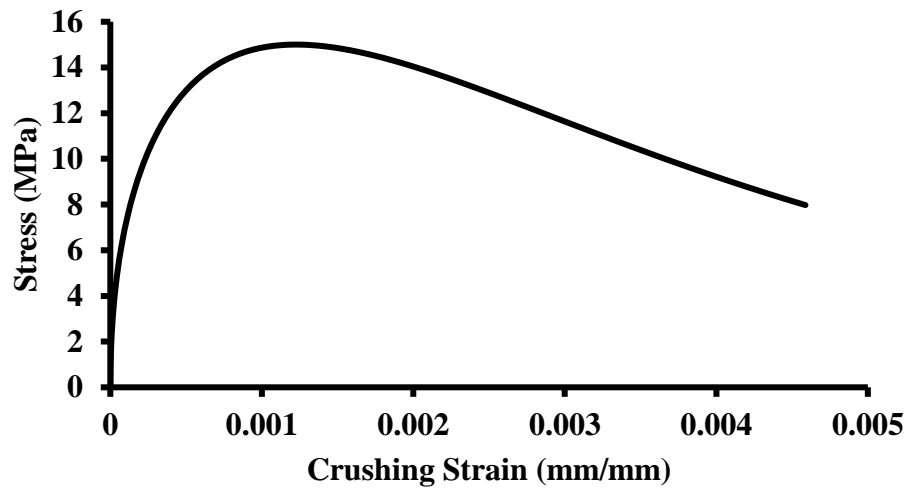


Figure 4. 28 : Compression behavior of concrete in non-linear range expressed as a function of crushing

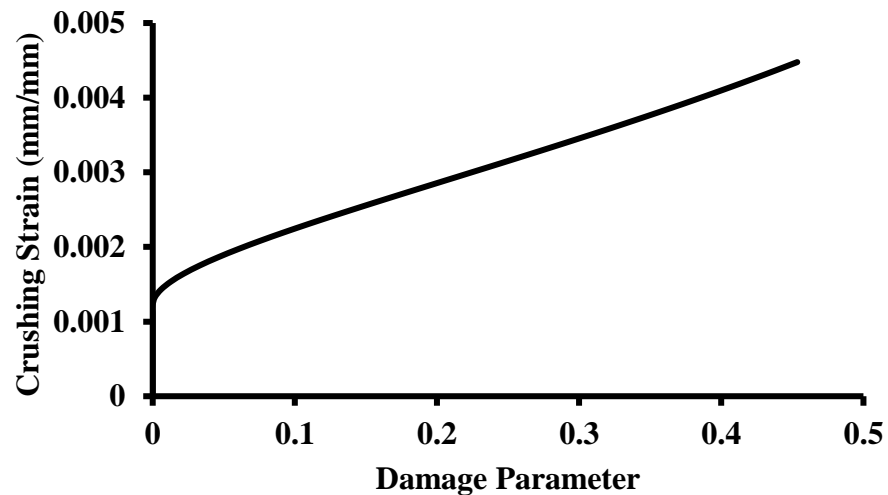


Figure 4. 29 : Compression damage of concrete

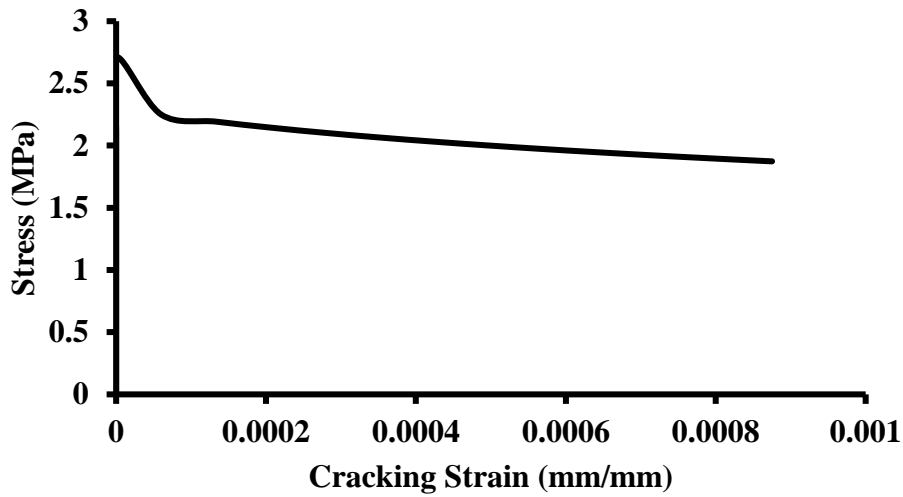


Figure 4.30 : Tension behavior of concrete in non-linear range expressed as a function of crushing

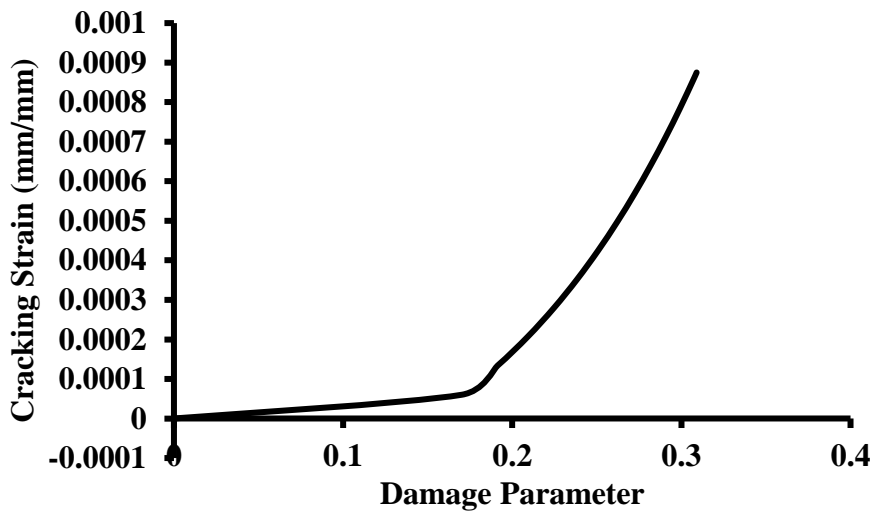


Figure 4.31 : Tension damage of concrete

4.10.2 Material Properties of Steel Reinforcement

The stress-strain graph for Fe250 given in (Pillai, 2010) is used to calculate the plastic strain (Abaqus manual 2013) (Figure 4.32) and is further used in the analysis.

The Poisson's ratio of 0.3 is used in this analysis (Pillai 2010)

The density of the steel is 7850 kg/m^3 (IS 875 (Part 1): 1987)

Modulus of elasticity of steel is $2 \times 10^{11} \text{ N/m}^2$ (IS 456: 2000)

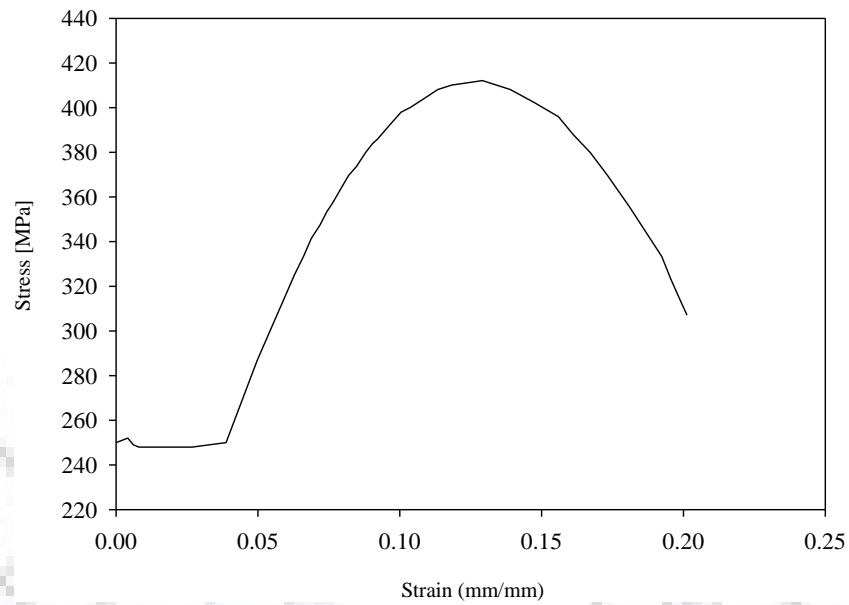


Figure 4. 32 : Stress-plastic strain curve for steel

4.11 MODELING OF URM MODEL

The structure is modeled using a finite element software Abaqus/CAE. The walls were modeled using solid 8-nodes linear hexahedral elements (C3D8), commonly known as “brick element”. The lintel and the roof were modeled using the same brick element (C3D8) (Figure. 4.33). The reinforcement in roof and lintel were modeled as 2-node, linear truss element (T3D2) and were embedded inside concrete. The connections between the structural members were modeled as tie constraint.

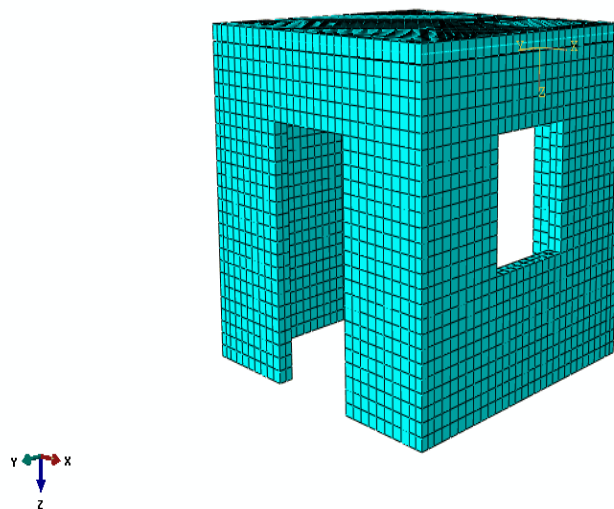


Figure 4. 33 : Finite element model of URM model with mesh

4.11.1 Modeling of Strengthened Masonry Model

The structure is modeled using a finite element software Abaqus/CAE. The masonry, concrete slab, coarse sand mortar was modeled using solid 8-nodes linear hexahedral elements (C3D8), commonly known as “brick element” (Figure 4.34). The reinforcement in the roof was modeled as 2-node, linear truss element (T3D2) and was embedded inside concrete. The lintel and corner mesh WWM reinforcement was modeled using the same T3D2 element and were embedded on the wall surface. The connections between the structural members were modeled as tie constraint.

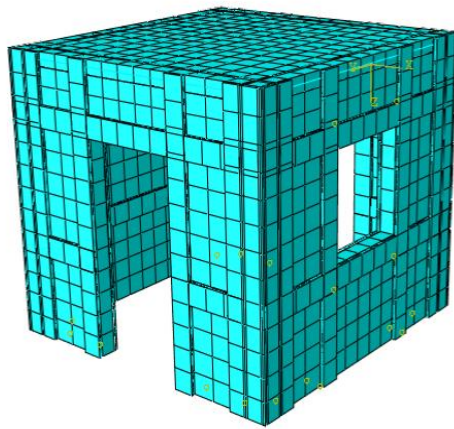


Figure 4. 34 : Finite element model of strengthened masonry model with mesh

A non-linear explicit analysis was carried out in Abaqus/CAE to simulate the behavior of both the half-scale masonry models numerically. The behavior of the numerical model was almost similar to that of experimental observation. The time versus acceleration graph obtained from the numerical model is given in Figures 4.35, 4.36, 4.38 to 4.41. The acceleration obtained numerically was almost matching with the experimental results. The damage pattern at various loading stages of URM and RM model can be seen in Figures 4.37 and 4.42.

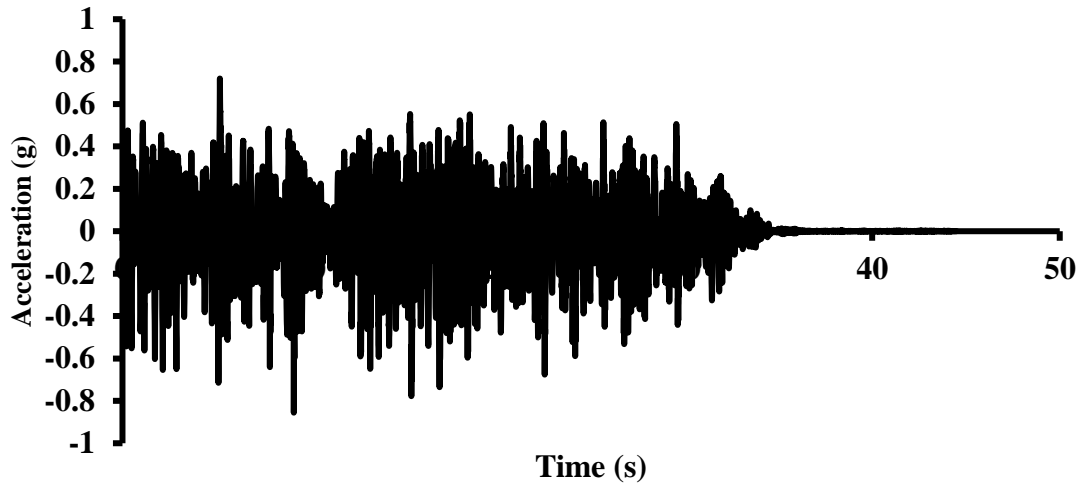


Figure 4. 35 : Numerical acceleration at roof level in the X direction in URM model - DBE

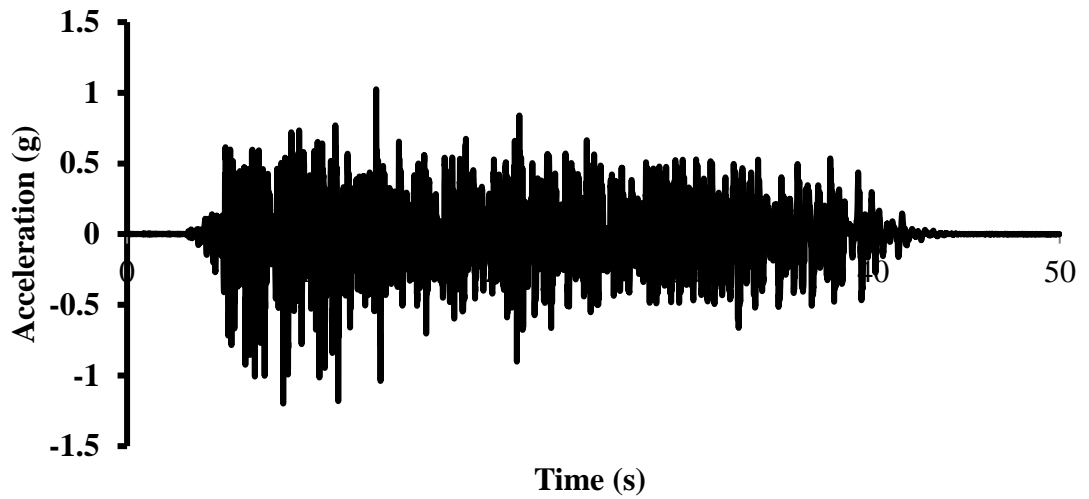
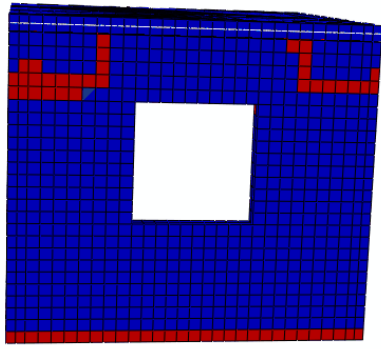
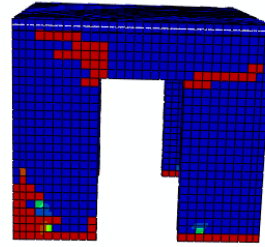


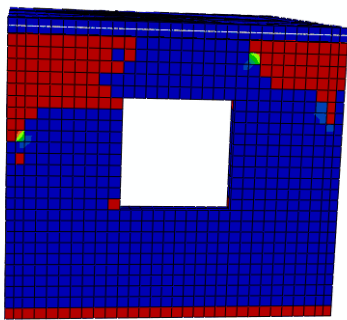
Figure 4. 36 : Numerical acceleration at roof level in the X direction in URM model - MCE



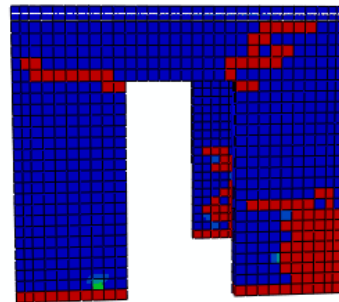
(a) Damage after first shock in west wall



(b) Damage after first shock in north wall



(c) Damage after second shock in west wall



(d) Damage after second shock in north wall

Figure 4. 37 : (a)-(d) Damage in URM model after shake loading

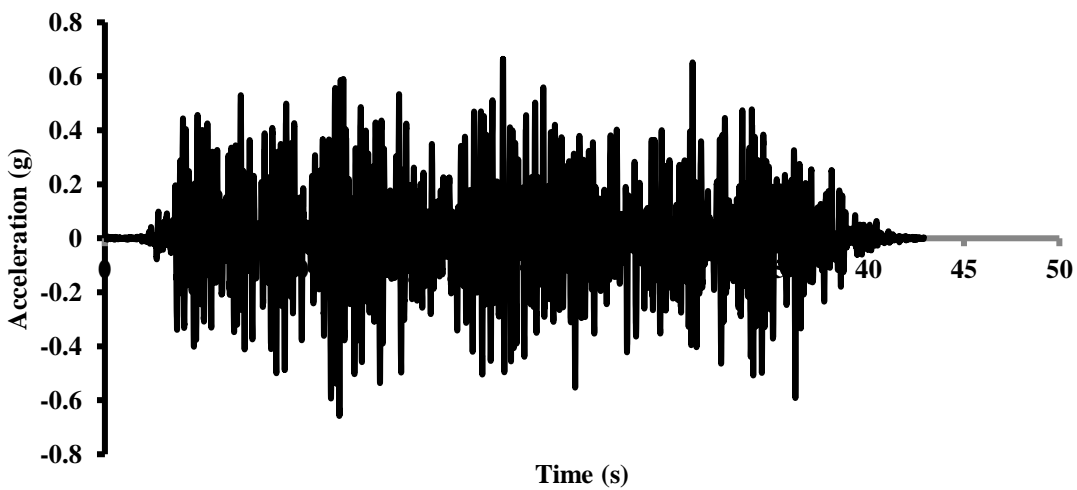


Figure 4. 38 : Numerical acceleration at roof level in the X direction in RM model - DBE

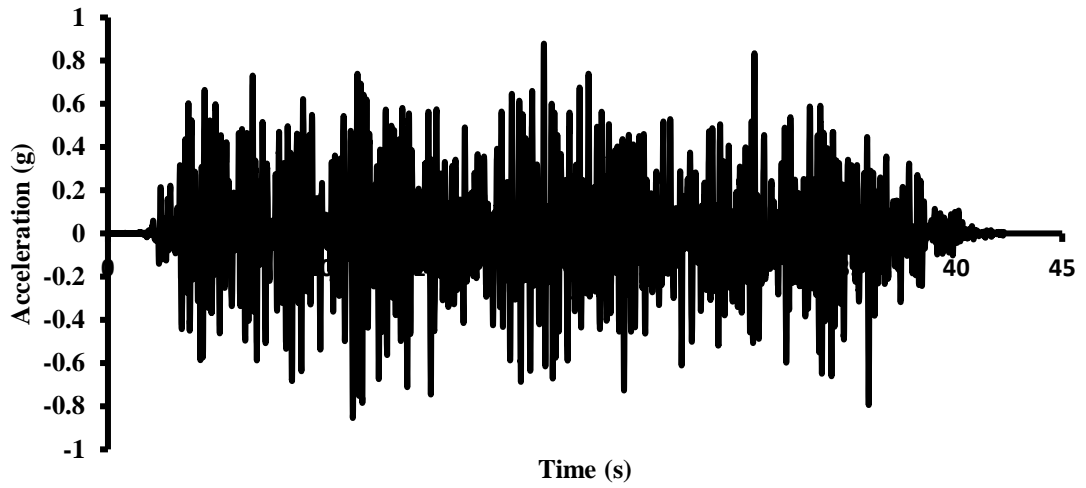


Figure 4.39 : Numerical acceleration at roof level in the X direction in RM model - 2 DBE

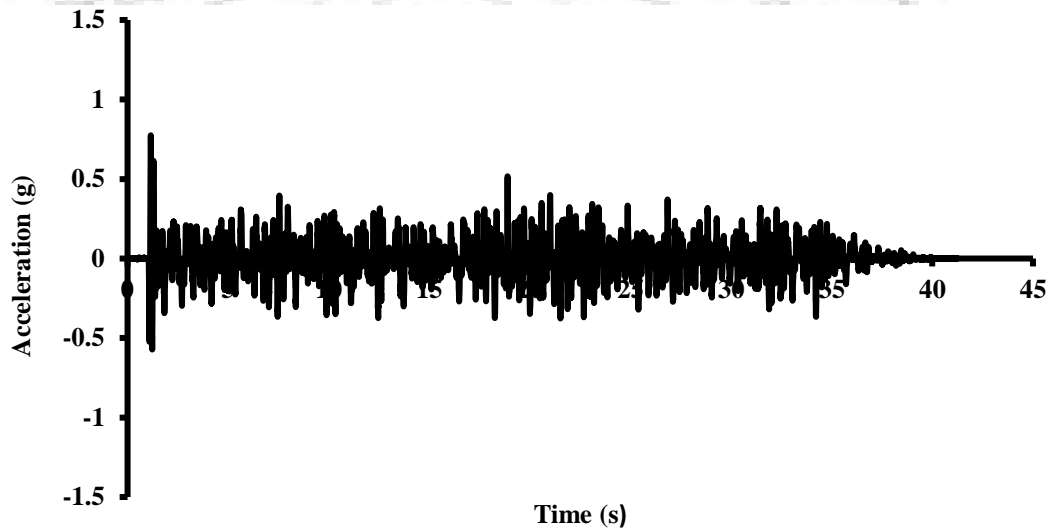


Figure 4.40 : Numerical acceleration at roof level in the X direction in RM model - 3 DBE

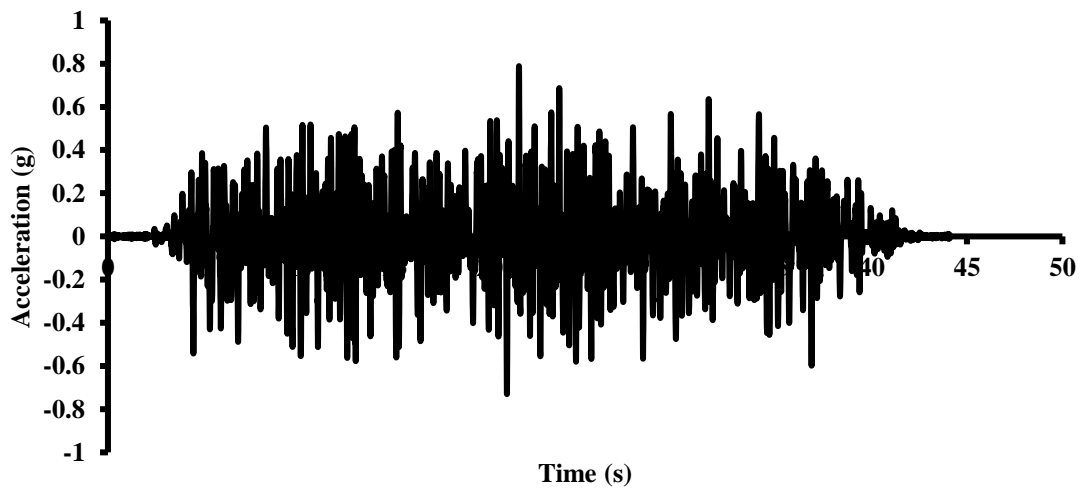


Figure 4.41 : Numerical acceleration at roof level in the X direction in RM model - 4 DBE

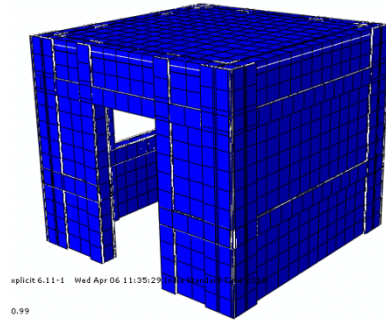


Figure 4. 42 : No damage in strengthened model after shake loading

4.12 SUMMARY

URM and RM models were constructed on a steel base plate and the tests were performed on the shake table. During the time of testing, behavior and response of both the models subjected to dynamic loading were examined. The URM model was constructed as per conventional procedure while the RM model was constructed as per the IS code provisions for seismic zone V. The earthquake resistant features included reinforcement in the form of WWM at sill level, lintel level, and at all the four corners and near the openings.

Total of two ground motions was applied to the URM model. Third shaking was not given to avoid the collapse of the model, which could have damaged the components/ parts of the shake table. In RM model, a total of four ground motions was applied with increasing intensity. Tri-axial accelerometers were used to record the base motion of the table and the roof motion of the models.

Minor cracks were observed in the URM model after the first shake and the cracks widened further during the second shake, resulting in severe damage to the model leading to the verge of its collapse. The inertia force transferred from the roof to the shear walls on northern and southern side led to the development of cracks originating near the openings. Though the in-plane shear walls offer greater resistance because of their larger depths, unreinforced masonry shear walls developed horizontal cracks at its base and around the window and door openings.

The RM model was subjected to intense ground motions as compared to URM model. The earthquake resistant features provided in the strengthened model in the form of sill band, lintel band and vertical corner band in all the four walls contributed in transferring the out-of-plane inertia force to the shear walls. The walls have been effectively tied together by placing vertical reinforcements to avoid the separation of vertical joints at the corners during shaking. North and south shear walls can resist lateral forces due to their own mass and those transmitted

to it from the roof. Further, the roof was properly anchored to the walls with the help of vertical reinforcement at all the four corners and near the openings starting from the foundation level, for exhibiting diaphragm action. All these earthquake resistant features incorporated in the strengthened model have not created any damage in the model even after the fourth shaking (higher than MCE). The following conclusions were arrived from the above experimental and numerical studies.

- The URM model was designed for gravity loads can resist only mild earthquakes while under moderate earthquakes, the brick masonry cracks which may lead to total collapse of the masonry building.
- Earthquake resistant features for brick masonry building are recommended in the Indian standard codes to enhance the seismic performance of the buildings.
- The proposed technique in this chapter can be implemented even to existing masonry structures without creating much damage to the structure.
- The experimental results concluded that the implementation of the proposed technique enhances the performance of the masonry structure during an earthquake.
- The numerical analysis using Abaqus, predicted the damage levels in both the building models with reasonable accuracy at all the shaking levels, justifying its application for estimating the seismic performance of URM and retrofitted buildings.
- The displacement and acceleration measured at the top level of the numerical model were quite close to those obtained experimentally, for both URM and strengthened models.



CHAPTER – 5

CONCLUSIONS AND SCOPE FOR FUTURE WORK

5.1 GENERAL

In this thesis, the efficacy of a retrofit methodology recommended in Indian standard code of practice for the strengthening of URM buildings has been evaluated both experimentally and numerically. Initially, 12 unreinforced masonry (URM) and 36 reinforced masonry (RM) panels were tested for both in-plane and out-of-plane loading and their behavior was observed for two types H2 and M2 (1:4 and 1:6) of mortar. Further, the experimental results of conventional URM panels were used to obtain material properties required to numerically simulate the non-linear material behavior of masonry. Seismic behavior of two half-scale masonry models was experimentally examined by shake table test for artificially generated acceleration time histories compatible with Indian standard response spectra for seismic zone V on hard soil. A finite element based micro-modeling approach using Concrete Damaged Plasticity (CDP) constitutive model has been used for both URM and RM panels for evaluating their performance in terms of damage pattern, shear stress-strain and load-deflection plots in case of both in-plane and out-of-plane loading. Similarly, half-scale masonry models were also numerically simulated and their behavior was compared with the shake table test results. Major findings of the foregoing study are discussed in the following sections.

5.2 URM PANELS

Material properties of masonry constituents i.e., brick and mortar and that of masonry prism under compression have been estimated using relevant ASTM standards. URM panels have been tested to study the in-plane and out-of-plane behavior as per ASTM (2010a, 2010b) guidelines. Finite element analysis, with CDP constitutive model, has been carried out to numerically simulate these experimental results. Summary of the experimental results and numerical study on the behavior of URM panels are given below:

- The behavior of URM specimens in diagonal shear test has been studied. During the testing, it was observed that the failure of the URM specimens was a combination of diagonal and sliding shear failure. These URM panels failed in a brittle manner.

- In the flexure tests, the failure of URM specimens was also sudden and brittle. After the development of first crack closer to the loading points, the specimens were not able to sustain any further load.
- It was found that non-linear finite element simulation using CDP constitutive model, could predict the behavior of URM panels under in-plane shear and out-of-plane bending. The numerically simulated results were found to be in good agreement with the experimental results in both the tests.

5.3 RM PANELS

WWM of three different spacing (1 inch, 1.5 inch and 2 inch) and coarse sand mortar has been used for strengthening of URM panels and were tested in both in-plane and out-of-plane action. To study the efficacy of the adopted strengthening (WWM) technique, the strengthened panels have been tested under diagonal compression and flexure according to ASTM standards. The effect of strengthening on the in-plane behavior of URM panels including failure modes, shear strength, maximum drift capacity and ductility have been investigated from experimental results. Similarly, the effect of strengthening on out-of-plane behavior has also been studied in terms of relative increase in strength and ductility. Finite element analyses have been carried out for in-plane and out-of-plane behavior of RM panels using CDP constitutive model to simulate the inelastic behavior of masonry and coarse sand mortar. The experimental and numerical results have been compared. Observations from the experimental and numerical studies on RM panels are as follows:

- The unreinforced masonry panels, when reinforced with WWM, have shown significant improvement in its shear strength and ductility because of the confining action of the strengthening technique adopted.
- An increase in ductility of about 5, 12 and 11 times was observed for RM panels strengthened with 1 inch, 1.5 inch and 2 inch spacing WWM respectively compared to URM panels with 1:4 mortar under diagonal shear compression.
- Further, an increase in ductility of about 4, 5 and 10 times was observed for RM panels strengthened with 1 inch, 1.5 inch and 2 inch spacing WWM respectively compared to URM panels with 1:6 mortar under diagonal shear compression.
- The RM panels showed better overall performance compared to URM panels when subjected to four point loading in out-of-plane action.

- The strengthened flexure specimen showed an increase in ductility of 1.7, 2.5 and 1.4 times in case of 1:4 RM panel with 1 inch, 1.5 inch and 2 inch spacing WWM respectively when compared with 1:4 URM panels.
- An increase in ductility of 1.6, 3.2 and 2.5 times was observed in case of 1:6 RM panel with 1 inch, 1.5 inch and 2 inch spacing WWM individually when compared to 1:4 URM panels.
- In case of flexure strengthened specimen, the initial failure pattern was much influenced by the masonry strength, but the final failure was influenced by the reinforcement provided.
- The test results build up the confidence in verifying the fact that WWM in combination with coarse sand mortar can significantly improve the performance of URM and can suitably be implemented in earthquake prone areas.
- It was found that non-linear finite element simulation using CDP constitutive model, could predict the behavior of strengthened panels under both in-plane and out-of-plane action reasonably well. The predicted strengths were also found to be in close agreement with experimental results.

5.4 DYNAMIC TESTING AND SIMULATION OF BUILDING MODELS

Two half-scale models, one traditionally built and the other strengthened with WWM and mortar have been tested for a series of artificially generated acceleration time history on the shake table test facility available at the Department of Earthquake Engineering, IIT Roorkee. These input ground motions were applied at the base of the model and the response in terms of acceleration has been recorded both at the base and at the top of both the models. The crack pattern, weaker zones, modes of failure and damages at different locations were identified with increasing intensity of shaking and conclusions were drawn with respect to the effectiveness of the strengthening technique adopted. The acceleration at top of the model obtained numerically was compared with the experimental observation. The major observations are as follows:

- Minor cracks were observed in the URM model after the first shake and the cracks widened further during the second shake, resulting in severe damage to the model. The inertia force transferred from the roof to the shear walls on northern and southern side led to the development of cracks originating near the openings. Though the in-plane shear walls offered great resistance because of their larger depths, unreinforced masonry shear walls developed horizontal cracks at its base and around the window and door openings.

- The RM model was subjected to the ground motions of increasing intensity. The earthquake resistant features provided in the strengthened model, in the form of seismic band at lintel level, vertical corner steel band at all the four corners of the model and jamb steel (vertical) near openings of two doors and a window, contributed in transferring the out-of-plane inertia force to the shear walls. The walls have been effectively tied together by placing reinforcements at appropriate locations as recommended in the code to avoid separation of vertical joints and any further damage during dynamic loading. North and south shear walls were capable of resisting horizontal forces due to their own mass and those transmitted to it from the roof. The roof was properly anchored to the walls with the help of vertical reinforcement in all the corners and near the opening to ensure appropriate diaphragm action. All these earthquake resistant features incorporated in the strengthened model enhanced the safety of RM model and no damage was observed even after the model was subjected to ground motion three times intense as was imparted to the URM model.
- The URM is most vulnerable to inertia forces leading to its damage/ collapse during earthquakes. The proposed technique can be implemented to any existing masonry structures without causing any structural damage to it and improve its seismic performance.
- It was found that non-linear finite element simulation using CDP constitutive model, could predict the behavior, of both URM and RM half-scale models tested on the shake table, reasonably well. The numerically simulated damage pattern and mode of failure were found to be in good agreement with the experimental results.

5.5 SCOPE FOR FUTURE WORK

The retrofit procedure recommended in IS 13935: 2009 and adopted in this study has been applied on both sides of the wall of a half-scale single story masonry building. Further, this study can be extended to full-scale and multi-storied masonry building (up to G+3) as well to evaluate their performance. In the present study, experiments have been conducted on half-scale models for uni-directional excitation. This can further be extended on prototype masonry buildings subjected to all three components of ground motion which would be the more realistic.

The scope of this study includes estimation of efficacy and developing numerical models for WWM, which can be extended to other strengthening materials including fibre reinforced polymer and engineered cementitious composites. This will require extensive experimental

investigations. The durability issues associated with the galvanised WWM should also be explored. Extensive experimental studies under bi-directional seismic excitation will be another challenging area to develop models for combined in-plane and out-of-plane action.

Fragility curve for masonry can also be developed by carrying out extensive experimental and numerical work by studying all the possible failure mechanism (in-plane, out-of-plane, combined in-plane and out-of-plane).





BIBLIOGRAPHY

1. ABAQUS, C. (2013). ABAQUS 6.13 Online documentation collection. Computer Software, Providence, RI.
2. Abboud, B.E., Hamid, A. and Harris, H.G. (1996). Flexural behaviour of reinforced concrete masonry walls under out-of-plane monotonic loads. *ACI Structural Journal*, 93(3), pp. 327-335.
3. Abrams, D., Smith, T., Lynch, J. and Franklin, S. (2007). Effectiveness of rehabilitation on seismic behaviour of masonry piers. *Journal of Structural Engineering*, 133(1), pp. 32-43.
4. ACI 531-79(1979). Building code requirements for concrete masonry structures, American Concrete Institute, Farmington Hills, MI 48331, U.S.A.
5. Adanur, S. (2010). Performance of masonry buildings during the 20 and 27 December 2007 Bala (Ankara) earthquakes in Turkey. *Natural Hazards and Earth System Sciences*, 10(12), pp. 2547-2556.
6. Agarwal, P., (1999). Experimental studies of seismic strengthening and retrofitting measure in masonry buildings. Ph.D. Thesis, Department of Earthquake Engineering, University of Roorkee, Roorkee.
7. Agrawal, P. and Shrikhande, M. (2006). Earthquake resistant design of structures. PHI Learning Pvt. Ltd.
8. Ahmad, N., Ali, Q., Ashraf, M., Naeem, A. and Alam, B. (2012). Seismic performance evaluation of reinforced plaster retrofitting technique for low-rise block masonry structures. *International Journal of Earth Sciences and Engineering*, 5(2), pp. 01-14.
9. Aiello, M.A., Micelli, F. and Valente, L. (2007). Structural upgrading of masonry columns by using composite reinforcements. *Journal of Composites for Construction*, 11(6), pp. 650-658.
10. Albert, M.L., Elwi, A.E. and Cheng, J.R. (2001). Strengthening of unreinforced masonry walls using FRPs. *Journal of Composites for Construction*, 5(2), pp. 76-84.
11. Al-Chaar, G.K. and Hasan, H.A. (2002). Dynamic response and seismic testing of CMU walls rehabilitated with composite material applied to only one side. *Proceedings of the Institution of Civil Engineers-Structures and Buildings*, 152(2), pp. 135-146.
12. Alcocer, S.M., Arias, J.G. and Vázquez, A. (2004). Response assessment of Mexican confined masonry structures through shaking table tests. *Proceedings of the 13th World Conference on Earthquake Engineering*, Vancouver, Canada, Paper No. 2130.

13. AlShawa, O., Sorrentino, L. and Liberatore, D. (2016). Simulation of shake table tests on out-of-plane masonry buildings. Part (II): Combined Finite-Discrete Elements. *International Journal of Architectural Heritage*, pp. 1-15.
14. Altin, S., Anil, Ö., Kara, M.E. and Kaya, M. (2008). An experimental study on strengthening of masonry infilled RC frames using diagonal CFRP strips. *Composites Part B: Engineering*, 39(4), pp. 680-693.
15. ASCE 41-06(2007). *Seismic Rehabilitation of Existing Buildings*. American Society of Civil Engineers, Virginia, USA.
16. Ashraf, M., Khan, A.N., Naseer, A., Ali, Q. and Alam, B. (2012). Seismic behaviour of unreinforced and confined brick masonry walls before and after ferrocement overlay retrofitting. *International Journal of Architectural Heritage*, 6(6), pp. 665-688.
17. Ashraf, M., Naeem Khan, A., Ali, Q., Shahzada, K. and Naseer, A. (2011). Experimental behaviour of full scale URM building retrofitted with ferrocement overlay. *Advanced Materials Research* (Vol. 255, pp. 319-323). Trans Tech Publications.
18. Asteris, P.G. (2003). Lateral stiffness of brick masonry infilled plane frames. *Journal of Structural Engineering*, 129(8), pp. 1071-1079
19. Asteris, P.G. (2008). On the structural analysis and seismic protection of historical masonry structures. *Open Construction and Building Technology Journal*, 2, pp. 124-133.
20. Asteris, P.G. and Tzamtzis, A.D. (2002). Non-linear analysis of masonry shear walls. *Proceedings of the 6th International Masonry Conference, London*, pp. 1-6.
21. Asteris, P.G., Cavaleri, L., Di Trapani, F. and Sarhosis, V. (2016). A macro-modelling approach for the analysis of infilled frame structures considering the effects of openings and vertical loads. *Structure and Infrastructure Engineering*, 12(5), pp. 551-566.
22. Asteris, P.G., Giannopoulos, I.P. and Chrysostomou, C.Z. (2012). Modeling of infilled frames with openings. *The Open Construction and Building Technology Journal*, 6(1), pp. 81-91.
23. ASTM (1991). "Standard test method for in situ compressive stress within solid unit masonry estimated using flat jack measurements." ASTM C1196-91
24. ASTM (2002). "Standard test method for pulse velocity through concrete." ASTM C597-02
25. ASTM (2010). "Standard test method for measuring the p-wave speed and the thickness of concrete plates using the impact-echo method." ASTM C1383-10
26. ASTM (2010a). "Standard test method for diagonal tension (shear) in masonry assemblages." ASTM E519/ E519M

27. ASTM (2010b). "Standard Test Method for Flexural Bond Strength of Masonry." ASTM E518/E518M-10
28. ASTM (2011a). "Standard test method and definitions for mechanical testing of steel products." ASTM A370-11
29. ASTM (2011b). "Standard test method for compressive strength of hydraulic cement mortars (using 2-in. or [50-mm] cube specimens)." ASTM C109/C109M
30. ASTM (2011C). "Standard test method for sampling and testing brick and structural clay tile." ASTM C67-11
31. ASTM (2011d). "Standard Test Method for compressive strength of masonry prism." ASTM C1314-11
32. Astroza, M., Moroni, O., Brzev, S. and Tanner, J. (2012). Seismic performance of engineered masonry buildings in the 2010 Maule earthquake. *Earthquake Spectra*, 28(S1), S385-S406.
33. Bajpai, K. and Duthinh, D. (2003). Bending performance of masonry walls strengthened with near-surface mounted FRP bars. *Proceedings of the 9th North American Masonry Conference*, pp. 1-4.
34. Bencardino, F., Spadea, G. and Swamy, R.N. (2002). Strength and ductility of reinforced concrete beams externally reinforced with carbon fiber fabric. *Structural Journal*, 99(2), pp. 163-171.
35. Benedetti, D. and Pezzoli, P. (1996). *Shaking table tests on masonry buildings, results and comments: experimental evaluation of technical interventions to reduce the seismic vulnerability of masonry buildings - A Monograph*, Bergamo, Italy
36. Benedetti, D., Carydis, P. and Pezzoli, P. (1998). Shaking table tests on 24 simple masonry buildings. *Earthquake Engineering & Structural Dynamics*, 27(1), pp. 67-90.
37. Blondet, M., Garcia, G.V., Brzev, S. and Rubiños, A. (2003). Earthquake-resistant construction of adobe buildings: A tutorial. *EERI/IAEE World Housing Encyclopaedia*.
38. Bocca, P. and Grazzini, A. (2008). Experimental techniques for the evaluation of the long-term behaviour of masonry strengthening materials. *Proceedings of 6th Conference on Structural Analysis of Historical Construction (SAHC08)*, pp. 339-347.
39. Borri, A., Castori, G. and Corradi, M. (2011). Shear behaviour of masonry panels strengthened by high strength steel cords. *Construction and Building Materials*, 25(2), pp. 494-503.

40. Borri, A., Castori, G., Corradi, M. and Sisti, R. (2014). Masonry wall panels with GFRP and steel-cord strengthening subjected to cyclic shear: An experimental study. *Construction and Building Materials*, 56, pp. 63-73.
41. Bothara, J.K., Dhakal, R.P. and Mander, J.B. (2010). Seismic performance of an unreinforced masonry building: an experimental investigation. *Earthquake Engineering & Structural Dynamics*, 39(1), pp. 45-68.
42. Bruneau, M. (1994). State-of-the-art report on seismic performance of unreinforced masonry buildings. *Journal of Structural Engineering*, 120(1), pp. 230-251.
43. Brzev, S. (2007). Earthquake-resistant confined masonry construction. National Information Center of Earthquake Engineering (NICEE), Indian Institute of Technology Kanpur, India.
44. Brzev, S. (2008). Earthquake-resistant confined masonry construction. National Information Center for Earthquake Engineering (NICEE), Indian Institute of Technology Kanpur, India.
45. Calvi, G.M., Kingsley, G.R. and Magenes, G. (1996). Testing of masonry structures for seismic assessment. *Earthquake Spectra*, 12(1), pp. 145-162.
46. Candeias, P., Costa, A.C. and Coelho, E. (2004). Shaking table tests of 1:3 reduced scale models of four story unreinforced masonry buildings. *Proceedings of the 13th World Conference on Earthquake Engineering*. Vancouver, Canada.
47. Capozucca, R. (2016). Double-leaf masonry walls under in-plane loading strengthened with GFRP/SRG strips. *Engineering Structures*, 128, pp. 453-473.
48. Carozzi, F.G. and Poggi, C. (2015). Mechanical properties and debonding strength of Fabric Reinforced Cementitious Matrix (FRCM) systems for masonry strengthening. *Composites Part B: Engineering*, 70, pp. 215-230.
49. Carozzi, F.G., Milani, G. and Poggi, C. (2014). Mechanical properties and numerical modeling of fabric reinforced cementitious matrix (FRCM) systems for strengthening of masonry structures. *Composite Structures*, 107, pp. 711-725.
50. Cecchi, A. and Barbieri, A. (2008). Homogenisation procedure to evaluate the effectiveness of masonry strengthening by CFRP repointing technique. *WSEAS Transactions on Applied and Theoretical Mechanics*, 3(1), pp. 12-27.
51. Chácará, C., Mendes, N., & Lourenço, P. B. (2017). Simulation of shake table tests on out-of-plane masonry buildings. Part (IV): macro and micro FEM based approaches. *International Journal of Architectural Heritage*, 11(1), 103-116.

52. Chávez, Marcos and Roberto, Meli. (2012). Shaking table testing and numerical simulation of the seismic response of a typical Mexican colonial temple. *Earthquake Engineering & Structural Dynamics* 41.2, pp. 233-253.
53. Chen, X. and Liu, Y. (2017). Finite element study of the effect of interfacial gaps on the in-plane behaviour of masonry infills bounded by steel frames. *Structures* (Vol. 10, pp. 1-12.
54. Chen, Y., Ashour, A. F., & Garrity, S. W. (2007). Modified four-hinge mechanism analysis for masonry arches strengthened with near-surface reinforcement. *Engineering structures*, 29(8), pp. 1864-1871.
55. Chen, Y., Ashour, A.F. and Garrity, S.W. (2008). Moment/thrust interaction diagrams for reinforced masonry sections. *Construction and Building Materials*, 22(5), pp. 763-770.
56. Churilov, S. and Dumova-Jovanoska, E. (2012). Analysis of masonry walls strengthened with RC jackets. 15th WCEE, Lisbon, Portugal.
57. Corradi, M., Borri, A. and Vignoli, A. (2003). Experimental study on the determination of strength of masonry walls. *Construction and Building Materials*, 17(5), pp. 325-337.
58. Corradi, M., Borri, A., Castori, G. and Sisti, R. (2014). Shear strengthening of wall panels through jacketing with cement mortar reinforced by GFRP grids. *Composites Part B: Engineering*, 64, pp. 33-42.
59. Costa, A.A., Arêde, A., Costa, A.C., Penna, A. and Costa, A. (2013). Out-of-plane behaviour of a full scale stone masonry façade. Part 2: shaking table tests. *Earthquake Engineering & Structural Dynamics*, 42(14), pp. 2097-2111.
60. D'Ambrisi, A., Feo, L. and Focacci, F. (2013). Experimental and numerical investigation on bond between Carbon-FRCM materials and masonry. *Composites Part B: Engineering*, 46, pp. 15-20.
61. Das, A., Deb, S.K. and Dutta, A. (2016). Comparison of numerical and experimental seismic responses of FREI-supported un-reinforced brick masonry model building. *Journal of Earthquake Engineering*, 20(8), pp. 1239-1262.
62. Das, A., Deb, S.K. and Dutta, A. (2016). Shake table testing of un-reinforced brick masonry building test model isolated by U-FREI. *Earthquake Engineering & Structural Dynamics*, 45(2), pp. 253-272.
63. De Felice, G., De Santis, S., Garmendia, L., Ghiassi, B., Larrinaga, P., Lourenço, P. B. and Papanicolaou, C.G. (2014). Mortar-based systems for externally bonded strengthening of masonry. *Materials and structures*, 47(12), pp. 2021-2037.

64. De Lorenzis, L., Tinazzi, D. and Nanni, A. (2000). Near surface mounted FRP rods for masonry strengthening: bond and flexural testing. Proceedings of the International Conference on Composite Engineering.
65. Dhanasekar, Manicka, and Waheed Haider. (2008). Explicit finite element analysis of lightly reinforced masonry shear walls. Computers & Structures 86.1, pp. 15-26.
66. Dizhur, D., Griffith, M. and Ingham, J. (2014). Out-of-plane strengthening of unreinforced masonry walls using near surface mounted fibre reinforced polymer strips. Engineering structures, 59, pp. 330-343.
67. Dolatshahi, K.M. and Yekrangnia, M. (2015). Out-of-plane strength reduction of unreinforced masonry walls because of in-plane damages. Earthquake Engineering & Structural Dynamics, 44(13), pp. 2157-2176.
68. Drysdale, R.G., Hamid, A.A. and Baker, L.R. (1994). Masonry structures: Behaviour and design. Prentice Hall.
69. Dubey, R.N., (2011). Experimental studies to verify the efficacy of earthquake resistant measures in masonry buildings. Ph.D. Thesis, Department of Earthquake Engineering, Indian Institute of Technology Roorkee, Roorkee.
70. Ehsani, M.R. (1995). Strengthening of earthquake-damaged masonry structures with composite materials. RILEM Proceedings, Chapman & Hall, pp. 680-680.
71. ElGawady, M.A., Lestuzzi, P. and Badoux, M. (2004). A review of conventional seismic retrofitting techniques for URM. 13th International Brick and Block Masonry Conference, Amsterdam (Vol. 10, No. 10).
72. ElGawady, M.A., Lestuzzi, P. and Badoux, M. (2006). Aseismic retrofitting of unreinforced masonry walls using FRP. Composites Part B: Engineering, 37(2), pp. 148-162.
73. ElGawady, M.A., Lestuzzi, P. and Badoux, M. (2006). Retrofitting of masonry walls using shotcrete. Proceedings of the NZSEE Conference, Paper (Vol. 45).
74. Eurocode 6 (2005). "Design of masonry structures Part1-2, General rules-structural fire design", European Committee for standardization (CEN), Brussels, Belgium.
75. Eurocode 8 (2004). "Design for structures for earthquake resistance, Part-1, General Rules, Seismic actions and rules for buildings", European Committee for standardization (CEN), Brussels, Belgium.
76. Faella, C., Martinelli, E., Nigro, E. and Paciello, S. (2004). Tuff masonry walls strengthened with a new kind of C-FRP sheet: experimental tests and analysis. Proceedings of the 13th World Conference on Earthquake Engineering. Paper (No. 923).

77. Farooq, S.H., Ilyas, M. and Ghaffar, A. (2006). Technique for strengthening of masonry wall panels using steel strips. *Asian Journal of Civil Engineering (Building and Housing)*, 7(6), pp. 621-638.
78. FEMA 172 (1992). "NEHRP Handbook of techniques for seismic rehabilitation of existing buildings." Federal Emergency Management Agency, Washington, D.C., USA.
79. FEMA 306 (1998) "Evaluation of earthquake damaged concrete and masonry wall buildings: Basic procedures manual." Federal Emergency Management Agency, Washington, D.C., USA.
80. FEMA 356 (2000). "Prestandard and commentary for the seismic rehabilitation of buildings." Federal Emergency Management Agency, Washington, D.C., USA.
81. Furtado, A., Rodrigues, H., Arêde, A. and Varum, H. (2016). Simplified macro-model for infill masonry walls considering the out-of-plane behaviour. *Earthquake Engineering & Structural Dynamics*, 45(4), pp. 507-524.
82. Gabor, A., Bennani, A., Jacquelin, E. and Lebon, F. (2006). Modelling approaches of the in-plane shear behaviour of unreinforced and FRP strengthened masonry panels. *Composite Structures*, 74(3), pp. 277-288.
83. Galal, K. and Sasanian, N. (2010). Out-of-plane flexural performance of GFRP-reinforced masonry walls. *Journal of Composites for Construction*, 14(2), 162-174.
84. Garofano, A., Ceroni, F. and Pecce, M. (2016). Modelling of the in-plane behaviour of masonry walls strengthened with polymeric grids embedded in cementitious mortar layers. *Composites Part B: Engineering*, 85, pp. 243-258.
85. Ghobarah, A. and El Mandooh Galal, K. (2004). Out-of-plane strengthening of unreinforced masonry walls with openings. *Journal of Composites for Construction*, 8(4), pp. 298-305.
86. Giordano, A., Mele, E. and De Luca, A. (2002). Modelling of historical masonry structures: comparison of different approaches through a case study. *Engineering Structures*, 24(8), pp. 1057-1069.
87. Grecchi, G. (2010). Material and structural behaviour of masonry: simulation with a commercial code. *Laurea Thesis, University of Pavia, Lombardy, Italy.*
88. Griffith, M.C., Lam, N.T., Wilson, J.L. and Doherty, K. (2004). Experimental investigation of unreinforced brick masonry walls in flexure. *Journal of Structural Engineering*, 130(3), pp. 423-432.

89. Gumaste, K.S., Rao, K.N., Reddy, B.V. and Jagdish, K.S. (2007). Strength and elasticity of brick masonry prisms and wallettes under compression. *Materials and Structures*, 40(2), pp. 241-253.
90. Hall, J.D., Schuman, P.M. and Hamilton III, H.R. (2002). Ductile anchorage for connecting FRP strengthening of under-reinforced masonry buildings. *Journal of Composites for Construction*, 6(1), pp. 3-10.
91. Hamid, A., Mahmoud, A. and El Magd, S.A. (1994). Strengthening and repair of unreinforced masonry structures: state-of-the-art. *Proceedings of the 10th International Brick and Block Masonry Conference*, Vol. 2, pp. 485-497.
92. Hamid, A.A. and Drysdale, R.G. (1988). Flexural tensile strength of concrete block masonry. *Journal of Structural Engineering*, 114(1), pp. 50-66.
93. Hamid, A.A., El-Dakhakhni, W.W., Hakam, Z.H. and Elgaaly, M. (2005). Behaviour of composite unreinforced masonry–fiber-reinforced polymer wall assemblages under in-plane loading. *Journal of Composites for Construction*, 9(1), pp. 73-83.
94. Hamilton III, H.R. and Dolan, C.W. (2001). Flexural capacity of glass FRP strengthened concrete masonry walls. *Journal of Composites for Construction*, 5(3), pp. 170-178.
95. Hamilton III, H.R., Holberg, A., Caspersen, J. and Dolan, C.W. (1999). Strengthening concrete masonry with fiber reinforced polymers. *Special Publication*, 188, pp. 1103-1116.
96. Hamoush, S.A., McGinley, M.W., Mlakar, P., Scott, D. and Murray, K. (2001). Out-of-plane strengthening of masonry walls with reinforced composites. *Journal of Composites for Construction*, 5(3), 139-145.
97. Hashemi, A., & Mosalam, K.M. (2006). Shake-table experiment on reinforced concrete structure containing masonry infill wall. *Earthquake Engineering & Structural Dynamics*, 35(14), pp. 1827-1852.
98. Hashmi, A. K., & Madan, A. (2008). Damage forecast for masonry infilled reinforced concrete framed buildings subjected to earthquakes in India. *Current Science*, 61-73.
99. Hollaway, L.C. and Teng, J.G. (Eds.). (2008). *Strengthening and rehabilitation of civil infrastructures using fibre-reinforced polymer (FRP) composites*. Elsevier.
100. Hu, H. T., and Schnobrich, W. C. (1989). Constitutive modeling of concrete by using nonassociated plasticity. *Journal of Materials in Civil Engineering*, 1(4), 199-216.
101. Hu, H.T., Lin, F.M. and Jan, Y.Y. (2004). Non-linear finite element analysis of reinforced concrete beams strengthened by fiber-reinforced plastics. *Composite Structures*, 63(3), pp. 271-281.

102. Huang, H.C. and Usmani, A.S. (2012). Finite element analysis for heat transfer: theory and software. Springer Science & Business Media.
103. IITK-GSDMA. (2005). Guidelines for structural use of reinforced masonry, NICEE, Indian Institute of Technology Kanpur.
104. IS 1077 (1992). "Common Burnt Clay Building Bricks-Specification." Bureau of Indian Standard, New Delhi. India.
105. IS 13828 (1993). "Indian Standard Guidelines for Improving Earthquake Resistance of Low Strength Masonry." Bureau of Indian Standard, New Delhi. India.
106. IS 13935 (2009). "Indian Standard Code of Evaluation, Repair and Strengthening of Masonry Buildings." Bureau of Indian Standard, New Delhi. India.
107. IS 1893 Part I (2002). "Indian Standard Criteria for Earthquake Design of Structures." Bureau of Indian Standard, New Delhi. India.
108. IS 1905 (1987). "Indian Standard Code of Practice for Structural Use of Unreinforced Masonry (Third Revision)." Bureau of Indian Standard, New Delhi. India.
109. IS 4326 (1993). "Indian Standard Code of Earthquake Resistant Design and Construction of Building." Bureau of Indian Standard, New Delhi. India.
110. IS 456 (2000). "Plain and Reinforced Concrete-Code of practice." Bureau of Indian Standard, New Delhi. India.
111. IS 516 (1959). "Indian Standard Methods of Tests for Concrete." Bureau of Indian Standard, New Delhi. India.
112. IS 875 Part I (1987). "Code of practice for Design Loads (other than Earthquake) for Buildings and Structures." Bureau of Indian Standard, New Delhi. India.
113. Ismail, N., Petersen, R.B., Masia, M.J. and Ingham, J.M. (2011). Diagonal shear behaviour of unreinforced masonry wallettes strengthened using twisted steel bars. *Construction and Building Materials*, 25(12), pp. 4386-4393.
114. Jagadish, K. S., Raghunath, S., & Rao, K. N. (2003). Behaviour of masonry structures during the Bhuj earthquake of January 2001. *Journal of Earth System Science*, 112(3), 431-440.
115. Jain, S. K. (2016). Earthquake safety in India: achievements, challenges and opportunities. *Bulletin of Earthquake Engineering*, 14(5), 1337-1436.
116. Jain, S.K., Murty, C.V.R., Arlekar, J.N., Sinha, R., Goyal, A. and Jain, C.K. (1997). Some observations on engineering aspects of the Jabalpur earthquake of 22 May 1997. *EERI Special Earthquake Report, EERI Newsletter*, 32(2), pp. 1-18.

117. Janaraj, T. and Dhanasekar, M. (2014). Finite element analysis of the in-plane shear behaviour of masonry panels confined with reinforced grouted cores. *Construction and Building Materials*, 65, pp. 495-506.
118. Janaraj, T. and Dhanasekar, M. (2016). Studies on the existing in-plane shear equations of partially grouted reinforced masonry. *Australian Journal of Structural Engineering*, pp. 1-8.
119. Jankowiak, T. and Lodygowski, T. (2005). Identification of parameters of concrete damage plasticity constitutive model. *Foundations of Civil and Environmental Engineering*, 6(1), pp. 53-69.
120. Joshua Daniel., (2012). Seismic analysis of masonry buildings, M.Tech. Dissertation, Department of Earthquake Engineering, Indian Institute of Technology Roorkee, Roorkee.
121. Kadam, S.B., Singh, Y. and Li, B. (2014). Strengthening of unreinforced masonry using welded wire mesh and micro-concrete—behaviour under in-plane action. *Construction and Building Materials*, 54, pp. 247-257.
122. Kadam, S.B., Singh, Y. and Li, B. (2015). Out-of-plane behaviour of unreinforced masonry strengthened using ferrocement overlay. *Materials and Structures*, 48(10), pp. 3187-3203.
123. Kalali, A. and Kabir, M.Z. (2012). Experimental response of double-wythe masonry panels strengthened with glass fiber reinforced polymers subjected to diagonal compression tests. *Engineering Structures*, 39, pp. 24-37.
124. Karantoni, F.V. and Fardis, M.N. (1992). Effectiveness of seismic strengthening techniques for masonry buildings. *Journal of Structural Engineering*, 118(7), pp. 1884-1902.
125. Kaushik, H.B., Rai, D.C. and Jain, S.K. (2006). Code approaches to seismic design of masonry-infilled reinforced concrete frames: A State-of-the-art review. *Earthquake Spectra*, 22(4), pp. 961-983.
126. Kaushik, H.B., Rai, D.C. and Jain, S.K. (2007). Stress-strain characteristics of clay brick masonry under uniaxial compression. *Journal of Materials in Civil Engineering*, 19(9), pp. 728-739.
127. Kaushik, H.B., Rai, D.C. and Jain, S.K. (2007). Uniaxial compressive stress-strain model for clay brick masonry. *Current Science*, 92(4), pp. 497-501.
128. Kazemi, M.T., Asl, M.H., Bakhshi, A. and Rofooei, F.R. (2010). Shaking table study of a full-scale single storey confined brick masonry building. *Scientia Iranica. Transaction A, Civil Engineering*, 17(3), 184.

129. Kolsch, H. (1998). Carbon fiber cement matrix (CFCM) overlay system for masonry strengthening. *Journal of Composites for Construction*, 2(2), 105-109.
130. Korany, Y. and Drysdale, R. (2006). Rehabilitation of masonry walls using unobtrusive FRP techniques for enhanced out-of-plane seismic resistance. *Journal of Composites for Construction*, 10(3), pp. 213-222.
131. Krevaikas, T.D. and Triantafillou, T.C. (2005). Masonry confinement with fiber-reinforced polymers. *Journal of Composites for Construction*, 9(2), pp. 128-135.
132. Kumar, A. and Sinha, R. (2003). Rural mud house with pitched roof. *World housing Encyclopaedia Report*, (23).
133. Lang, D.H. (2004). Damage potential of seismic ground motion considering local site effects.
134. Lang, D.H., Molina-Palacios, S. and Lindholm, C.D. (2008). Towards near-real-time damage estimation using a CSM-based tool for seismic risk assessment. *Journal of Earthquake Engineering*, 12(S2), pp. 199-210.
135. Lang, D.H., Singh, Y. and Prasad, J.S.R. (2012). Comparing empirical and analytical estimates of earthquake loss assessment studies for the city of Dehradun, India. *Earthquake Spectra*, 28(2), pp. 595-619.
136. Lee, H.K., Kim, B.R. and Ha, S.K. (2008). Numerical evaluation of shear strengthening performance of CFRP sheets/strips and sprayed epoxy coating repair systems. *Composites Part B: Engineering*, 39(5), pp. 851-862.
137. Lewis, R.W., Zheng, Y. and Usmani, A.S. (1995). Aspects of adaptive mesh generation based on domain decomposition and Delaunay triangulation. *Finite Elements in Analysis and Design*, 20(1), pp. 47-70.
138. Li, T., Galati, N., Tumialan, J.G. and Nanni, A. (2005). Analysis of unreinforced masonry concrete walls strengthened with glass fiber-reinforced polymer bars. *ACI Structural Journal*, 102(4), 569.
139. Lin, Y., Ingham, J. and Lawley, D. (2010). Testing of unreinforced masonry walls seismically retrofitted with ECC shotcrete. *Shotcrete: Elements of a System*, 191.
140. Lin, Y., Lawley, D., Wotherspoon, L. and Ingham, J.M. (2016). Out-of-plane testing of unreinforced masonry walls strengthened using ECC shotcrete. *Structures (Vol. 7)*, Elsevier, pp. 33-42.
141. Lotfi, H.R. and Shing, P.B. (1991). An appraisal of smeared crack models for masonry shear wall analysis. *Computers & structures*, 41(3), pp. 413-425.

- 142.Lourenco, P.B. (1996). Computational strategies for masonry structures. TU Delft, Delft University of Technology.
- 143.Lourenço, P.B. and Barros, J. (2000). Size effect on masonry subjected to out-of-plane loading. Proceedings of 12th International Brick/Block Masonry Conference (Vol. 2), pp. 1085-1098.
- 144.Lourenço, P.B., Avila, L., Vasconcelos, G., Alves, J.P.P., Mendes, N. and Costa, A.C. (2013). Experimental investigation on the seismic performance of masonry buildings using shaking table testing. Bulletin of Earthquake Engineering, 11(4), pp. 1157-1190.
- 145.Lu, X., Fu, G., Shi, W. and Lu, W. (2008). Shake table model testing and its application. The Structural Design of Tall and Special Buildings, 17(1), pp. 181-201.
- 146.Luccioni, B. and Rougier, V.C. (2011). In-plane retrofitting of masonry panels with fibre reinforced composite materials. Construction and Building Materials, 25(4), pp. 1772-1788.
- 147.Maalej, M., Lin, V.W.J., Nguyen, M.P. and Quek, S.T. (2010). Engineered cementitious composites for effective strengthening of unreinforced masonry walls. Engineering Structures, 32(8), pp. 2432-2439.
- 148.Maddaloni, G., Di Ludovico, M., Balsamo, A. and Prota, A. (2016). Out-of-plane experimental behaviour of T-shaped full scale masonry wall strengthened with composite connections. Composites Part B: Engineering, 93, pp. 328-343.
- 149.MagarPatil, H. R. and Jangid, R.S. (2013). Seismic vulnerability assessment of steel moment resisting frame due to infill masonry wall, variation in column size and horizontal buckling restrained braces. International Journal of Civil and Environmental Engineering, 2(1), pp. 20-27.
- 150.MagarPatil, H.R. and Jangid, R.S. (2012). Seismic assessment of steel moment resisting frame with and without masonry walls. Proceeding of International Conference on Structural and Civil Engineering, Bangalore, pp. 05-08.
- 151.MagarPatil, H.R. and Jangid, R.S. (2015). Numerical study of seismic performance of steel moment-resisting frame with buckling-restrained brace and viscous fluid damper. The IES Journal Part A: Civil & Structural Engineering, 8(3), pp.165-174.
- 152.Magenes, G. and Calvi, G.M. (1997). In-plane seismic response of brick masonry walls. Earthquake Engineering & Structural Dynamics, 26(11), pp. 1091-1112.
- 153.Mahmood, H. and Ingham, J.M. (2011). Diagonal compression testing of FRP-retrofitted unreinforced clay brick masonry wallettes. Journal of Composites for Construction, 15(5), pp. 810-820.

154. Maoxin, J.L.Z. (2004). Review of research on strengthening of structure with ferrocement laminates. *Journal of Building Structure*, 3, 001.
155. Marcari, G., Manfredi, G., Prota, A. and Pecce, M. (2007). In-plane shear performance of masonry panels strengthened with FRP. *Composites Part B: Engineering*, 38(7), pp. 887-901.
156. Marcari, G., Oliveira, D.V., Fabbrocino, G. and Lourenço, P.B. (2011). Shear capacity assessment of tuff panels strengthened with FRP diagonal layout. *Composites Part B: Engineering*, 42(7), pp.1956-1965.
157. Marshall Jr, O.S., Sweeney, S.C. and Trovillion, J.C. (2000). Performance testing of fiber-reinforced polymer composite overlays for seismic rehabilitation of unreinforced masonry walls. Engineer Research and Development Center Champaign IL Construction Engineering Research Lab, (No. ERDC/CERL-TR-00-18).
158. Matsagar, V.A. and Jangid, R.S. (2008). Base isolation for seismic retrofitting of structures. *Practice Periodical on Structural Design and Construction*, 13(4), pp. 175-185.
159. McNary, W.S. and Abrams, D.P. (1985). Mechanics of masonry in compression. *Journal of Structural Engineering*, 111(4), pp. 857-870.
160. Meisl, C.S., Elwood, K.J. and Ventura, C.E. (2007). Shake table tests on the out-of-plane response of unreinforced masonry walls. *Canadian Journal of Civil Engineering, Special Issue on Masonry*, 34(11), pp. 1381-1392.
161. Mele, E., De Luca, A. and Giordano, A. (2003). Modelling and analysis of a basilica under earthquake loading. *Journal of Cultural Heritage*, 4(4), pp. 355-367.
162. Mendes, N., Costa, A. A., Lourenço, P. B., Bento, R., Beyer, K., de Felice, G., & Lemos, J. V. (2017). Methods and approaches for blind test predictions of out-of-plane behavior of masonry walls: A numerical comparative study. *International Journal of Architectural Heritage*, 11(1), 59-71.
163. Mendes, N., Lourenço, P.B. and Campos-Costa, A. (2014). Shaking table testing of an existing masonry building: assessment and improvement of the seismic performance. *Earthquake Engineering & Structural Dynamics*, 43(2), pp. 247-266.
164. Menna, C., Asprone, D., Durante, M., Zinno, A., Balsamo, A. and Prota, A. (2015). Structural behaviour of masonry panels strengthened with an innovative hemp fibre composite grid. *Construction and Building Materials*, 100, pp. 111-121.
165. Miltiadou-Fezans, A. and Tassios, T.P. (2013). Stability of hydraulic grouts for masonry strengthening. *Materials and Structures*, 46(10), pp. 1631-1652.

166. Moon, F. L., Yi, T., Leon, R. T., & Kahn, L. F. (2007). Testing of a full-scale unreinforced masonry building following seismic strengthening. *Journal of Structural Engineering*, 133(9), pp. 1215-1226.
167. Mordanova, A., De Santis, S. and de Felice, G. (2016). State-of-the-art review of out-of-plane strengthening of masonry walls with mortar-based composites.
168. Mosallam, A.S. (2007). Out-of-plane flexural behaviour of unreinforced red brick walls strengthened with FRP composites. *Composites Part B: Engineering*, 38(5), pp. 559-574.
169. Moșoarcă, M., Petruș, C., Stoian, V. and Anastasiadis, A. (2016). Behaviour of masonry infills subjected to out of plane seismic actions. Part 1: Theoretical analysis.
170. MSJC (2013). "Building code requirements and specification for masonry structures" TMS 402-13/ACI 530-13/ASCE 5-13, The Masonry Society.
171. Nanni, A. and Tumialan, J.G. (2003). Fiber-reinforced composites for the strengthening of masonry structures. *Structural Engineering International*, 13(4), pp. 271-278.
172. Naqvi, T., Datta, T.K. and Ramana, G.V. (2010). Fragility analysis of concrete building structures. *International Journal of Earth Science and Engineering*, 3(5).
173. Naqvi, T., Datta, T.K. and Ramana, G.V. (2010). Fragility analysis of flexible base buildings. *IUP Journal of Structural Engineering*, 3(4).
174. Nateghi, A.F. and Alemi, F. (2008). Experimental study of seismic behaviour of typical Iranian URM brick walls. *Proc. of the 14th World Conference on Earthquake Engineering*, Beijing, China.
175. Nath, R.J., Deb, S.K. and Dutta, A. (2013). Base isolated RC building-performance evaluation and numerical model updating using recorded earthquake response. *Earthquakes and Structures*, 4(5), pp. 471-487.
176. NBCC (2010). "National building code of Canada" National Research Council 1200 Montreal Road, Ottawa ON K1A 0R6.
177. NCPDP (2006). "Intervention for capacity building for earthquake risk reduction in earthquake affected part of Kashmir" Building materials and Technology Promotion Council, New Delhi.
178. Noor-E-Khuda, S., Dhanasekar, M. and Thambiratnam, D. P. (2016). Out-of-plane deformation and failure of masonry walls with various forms of reinforcement. *Composite Structures*, 140, pp. 262-277.
179. Noor-E-Khuda, S., Dhanasekar, M. and Thambiratnam, D.P. (2016). An explicit finite element modelling method for masonry walls under out-of-plane loading. *Engineering Structures*, 113, pp. 103-120.

- 180.NZS 4230(1990). “Code of practice for design of masonry structures”, Standards New Zealand, Wellington, 6020.
- 181.NZS 4230(2004). “Design of reinforced concrete masonry structures”, Standards New Zealand, Wellington, 6020.
- 182.Oliveira, D.V., Basilio, I. and Lourenço, P.B. (2010). Experimental behaviour of FRP strengthened masonry arches. *Journal of Composites for Construction*, 14(3), pp.312-322.
- 183.Ottazzi, G., Yep, J., Blondet, M., Villa-Garcia, G. and Ginocchio, J. (1989). Shaking table tests of improved adobe masonry houses. *Proceedings of the Ninth World Conference on Earthquake Engineering*, 1988, Tokyo-Kyoto, Japan, pp. 1123-28.
- 184.Oyarzo-Vera, C., Abdul Razak, A.K. and Chouw, N. (2009). Modal testing of an unreinforced masonry house. *International Operational Modal Analysis Conference*, Portonovo, Ancona, Italy.
- 185.Page, A.W. (1978). Finite element model for masonry. *Journal of the Structural Division*, 104(8), pp. 1267-1285.
- 186.Panizza, M., Garbin, E., Valluzzi, M.R. and Modena, C. (2012). Experimental investigation on bond of FRP/SRP applied to masonry prisms. *Proceedings of 6th International Conference on FRP Composites in Civil Engineering (CICE 2012)*, Rome, Italy.
- 187.Papanicolaou, C., Triantafillou, T. and Lekka, M. (2011). Externally bonded grids as strengthening and seismic retrofitting materials of masonry panels. *Construction and Building Materials*, 25(2), pp. 504-514.
- 188.Papanicolaou, C.G., Triantafillou, T.C., Papatheanasiou, M. and Karlos, K. (2008). Textile reinforced mortar (TRM) versus FRP as strengthening material of URM walls: out-of-plane cyclic loading. *Materials and Structures*, 41(1), pp. 143-157.
- 189.Paquette, J., Bruneau, M. and Brzev, S. (2004). Seismic testing of repaired unreinforced masonry building having flexible diaphragm. *Journal of Structural Engineering*, 130(10), pp. 1487-1496.
- 190.Penazzi, D., Valluzzi, M.R., Saisi, A., Binda, L. and Modena, C. (2001). Repair and strengthening of historic masonry buildings in seismic areas. *International Congress, More than two thousand years in the history of Architecture Safeguarding the Structure of our Architectural Heritage*, Bethlehem, Palestine, pp. 1-6.
- 191.Penner, O. and Elwood, K. J. (2016). Out-of-plane dynamic stability of unreinforced masonry walls in one-way bending: Shake Table Testing. *Earthquake Spectra*.

192. Petersen, R.B., Masia, M.J. and Seracino, R. (2010). In-plane shear behaviour of masonry panels strengthened with NSM CFRP strips. I: Experimental investigation. *Journal of Composites for Construction*, 14(6), pp. 754-763.
193. Pillai, Unnikrishna. S. and Devdas, M. (2003). *Reinforced concrete design*. Tata McGraw Hill, New Delhi.
194. Plevris, V. and Asteris, P.G. (2014). Modeling of masonry failure surface under biaxial compressive stress using Neural Networks. *Construction and Building Materials*, 55, pp. 447-461.
195. Prajapati, S., AlShawa, O. and Sorrentino, L. (2015). Out-of-plane behaviour of single-body unreinforced-masonry wall restrained by a flexible diaphragm. In *Proceedings of the 5th ECCOMAS Thematic Conference on Computational Methods in Structural Dynamics and Earthquake Engineering*, paper C (Vol. 1552), pp. 25-27.
196. Prakash, S.S. and Alagusundaramoorthy, P. (2008). Load resistance of masonry wallettes and shear triplets retrofitted with GFRP composites. *Cement and Concrete Composites*, 30(8), pp. 745-761.
197. Prawel, S.P. and Lee, H.H. (1988). The performance of upgraded brick masonry piers subjected to in-plane motion. *Proceedings of the 8th International Brick/Block Masonry Conference*, Dublin, Ireland.
198. Priestley, M.J.N. and Paulay, T. (1992). *Seismic design of reinforced concrete and masonry buildings*. New York: John Wiley & Sons, Inc.
199. Prota, A., Manfredi, G. and Nardone, F. (2008). Assessment of design formulas for in-plane FRP strengthening of masonry walls. *Journal of Composites for Construction*, 12(6), pp. 643-649.
200. Raghunath, S. (2003). *Static and dynamic behaviour of brick masonry with containment reinforcement*. PhD thesis, Department of Civil Engineering, Indian Institute of Science, India.
201. Rai, D.C. and Goel, S.C. (1996). Seismic strengthening of unreinforced masonry piers with steel elements. *Earthquake spectra*, 12(4), pp. 845-862.
202. Rai, D.C. and Goel, S.C. (2003). Seismic evaluation and upgrading of chevron braced frames. *Journal of Constructional Steel Research*, 59(8), pp. 971-994.
203. Rai, D.C., Agnihotri, P. and Singhal, V. (2011). Out-of-plane strength of damaged unreinforced masonry walls. *2nd North American Masonry Conference*, Minneapolis, Minnesota, USA.

204. Rao, K.N., Raghunath, S. and Jagadish, K.S. (2004). Containment reinforcement for earthquake resistant masonry buildings. 13th World Conference on Earthquake Engineering Conference Proceedings.
205. Raparla, H.B. and Kumar, R.P. (2011). Linear analysis of reinforced concrete buildings subjected to blast loads. ICI Journal, pp. 1-16.
206. Robazza, B.R., Brzev, S., Elwood, K.J., Anderson, D.L., Yang, T.Y. and McEwen, B. (2015). A Study on the out-of-plane stability of ductile reinforced masonry shear walls subjected to in-plane reversed cyclic loading. 12th North American Masonry Conference.
207. Rossetto, T. and Peiris, N. (2009). Observations of damage due to the Kashmir earthquake of October 8, 2005 and study of current seismic provisions for buildings in Pakistan. Bulletin of Earthquake Engineering, 7(3), pp. 681-699.
208. Rossi, M., Calderini, C. and Lagomarsino, S. (2016). Experimental testing of the seismic in-plane displacement capacity of masonry cross vaults through a scale model. Bulletin of Earthquake Engineering, 14(1), pp. 261-281.
209. Santa-Maria, H., Duarte, G. and Garib, A. (2004, August). Experimental investigation of masonry panels externally strengthened with CFRP laminates and fabric subjected to in-plane shear load. 8th US National Conference on Earthquake Engineering, San Francisco, USA, Paper No. 1042.
210. Sarangapani, G., Reddy, B.V. and Jagadish, K.S. (2010). Structural characteristics of bricks mortars and masonry.
211. Sathiparan, N., Mayorca, P. and Meguro, K. (2012). Shake table tests on one-quarter scale models of masonry houses retrofitted with PP-band mesh. Earthquake Spectra, 28(1), pp. 277-299.
212. Schwegler, G. and Kelterborn, P. (1996). Earthquake resistance of masonry structures strengthened with fiber composites. Eleventh World Conference on Earthquake Engineering, Acapulco, Mexico.
213. Seible, F., Priestley, M.J.N., Kingsley, G.R. and K rkch basche, A.G. (1994). Seismic response of full-scale five-story reinforced-masonry building. Journal of Structural Engineering, 120(3), pp. 925-946.
214. Shah, A.A. (2011). Applications of ferrocement in strengthening of unreinforced masonry columns. International Journal of Geology, 5(1), pp. 21-27.
215. Shahzada, K., Javed, M., Alam, B., Khan, M., Ali, Z., Khan, H. and Shah, S.S.A. (2012). Strengthening of brick masonry walls against earthquake loading. International Journal of Advanced Structures and Geotechnical Engineering, 1, pp. 10-14.

216. Silva, P.F., Yu, P. and Nanni, A. (2008). Monte Carlo simulation of shear capacity of URM walls retrofitted by polyurea reinforced GFRP grids. *Journal of Composites for Construction*, 12(4), pp. 405-415.
217. Singh, K.K., Kaushik, S.K. and Parakash, A. (1998). Strengthening of brick masonry columns by ferrocement. *Proceedings of the Third International Symposium on Ferrocement*, University of Roorkee, pp. 306-315.
218. Sinha, R. and Brzev, S. (2002). Housing Report: Unreinforced brick masonry building with reinforced concrete roof slab. Earthquake Engineering Research Institute (EERI), International Association for Earthquake Engineering (IAEE).
219. Sinha, R. and Goyal, A. (1994). Damage to buildings in Latur earthquake.
220. Sinha, R. and Murnal, P. (2001). Earthquake resistant design of torsionally coupled structures using VFPI. *Structures 2001: A Structural Engineering Odyssey*, pp. 1-12.
221. Sinha, R. and Murty, C.V.R. (1998). The 1993 Killari earthquake: engineering lessons and challenges. *Indian Concrete Journal*, 72(11), pp. 591-601.
222. Sinha, R., Brzev, S. and Kharel, G. (2004). Indigenous earthquake-resistant technologies— an overview. 13th World Conference on Earthquake Engineering.
223. Sorrentino, L., D' Ayala, D., de Felice, G., Griffith, M.C., Lagomarsino, S. and Magenes, G. (2016). Review of out-of-plane seismic assessment techniques applied to existing masonry buildings. *International Journal of Architectural Heritage*, pp. 1-20.
224. SP 20 (1991). "Handbook on masonry design and construction, part 2." Bureau of Indian Standard, New Delhi. India.
225. Sreerama, A.K. and Ramancharla, P.K. (2013). Earthquake behaviour of reinforced concrete framed buildings on hill slopes. *International Symposium on New Technologies for Urban Safety of Mega Cities in Asia (USMC-October 2013)*. Report No: IIIT/TR/2013/-1.
226. Srikanth, T., Kumar, R.P., Singh, A.P., Rastogi, B.K. and Kumar, S. (2010). Earthquake vulnerability assessment of existing buildings in Gandhidham and Adipur cities, Kachchh, Gujarat (India). *European Journal of Scientific Research*, 41(3), pp. 336-353.
227. Stratford, T., Pascale, G., Manfroni, O. and Bonfiglioli, B. (2004). Shear strengthening masonry panels with sheet glass-fiber reinforced polymer. *Journal of Composites for Construction*, 8(5), pp. 434-443.
228. Sundara Raja Iyengar, K.T., Desayi, P. and Reddy, K.N. (1970). Stress-strain characteristics of concrete confined in steel binders. *Magazine of Concrete Research*, 22(72), pp. 173-184.

229. Tan, K.H. and Patoary, M.K.H. (2004). Strengthening of masonry walls against out-of-plane loads using fiber-reinforced polymer reinforcement. *Journal of Composites for Construction*, 8(1), pp. 79-87.
230. Tinazzi, D., Modena, C. and Nanni, A. (2000). Strengthening of masonry assemblages with FRP rods and laminates. *Proceedings of International Meeting on Composite Materials, PLAST*, pp. 411-418.
231. Tomazevic, M. (1999). *Earthquake-resistant design of masonry buildings (Vol. 1)*. World Scientific.
232. Tomaževič, M. (2007). Damage as a measure for earthquake-resistant design of masonry structures: Slovenian experience. *Canadian Journal of Civil Engineering (Special Issue on Masonry)*, 34(11), pp. 1403-1412.
233. Tomaževič, M. (2009). Shear resistance of masonry walls and Eurocode 6: Shear versus tensile strength of masonry. *Materials and Structures*, 42(7), pp. 889-907.
234. Tomaževič, M. and Klemenc, I. (1997). Seismic behaviour of confined masonry walls. *Earthquake Engineering & Structural Dynamics*, 26(10), pp. 1059-1071.
235. Tomazevic, M. and Lutman, M. (1996). Seismic behaviour of masonry walls: modeling of hysteretic rules. *Journal of Structural Engineering*, 122(9), pp. 1048-1054.
236. Tomazevic, M. and Velochovsky, R. (2000). Some aspects of experimental testing of seismic behaviour of masonry walls and models of masonry buildings. *ISET Journal of Earthquake Technology*, 404, pp. 101-117.
237. Tomazevic, M. and Weiss, P. (1994). Seismic behaviour of plain-and reinforced-masonry buildings. *Journal of Structural Engineering*, 120(2), pp. 323-338.
238. Tomaževič, M., Klemenc, I. and Weiss, P. (2009). Seismic upgrading of old masonry buildings by seismic isolation and CFRP laminates: a shaking-table study of reduced scale models. *Bulletin of Earthquake Engineering*, 7(1), pp. 293-321.
239. Tomazevic, M., Lutman, M. and Petkovic, L. (1996). Seismic behaviour of masonry walls: experimental simulation. *Journal of Structural Engineering*, 122(9), pp. 1040-1047.
240. Tomaževič, M., Lutman, M. and Weiss, P. (1996). Seismic upgrading of old brick-masonry urban houses: tying of walls with steel ties. *Earthquake Spectra*, 12(3), pp. 599-622.
241. Toranzo, L.A., Restrepo, J.I., Mander, J.B. and Carr, A.J. (2009). Shake-table tests of confined-masonry rocking walls with supplementary hysteretic damping. *Journal of Earthquake Engineering*, 13(6), pp. 882-898.

242. Triantafillou, T.C. (1998). Strengthening of masonry structures using epoxy-bonded FRP laminates. *Journal of Composites for Construction*, 2(2), pp. 96-104.
243. Triantafillou, T.C. (1998). Strengthening of structures with advanced FRPs. *Progress in Structural Engineering and Materials*, 1(2), pp. 126-134.
244. Triantafillou, T.C. and Fardis, M.N. (1997). Strengthening of historic masonry structures with composite materials. *Materials and Structures*, 30(8), pp. 486-496.
245. Triantafillou, T.C., Papanicolaou, C.G., Zissimopoulos, P. and Laourdekis, T. (2006). Concrete confinement with textile-reinforced mortar jackets. *ACI Structural Journal*, 103(1), 28.
246. Tu, Y.H., Chuang, T.H., Liu, P.M. and Yang, Y.S. (2010). Out-of-plane shaking table tests on unreinforced masonry panels in RC frames. *Engineering Structures*, 32(12), pp. 3925-3935.
247. Tumialan, J.G. (2001). Strengthening of masonry structures with FRP composites. *Structures: A Structural Engineering Odyssey*, pp. 1-8
248. Tumialan, J.G., Galati, N. and Nanni, A. (2003). Field assessment of unreinforced masonry walls strengthened with fiber reinforced polymer laminates. *Journal of Structural Engineering*, 129(8), pp. 1047-1056.
249. Tumialan, J.G., Galati, N. and Nanni, A. (2003). FRP strengthening of UMR walls subject to out-of-plane loads. *ACI Structures Journal*, 100(3), pp. 312-329.
250. Tumialan, J.G., Galati, N., Namboorimadathil, S.M. and Nanni, A. (2002). Strengthening of masonry with FRP bars. *3rd. Int. Conf. on Composites in Infrastructure (ICCI 2002)*.
251. Tumialan, J.G., Morbin, A., Nanni, A. and Modena, C. (2001). Shear strengthening of masonry walls with FRP composites. *Composites*, pp. 3-6.
252. Turco, V., Secondin, S., Morbin, A., Valluzzi, M.R. and Modena, C. (2006). Flexural and shear strengthening of un-reinforced masonry with FRP bars. *Composites Science and Technology*, 66(2), pp. 289-296.
253. Turek, M., Ventura, C.E. and Kuan, S. (2007). In-plane shake-table testing of GFRP-strengthened concrete masonry walls. *Earthquake Spectra*, 23(1), pp. 223-237.
254. Turer, A. and Gölalmiş, M. (2008). Scrap tire ring as a low-cost post-tensioning material for masonry strengthening. *Materials and Structures*, 41(8), pp. 1345-1361.
255. Turer, A., Korkmaz, S.Z. and Korkmaz, H.H. (2007). Performance improvement studies of masonry houses using elastic post-tensioning straps. *Earthquake Engineering & Structural Dynamics*, 36(5), pp. 683-705.

256. Valluzzi, M.R., Tinazzi, D. and Modena, C. (2002). Shear behaviour of masonry panels strengthened by FRP laminates. *Construction and Building Materials*, 16(7), pp. 409-416.
257. Van Dam, J. (2015). Validation of efficient numerical model for out-of-plane bending of unreinforced masonry walls. Doctoral dissertation, TU Delft, Delft University of Technology.
258. Varma, M.N., Jangid, R.S. and Achwal, V.G. (2006). Tension ring in masonry domes. *Structural Analysis of Historical Constructions*, New Dehli, pp. 1187-1194.
259. Vecchio, F.J. (1990). Reinforced concrete membrane element formulations. *Journal of Structural Engineering*, 116(3), pp. 730-750.
260. Wei, C.Q., Zhou, X.G. and Ye, L.P. (2007). Experimental study of masonry walls strengthened with CFRP. *Structural Engineering and Mechanics*, 25(6), pp. 675-690.
261. Wel, S., Reinhorn, A.M. and Qazi, S.A. (1988). Upgrading the seismic resistance of unreinforced brick masonry using ferrocement coatings.
262. Wenzel, F., Bendimerad, F. and Sinha, R. (2007). Megacities–megarisks. *Natural Hazards*, 42(3), pp. 481-491.
263. Wight, G.D., Ingham, J.M. and Kowalsky, M. J. (2004). Shake table testing of post-tensioned concrete masonry walls. *Proceedings of the 13th International Brick/Block Masonry Conference*, Vol. 4, pp. 1059-68.
264. Wight, G.D., Kowalsky, M.J. and Ingham, J.M. (2007). Shake table testing of posttensioned concrete masonry walls with openings. *Journal of Structural Engineering*, 133(11), pp. 1551-1559.
265. Witzany, J., Cejka, T. and Zigler, R. (2011). Problems of masonry strengthening with carbon-and glass fibre fabric. *Procedia Engineering*, 14, pp. 2086-2093.
266. Yi, T., Moon, F.L., Leon, R.T. and Kahn, L.F. (2006). Lateral load tests on a two-story unreinforced masonry building. *Journal of Structural Engineering*, 132(5), pp. 643-652.
267. Yu, T., Teng, J.G., Wong, Y.L. and Dong, S.L. (2010). Finite element modeling of confined concrete-II: Plastic-damage model. *Engineering Structures*, 32(3), pp. 680-691.
268. Yuen, T.Y., Kuang, J.S. and Ali, B.S.M. (2016). Assessing the effect of bi-directional loading on non-linear static and dynamic behaviour of masonry-infilled frames with openings. *Bulletin of Earthquake Engineering*, 14(6), pp. 1721-1755.
269. Zhou, D., Lei, Z. and Wang, J. (2013). In-plane behaviour of seismically damaged masonry walls repaired with external BFRP. *Composite Structures*, 102, pp. 9-19.



LIST OF PUBLICATIONS

REFEREED JOURNALS

1. **Shermi, C., & Dubey, R. N.** (2017). Study on out-of-plane behaviour of unreinforced masonry strengthened with welded wire mesh and mortar. *Construction and Building Materials*, 143, 104-120. (Elsevier, UK)
2. **Shermi, C., & Dubey, R. N.** (2017). Performance Evaluation of a Reinforced Masonry Model and an Unreinforced Masonry Model Using a Shake Table Testing Facility. *Journal of Performance of Constructed Facilities*, 32(1). (ASCE)
3. **Shermi, C., & Dubey, R. N.** In-plane behaviour of unreinforced masonry strengthened with welded wire mesh and mortar. *Construction and Building Materials* (**Accepted**)

